

Ø7Ø
Ska
Lat
M.S.

JAN 12 1990

LATE TERTIARY TECTONIC EVOLUTION OF THE SEAFLOOR
SPREADING SYSTEM OFF THE COAST OF CALIFORNIA BETWEEN THE
MENDOCINO AND MURRAY FRACTURE ZONES

A THESIS SUBMITTED TO THE GRADUATE DIVISION OF
THE UNIVERSITY OF HAWAII IN PARTIAL FULFILLMENT
OF THE REQUIREMENTS FOR THE DEGREE OF

MASTER OF SCIENCE
IN GEOLOGY AND GEOPHYSICS

DECEMBER 1989

By

Laurie Elaine Skaer

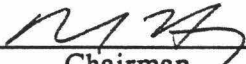
Thesis Committee:

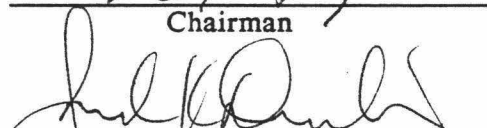
Richard N. Hey, Chairman
Frederick K. Duennebieer
John M. Sinton

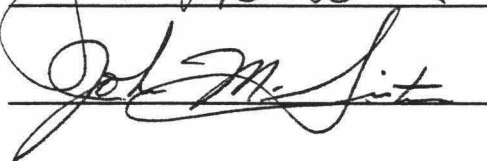
RETURN TO
HAWAII INSTITUTE OF GEOPHYSICS
LIBRARY ROOM

We certify that we have read this thesis and that, in our opinion, it is satisfactory in scope and quality as a thesis for the degree of Master of Science in Geology and Geophysics.

THESIS COMMITTEE



Chairman




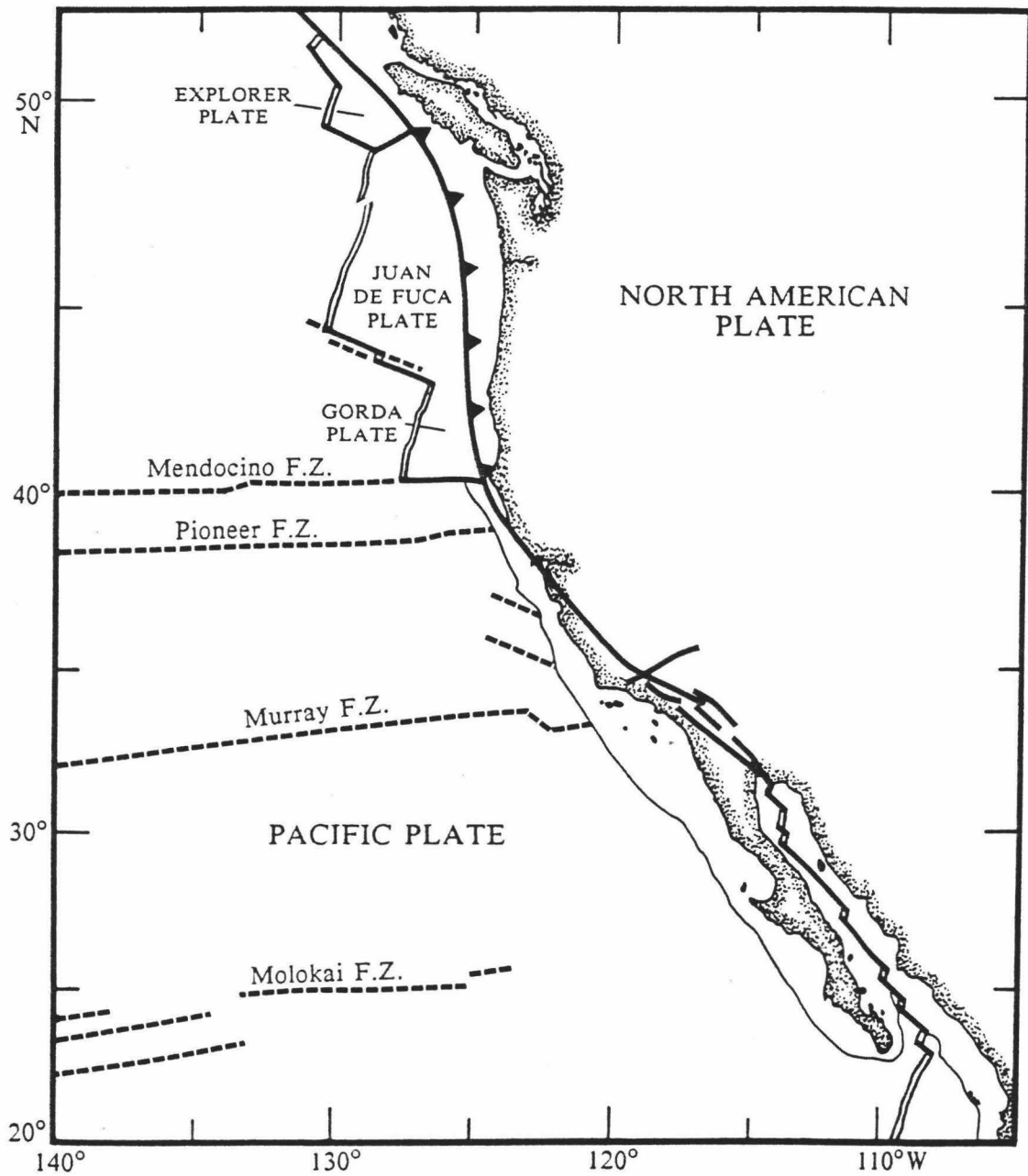


Fig. 1. Location map identifying present plates and plate boundaries (base map from Severinghaus and Atwater, 1989). Solid lines are active transform faults, dashed lines are fracture zones. Active spreading centers are shown by solid, double lines, subduction is indicated by the sawtoothed line.

ABSTRACT

A forward modelling program of two-plate spreading on a sphere was utilized to reconstruct the late Tertiary tectonic evolutionary history of the seafloor spreading system off the coast of California between the Mendocino and Murray fracture zones. This analytical technique was applied to a unique set of magnetic anomaly data consisting principally of a new digital data set: the original Raff-Mason data from one of the most significant marine geophysical surveys--the PIONEER survey. All the data, critical for the development of seafloor spreading and plate tectonic theory, were digitized (32° to 52°N), however, only the southern half was analyzed in this study.

Investigation of the Raff-Mason data, supplemented by additional magnetic anomaly data, indicates that the primary mechanism for reorganization of the Pacific-Farallon ridge as the spreading center migrated towards and arrived at the North American trench was rift propagation. The model presented here, containing a total of 21 propagation episodes from 36 Ma to 19.8 Ma (initiation time of the last propagator), shows excellent agreement with the isochrons identified from the magnetic anomaly pattern. Only minor exceptions exist locally in complex areas. A step-by-step evolution of the model is presented in a series of reconstructions documenting the history of spreading between the Pacific plate and five smaller plates created from the dissolution of the large ancestral Farallon plate. These plates include the Vancouver plate north of the Pioneer, the Farallon plate existing between the Murray and Pioneer transforms prior to the major reorganization at chron 10 (30.33 Ma), and the northwest-southeast spreading Arguello, Monterey, and Reyes microplates existing after chron 10.

TABLE OF CONTENTS

ACKNOWLEDGMENTS	iii
ABSTRACT.....	iv
LIST OF TABLES	vi
LIST OF FIGURES.....	vii
I INTRODUCTION	1
General Tectonic and Geologic Setting	1
Background for Data Set	3
Previous Studies.....	7
II DATA REDUCTION METHODS	20
The Digitizing Process	20
The Editing Process	21
The Merging Process.....	22
The Contouring Process	24
III ANALYTICAL METHODS	33
IV THE MODEL	45
V DISCUSSION	92
VI SUMMARY AND CONCLUSIONS.....	99
REFERENCES.....	101

LIST OF TABLES

Table		Page
1	Model Parameters for Pacific-Farallon Spreading.....	39
2	Model Parameters for Pacific-Vancouver Spreading.....	40
3	Model Parameters for Pacific-Arguello Spreading.....	41
4	Model Parameters for Pacific-Monterey Spreading	42
5	Model Parameters for Pacific-Reyes Spreading	43

LIST OF FIGURES

Figures	Page
1 Location map identifying present plates and plate boundaries	2
2 Physiographic provinces of the survey area.....	4
3 Shiptracks of the northern portion of the Raff-Mason data set.....	5
4 Shiptracks of the southern portion of the Raff-Mason data set.....	6
5 Original Esterline-Angus magnetic records from the PIONEER survey.....	8
6 Geometry of an oceanic propagator if propagation and rift failure are continuous.....	16
7 Magnetic anomaly profiles of the entire data set.....	25
8 Location and distribution of 1 minute by 1 minute gridded data points for the entire data set.....	27
9 Magnetic anomaly map of the entire data set gridded at 1 minute by 1 minute intervals	28
10 Location and distribution of 1 minute by 2 minute gridded data points for the definitive data set.....	29
11 Color contour anomaly map of the definitive data set	30
12 Shiptracks and magnetic anomaly map for the southernmost portion of the Raff-Mason data	32
13 Magnetic polarity time scale utilized in this study	34
14 Magnetic anomaly interpretation	35
15 Stepwise evolution of the ridge geometry for the model.....	44
16 Cartoon of plate boundary configuration at 36 Ma	46
17 Step-by-step evolution of the model.....	47
18 Detailed contour anomaly maps for complex areas.....	72
19 Three-dimensional color shaded relief magnetic anomaly plot.....	80
20 Bathymetry of the survey area.....	82
21 Cartoon of plate boundary configuration at time of major reorganization....	84
22 Final configuration of the model.....	90

23 Magnetic anomaly interpretation superimposed with fracture zones and
pseudofaults.....91

I. INTRODUCTION

Since the onset of seafloor spreading and plate tectonic theory, the evolution of the plate system off the west coast of North America has been extensively studied (Wilson, 1965; Vine and Wilson, 1965; Vine, 1966; Morgan, 1968; McKenzie and Morgan, 1969; Atwater, 1970; Hey, 1977; Hey and Wilson, 1982; Wilson et al., 1984; Nishimura et al., 1984; Riddihough, 1984; Wilson, 1988; Atwater, 1989; Severinghaus and Atwater, 1989). Currently, however, state of the art computer graphic techniques have only been applied to the Juan de Fuca area (Hey and Wilson, 1982; Wilson et al., 1984; Wilson, 1988). The objective of this paper is to apply these innovative analytical techniques to a new digital data set obtained from the original Raff-Mason data, one of the most significant marine geophysical surveys--the PIONEER survey (Mason, 1958; Mason and Raff, 1961; Raff and Mason, 1961), and to determine the spreading history in the area off the coast of California between the Murray and Mendocino fracture zones. A forward modelling program of two plate spreading on a sphere (Hey and Wilson, 1982; Wilson et al., 1984) was utilized to reconstruct the tectonic evolutionary history of this region by simulating the relatively complex magnetic pattern. The results indicate that a combination of seafloor spreading, rift propagation (Hey, 1977), and the fragmentation of the Farallon plate into microplates due to the arrival of the Pacific plate at the North American trench, can account for the complicated magnetic pattern.

General Tectonic and Geologic Setting

The present plate configuration of the region off the west coast of North America is shown in Figure 1. The area consists of two major plates: the Pacific and the North American, and 3 smaller plates: the Gorda, the Juan de Fuca, and the Explorer. The San Andreas fault system, the transform fault boundary between the

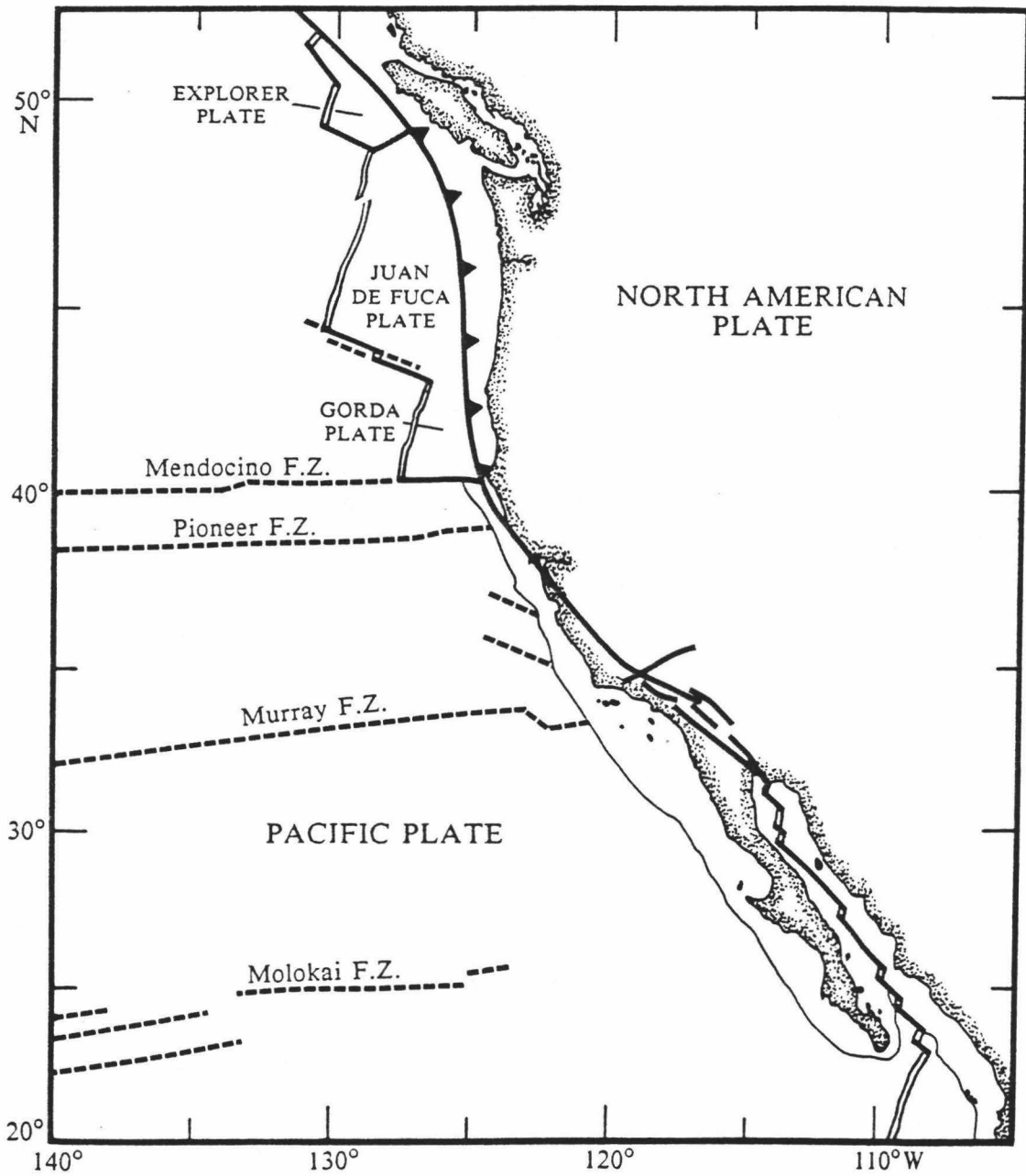


Fig. 1. Location map identifying present plates and plate boundaries (base map from Severinghaus and Atwater, 1989). Solid lines are active transform faults, dashed lines are fracture zones. Active spreading centers are shown by solid, double lines, subduction is indicated by the sawtoothed line.

Pacific and North American plates, lies to the east of the study area. The actual eastern border of the project, however, is the continental margin. The northern boundary of the area is defined by the Mendocino fracture zone/transform fault system while the southern boundary is delineated by the Murray fracture zone (FZ). Within the study area, the only other well known tectonic feature is the Pioneer FZ. The Pacific plate is currently moving northwest at a rate of 58 mm/yr with respect to the North American plate (Atwater, 1989).

The central California continental shelf and slope, and the adjacent abyssal plain and hills region constitute the main geological features of the study area. The topography is relatively subdued with only a few isolated seamounts compared to the rugged Baja California Seamount Province to the south of the Murray FZ. A continental-rise-type sediment wedge, composed of the Delgada and Monterey deep-sea fans, has built up at the base of the continental margin north of 34°N and south of the Mendocino FZ. These thick sediments cover a rugged volcanic basement whose irregularity is evident in the seismic profiles from the 1984 United States Geological Survey (USGS) Farnella Survey (EEZ-SCAN 84 Scientific Staff, 1986). The physiographic provinces of the survey area are shown in Figure 2.

Background for Data Set

From August 1955 to October 1956, an extensive high resolution magnetic survey of total field at sea level was conducted by the United States Coast and Geodetic Survey (USCGS) ship PIONEER while making detailed hydrographic surveys (Figures 3 and 4). The survey covers an area 250-300 miles wide off the west coast of the United States between latitudes 32°N and 52°N. Magnetic anomaly maps were generated for the area revealing a pattern of narrow anomalies of about 400 nT (nanoteslas) trending north-south for more than 500 miles over substantially flat abyssal plain (note: at the time of the original work, magnetic fields were measured in gammas, however, the SI

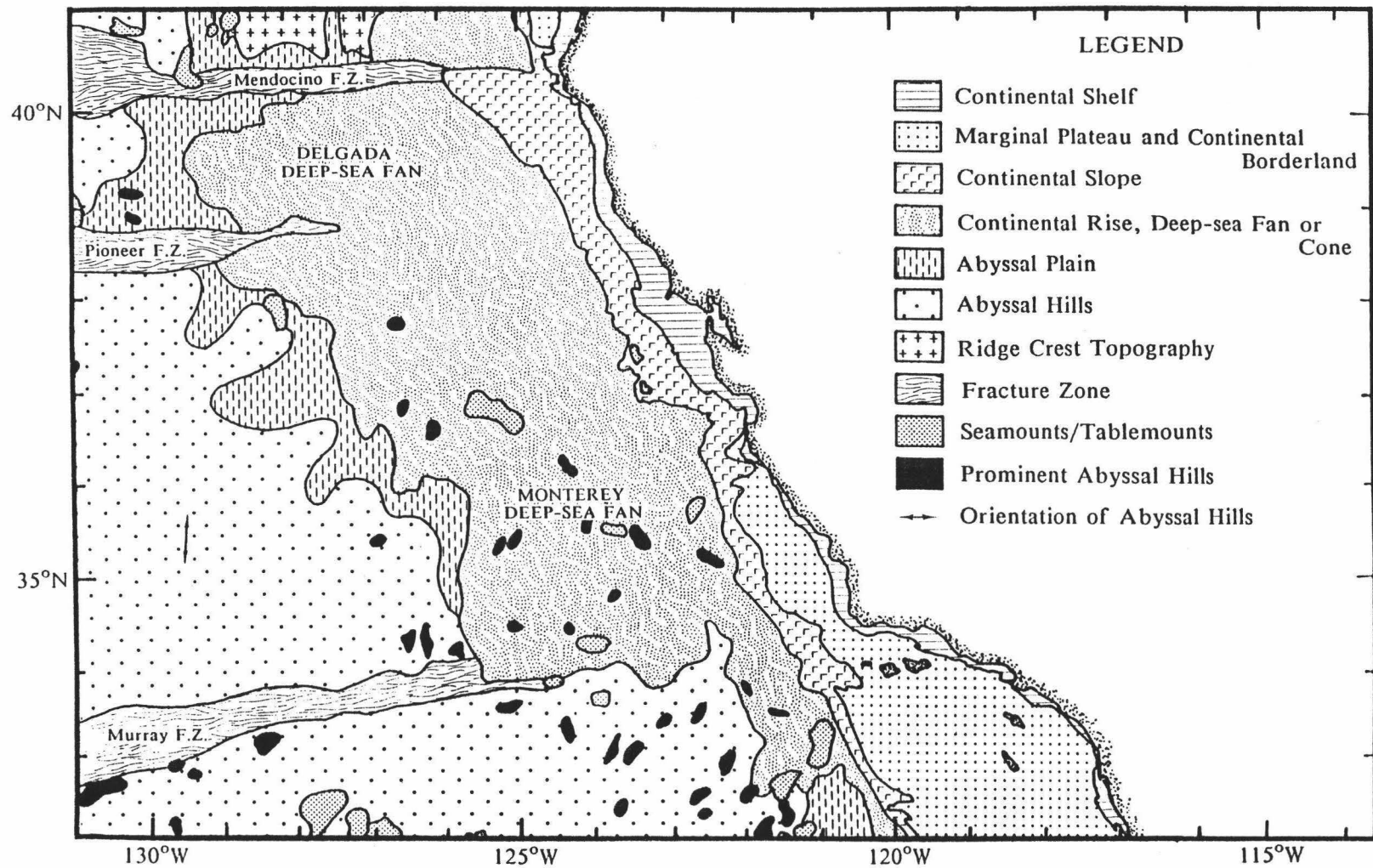


Fig. 2. Physiographic provinces of the survey area (modified from Morton and Lowrie, 1978).

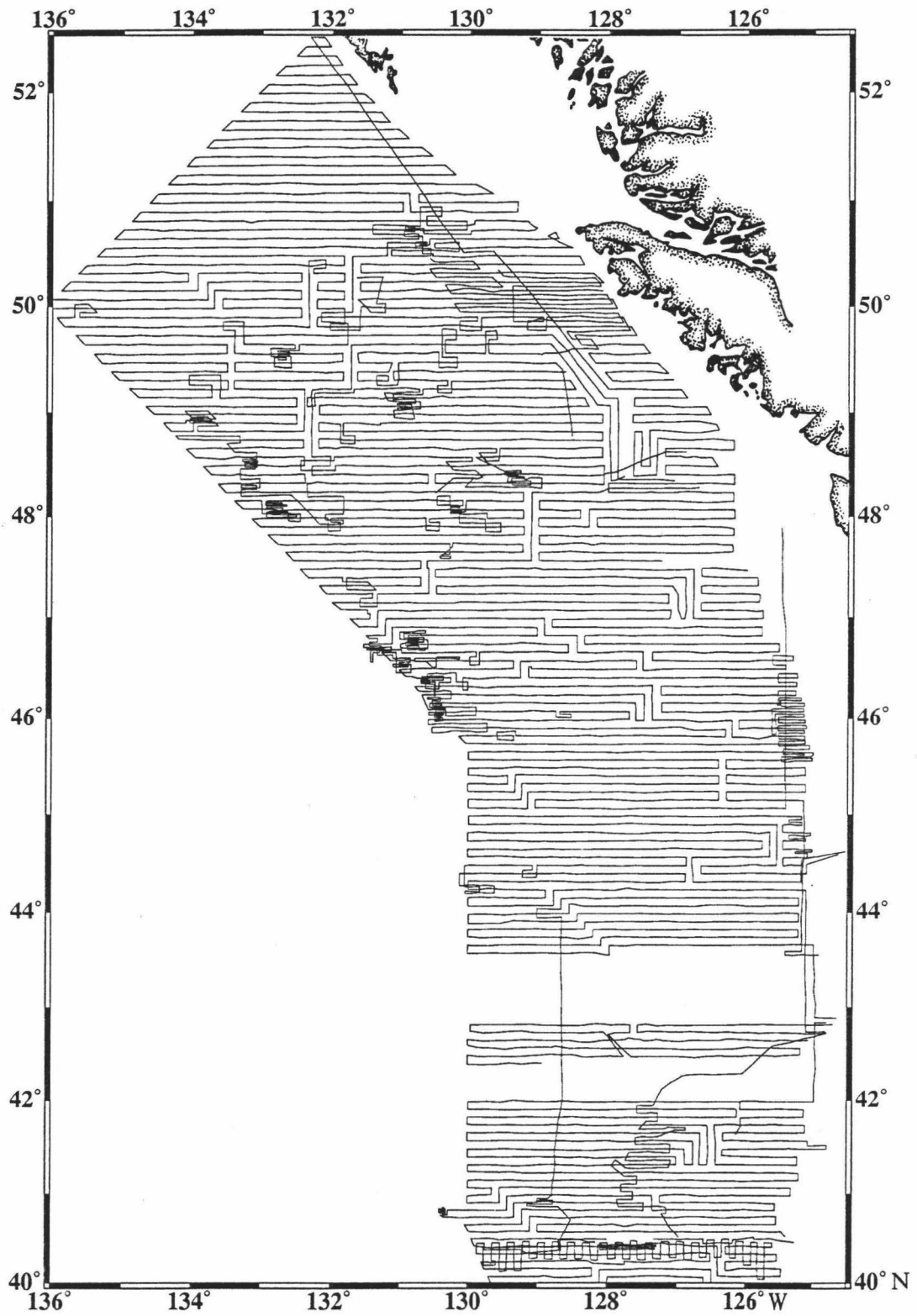


Fig. 3. Ship tracks of the northern portion of the Raff-Mason data set: surveys PIONEER 5 through PIONEER 11, and REHOBOTH.

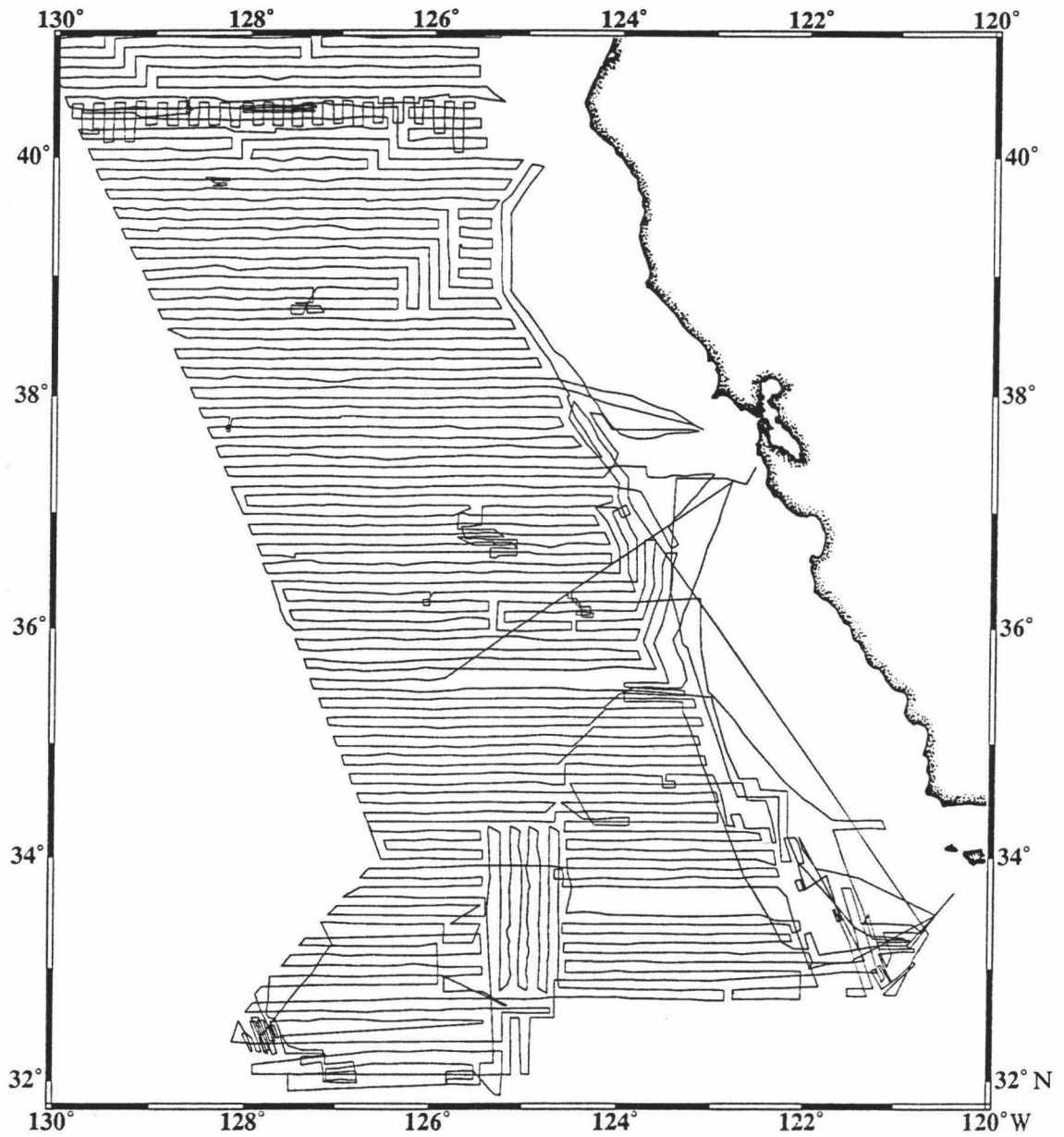


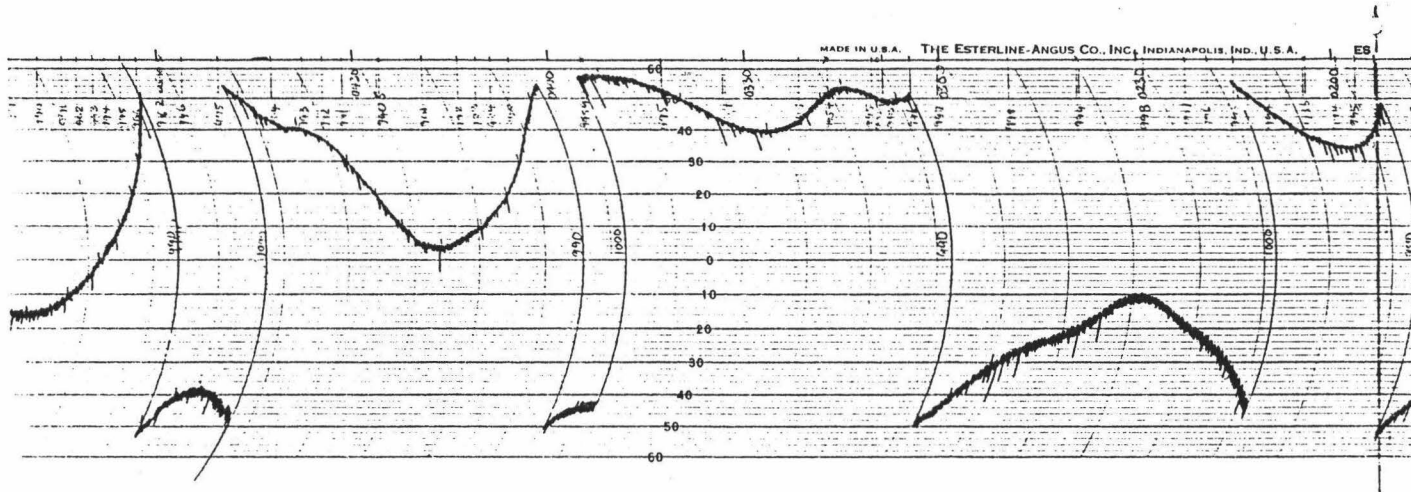
Fig. 4. Ship tracks of the southern portion of the Raff-Mason data set: surveys PIONEER 1 through PIONEER 6.

unit nanoteslas is used here (1 nanotesla = 1 gamma)). This was the initial discovery of magnetic stripes on the seafloor, features that would eventually play a major role in the plate tectonic revolution. The results of the PIONEER survey were published in Mason (1958), Menard and Vacquier (1958), Mason and Raff (1961), and Raff and Mason (1961).

Complete coverage of the survey area was obtained with a regular grid of surveyed track lines, approximately 5 nautical miles apart, except for highly anomalous areas where spacing was about 1 mile (Raff and Mason, 1961). The position of the ship was determined about every 8 miles by means of a radio-navigation system using ground wave propagation and fixed beacons on shore; the probable error was approximately ± 0.1 mile (Mason, 1958). The ship tracks are generally east-west, but sufficient lines were run in the north-south direction to eliminate ambiguity in magnetic contouring.

The magnetometer, a highly stabilized, self-orienting, total-field fluxgate, was mounted in a streamlined plastic fish and towed 500 feet behind the ship to reduce the effect of the ship's magnetism. The ship's effect ranged between ± 5 nT depending on the ship's heading (Mason, 1958). At approximately monthly intervals, the magnetometer was calibrated ashore against a proton-precession magnetometer. Total drift in the magnetometer during one survey was 20 nT (Mason, 1958). Taking into account the principal sources of error: inherent drift, inaccurate adjustment, and effect of the ship, the standard deviation of a single observation from the absolute value was about 15 nT (Mason and Raff, 1961; approximately 10 nT, Mason, 1958). Provided the instrument was kept in proper adjustment, the relative error between any two adjacent points was negligible (Mason, 1958). The diurnal variation of the total field was small compared to the value of the anomalies, so its effect was not removed (Mason, 1958). Examples of the original analog Esterline-Angus records are shown in Figure 5.

(A)



8

(B)

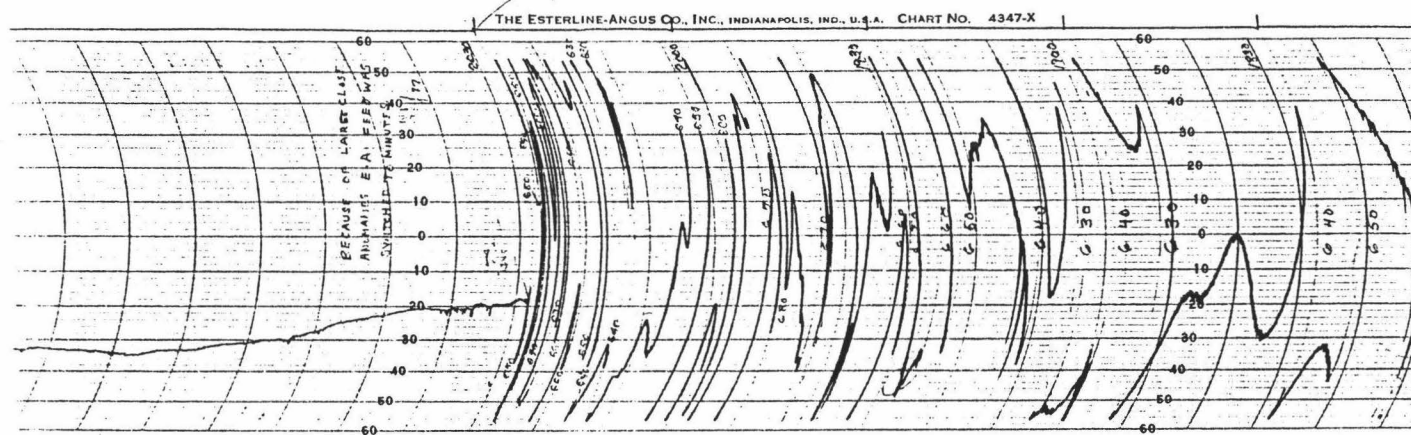


Fig. 5. Original Esterline-Angus magnetic records from the PIONEER survey. (a) An example of clean, clear-cut data. (b) An example of abstruse data. Magnetic offsets equal 500 nT. Times are annotated at the top of the record.

Previous Studies

Menard and Vacquier (1958) and Mason (1958) were the first to study and utilize the remarkable results of the PIONEER survey. By correlating the magnetic fabric north and south of the Murray FZ, they measured the direction and magnitude of horizontal slip of this 'transcurrent' fault to be 84 nautical miles (155 km). Vacquier et al. (1961) pursued this idea and measured the amount of slip along the Murray, Pioneer, and Mendocino 'transcurrent' faults. These huge horizontal displacements provided evidence for a "mobilitist" rather than "fixist" view of the Earth and helped pave the way for the acceptance of seafloor spreading and plate tectonics. In 1965, the findings of the PIONEER survey were utilized to advance the growing seafloor spreading idea; it was not until several years later that the survey results were important in developing plate tectonic theory.

Wilson (1965a) defined a new class of faults -- the transform fault, a type of horizontal shear fault that displays large offsets but terminates abruptly at both ends. He postulated that the San Andreas was a dextral transform fault (ridge-ridge type) and not a transcurrent fault as previously thought. He suggested that the magnetic offsets observed across the aseismic fracture zones off California may reflect the shape of a contemporary rift in the Pacific Ocean, and not be transcurrent fault displacements as previously supposed. This rift was, of course, the Pacific-Farallon spreading center. He also interpreted the San Andreas fault to be joined at the north to a short, isolated, oceanic ridge which he called the Juan de Fuca ridge, and at the south to the East Pacific Rise (Wilson, 1965b). He estimated the displacement along the transform fault to be approximately 400 km.

Using the magnetic stripes formed by the Juan de Fuca Ridge, Vine and Wilson (1965) reexamined the earlier speculation (Vine and Matthews, 1963) that ocean-floor spreading and periodic reversals of the earth's magnetic field might explain the

observed magnetic anomalies over oceanic ridges. Vine (1966) continued to study the symmetry and linearity of the unusual magnetic anomalies discovered by the 1955-56 PIONEER survey, and made an imposing conclusion that the "crest of the East Pacific Rise in the northeast Pacific has been overridden and modified by the westward drift of North America." He concluded that there was a change in direction of crustal spreading during Pliocene time from east-west to southeast-northwest; this more recent spreading created the northeast trending anomalies offshore between 35.5°N and 37°N. Consequently, these magnetic lineations were critical for the acceptance of seafloor spreading.

A residual magnetic anomaly map, the results of a U.S. Transcontinental Geophysical survey, was presented by Lattimore et al. (1968). This map extends west of the 1955 PIONEER survey. The magnetic survey, from the coast of California to 133°W longitude, 35°N to 39°N latitude, was conducted by the USCGS Ship PIONEER, from July to October, 1965. For this survey, ship tracks were primarily east-west and spaced approximately 18 km apart. The ship's position, whose accuracy was ± 1.8 km, was controlled by the U.S. Navy Satellite Navigation System. The Varian nuclear resonance magnetometer, used to measure the earth's total magnetic field intensity, was towed 230 m behind the ship except in water shallower than 200 m, where the tow length was reduced to 90 m.

Exciting discoveries transpired after the magnetic anomalies of the northeast Pacific were first identified and numbered by Pitman et al. (1968). The origin of the magnetic anomaly lineations were interpreted in accordance with the hypothesis of Vine and Matthews (1963). Menard and Atwater (1968) and Francheteau et al. (1970) further studied the characteristic patterns of the magnetic anomalies and fracture zones in detail. Menard and Atwater identified five trends in the northeast Pacific fracture zones and interpreted that at least five reorganization events in Pacific-Farallon spreading were manifested.

The motion of the Pacific 'block' relative to the North American 'block' was first considered by McKenzie and Parker (1967) and Morgan (1968). McKenzie and Parker obtained a pole position of 50°N, 85°W for motion between the Pacific plate and the plate containing North America and Kamchatka, using slip vectors from fault plane solutions. They plotted the slip vectors on a Mercator projection of the Pacific using the above pole and showed that the "paving stone theory of world tectonics" was correct and was applicable to about a quarter of the Earth's surface. Morgan deduced that large fracture zones lie on "circles of latitude" about the pole of relative rotation, and used the strike of the San Andreas fault system and associated faults between the Pacific and North American plates and azimuths from earthquake mechanism solutions to determine a pole of relative rotation at 53°N ($\pm 3^\circ$), 53°W ($\pm 5^\circ$).

Bassinger et al. (1969) interpreted the magnetic anomalies off central California to 133°W from a combination of maps from Lattimore et al. (1968) and Mason and Raff (1961). They noted "discontinuities occur in different parts of the magnetic pattern," but they believed local geology was responsible for these discontinuities, rather than global changes in sea-floor spreading. For the disturbed pattern between the Murray and Pioneer fracture zones, they felt a "combination of the nearness of the continent and the movements of crustal blocks" was possibly responsible for these local tectonic complications. They attributed the northeast-trending truncation and offsets of anomalies 11 and 12 to normal strike-slip faulting, and also attributed the possible fracture zone separating the northeast trending anomalies from the north-south trending anomalies to a strike-slip fault.

The next step in the progress of the plate tectonic theory occurred with McKenzie and Morgan (1969). They studied how the "simple geometric ideas of plate theory" extend to include some forms of plate evolution, particularly triple junctions. They defined two groups of triple junctions, stable and unstable, according to whether or not the triple junctions could retain their geometry as the plates move. With these

ideas, McKenzie and Morgan conceived a simplified tectonic history of the northeast Pacific dating back to the Tertiary by studying the evolution of the present triple junctions in the area.

First, they ascertained that there must have been a plate between the Pacific and the North American plates, the Farallon plate. Because only half of the Farallon anomaly pattern remains, this plate, along with its anomalies, must have been consumed by a trench between the Farallon-Pacific ridge and the coast of North America. They assumed all relative plate motions remained constant from the time of chron 13. According to McKenzie and Morgan, the Pacific plate first met the trench just south of the Mendocino transform fault. Two triple junctions were formed and strike-slip motion was initiated between the Pacific and North American plates. The northern triple junction (between the Mendocino transform fault, the San Andreas fault, and the trench (FFT)) migrated to the northwest, and the southern one (between the Pacific-Farallon ridge, the San Andreas fault, and the trench (RFT)) migrated to the southeast, joined by a constantly lengthening transform fault, the proto-San Andreas. The southern triple junction switched to a fault-fault-trench (FFT) type and migrated to the northwest when the Murray transform fault hit the North American plate. The motion of the southern triple junction flipped directions again when the Pacific-Farallon ridge was once more in contact with the trench. Thus, the evolution of these triple junctions provided a useful but very simple guide to the tectonic history of the ocean floor off California. The success of this effort, based in large part on the PIONEER survey data, was one of the key steps in the acceptance of plate tectonic theory.

A major reconstruction of the Cenozoic tectonic evolution of western North America was attempted by Atwater (1970). She was the first to stress the geological implications of the interactions of plates and believed that many of the "large scale

features of continental geology are related to plate motions" and that "the energy for tectonic activity was derived from the interactions of plates".

Atwater's first conclusions were that the initial portion of the Pacific plate to arrive at the mid-Tertiary trench was just south of the Mendocino transform fault, and that the Farallon plate had already begun to break up between the Pioneer and Murray fracture zones. When the North American and Pacific plates made contact, approximately 29 Ma (the age of the oldest offshore anomaly abutting the margin), a boundary formed between them accommodating the difference between their relative motions. This difference was probably similar to their present relative motion, and so began the San Andreas fault system and the present episode of strike-slip motion.

Atwater examined two models for late Cenozoic Pacific-North American plate motions: a model with constant motion throughout the late Cenozoic (model 1), and a model in which the plates were fixed with respect to one another until 5 Ma when they broke apart and began to move past one another (model 2). Atwater studied several different regions of Pacific-North American plate motions for information regarding the motion of the North American plate, i.e., to identify which model was correct. The first was the spreading at the mouth of the Gulf of California. The onset of spreading in the Gulf of California can be interpreted as either the onset of Pacific-North American motion in model 2 or the southward migration of a triple junction in model 1. She also studied spreading at the Juan de Fuca ridge, and noted spreading occurs parallel to the Blanco transform fault with a strike 25° different from the San Andreas trend. From this observation, she concluded that the Juan de Fuca plate is probably underthrusting the North American plate making the spreading direction at its ridge an unreliable indicator of Pacific-North American motion. Furthermore, Atwater noticed that there is a 50° to 60° difference in the pole position for the North American plate and the pole position determined from the trend of seamounts on the Pacific plate during the Cretaceous. These poles can be brought together assuming the

Pacific and North American plates moved with constant relative motion parallel to the present San Andreas fault system at a rate of approximately 60 mm/yr for the last m.y.. Thus, paleomagnetic separation supports model 1.

For the history of the North American plate motions, most of the evidence Atwater presented renders a constant motion model. Continental phenomena, mainly igneous rock distribution and amount and timing of deformation, supply inadequate evidence to distinguish between models, but substantiate the two active boundary regimes that were predicted for the edge of the North American plate: the trench regime and a strike-slip dominated regime. In conclusion, she believed that model 1 is the most probable even though it couldn't yet be definitely established, and she used this constant motion model to extrapolate the tectonic evolution for the Early Cenozoic.

A residual magnetic anomaly map, the results of a National Oceanic and Atmospheric Administration (NOAA) survey, was presented by Theberge (1971). The data, collected by the NOAA Ship SURVEYOR from March through September 1970, was reduced by means of the International Geomagnetic Reference Field (IGRF). Theberge characterized the central California continental shelf and continental slope as having a lack of magnetic expression. There are, however, three prominent, relatively low amplitude, positive anomalies found in the area trending northwesterly. The magnetic anomalies in the abyssal plain and hills region, extending between the Murray FZ and 40°N, define essentially the same pattern obtained by Mason and Raff (1961). There are two distinct trends: the north-south large amplitude anomalies, and the narrower, small amplitude, northeast trending anomalies inshore of 124°20'W.

The slightly rotated pattern of the magnetic anomalies off the coast of North America to a northeast trend suggested to Menard (1978) that the Farallon plate has been complexly fragmented by "pivoting fragments of the plate around points near ridge-trench-fault (RTF) triple junctions," beginning 55 Ma. Carlson (1981) proposed

that a 20° clockwise rotation for the Juan de Fuca and Gorda ridges occurred between approximately 9 and 3 Ma.

Observations of the magnetic anomalies in the Juan de Fuca area prompted Hey (1977) to develop the propagating rift hypothesis explaining oblique offsets commonly found in magnetic anomaly patterns while remaining compatible with rigid-plate tectonics. These offsets, called "pseudofaults," are en echelon arrays of fracture zones (if propagation is discontinuous) resulting from sequences of spreading center jumps propagating along a ridge (Hey, 1977). Prior to each jump, the propagating ridge is connected to the failing ridge by a transform fault which becomes inactive as a result of each jump. The new fracture zone and a segment of the old spreading center are transferred to one of the plates. Consequently, a series of failed rifts extinguished by each jump extend away from the corresponding doomed rift/transform juncture. The geometry of propagation and rift failure are continuous is presented in Figure 6. The past positions of propagating rift tips relative to both plates are recorded by V-shaped pseudofault pairs. The V points in the direction of propagation.

The transfer of lithosphere from one plate to the other during propagation may change the age pattern of the plate. If the plate is subducting (as in the case of the Farallon/Juan de Fuca plate), this age disruption may affect subduction rates and stresses, thus ridge configuration (Hey and Wilson, 1982). Another interesting characteristic of observed propagators is that the growing ridge frequently forms at a different azimuth from the dying ridge (Hey et al., 1980). Thus, propagating rifts constitute a mechanism by which spreading centers readjust to whatever forces are driving the plates (Hey, 1977), i.e. a method of ridge reorientation.

Sinton et al. (1983) studied the petrologic consequences of rift propagation on oceanic spreading ridges and concluded that "closed-system fractionation in non-replenished magma pockets is conducive to the development of high degrees of differentiation" at propagating rift tips. The greatest degree of differentiation and

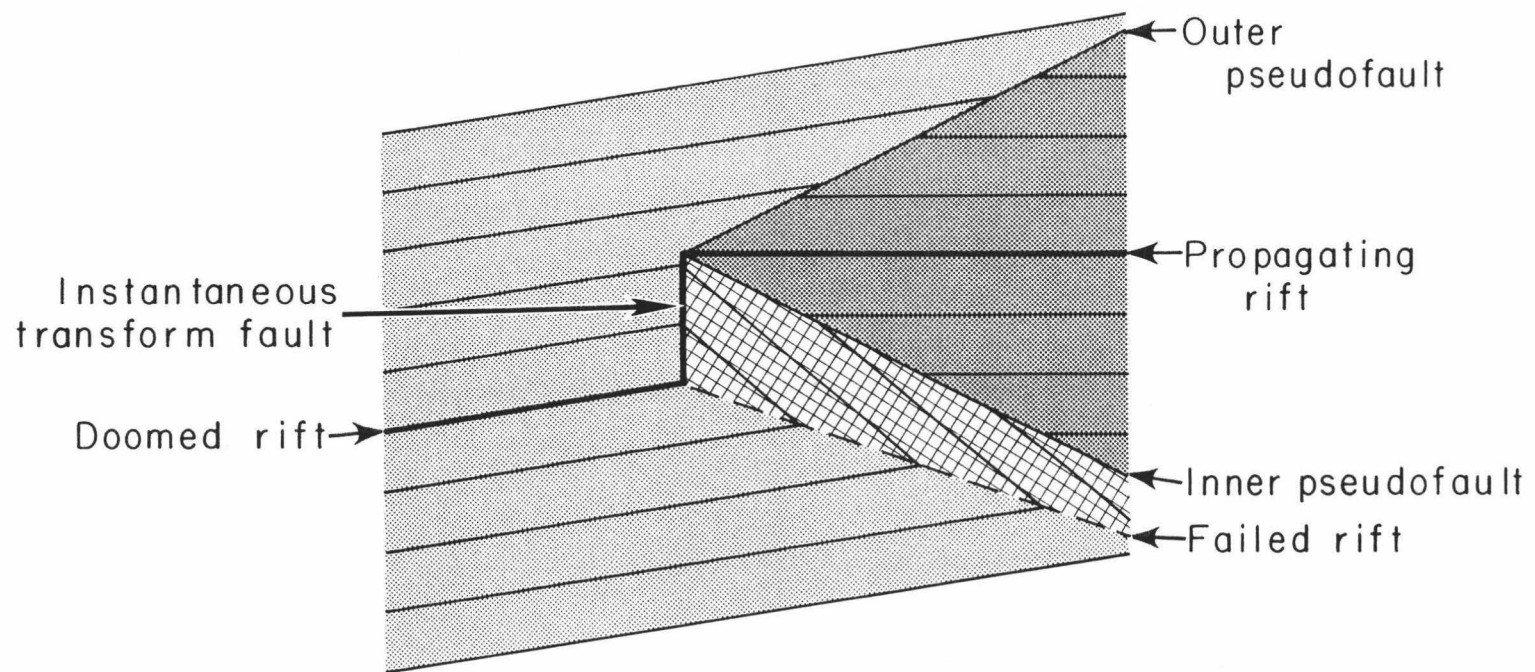


Fig. 6. Geometry of an oceanic propagator if propagation and rift failure are continuous. Tectonic elements are labelled. Propagator lithosphere is shown by dark stipple, normal lithosphere created at the doomed rift is shown by light stipple. Transferred lithosphere is indicated by crosshatching. Unidentified light lines show evenly spaced isochrons. Modified from Hey et al. (1986; 1988).

maximum compositional variability occurs within 50 km behind these special ridge-transform intersections. Vogt and Byerly (1976) noted that ferrobasalts recovered at Deep Sea Drilling Project (DSDP) Site 32, approximately 1.5° south of the Pioneer FZ, correlated with a high amplitude magnetic anomaly (chron 13). Sinton et al. (1983) noticed oblique truncations of some of the anomalies, an integral part of the propagating rift process. They tentatively interpreted the southeast-trending oblique truncation of anomaly 13 to represent the western pseudofault of a southward propagating rift; DSDP Site 32 would then lie just inside this outer pseudofault, analogous in position to highly differentiated lavas recovered from the Galapagos and Juan de Fuca areas.

Wilson et al. (1984) presented a detailed model of the tectonic evolution of the Juan de Fuca ridge. The model assumes that rift propagation provided the only mechanism of ridge reorientation in the area, occurring in response to changes in the spreading direction. This basic concept was also applied to my current analysis.

Engebretson et al. (1984) derived relative motion poles that describe the displacement histories between the Pacific and past adjacent oceanic plates. For stages of time of the order of 10^7 years, relative motion poles for plate pairs remained nearly fixed. Yet, between these stages "shifts in poles were commonly both large and abrupt" and within the stages the rates of plate motion changed. This indicated that the plates' speed changed more frequently than their direction (or that there are errors in the time scale). According to Engebretson et al. (1984), for the stage between chrons 21 and 8 (48 to 28 Ma), the Pacific-Farallon relative motion pole remained nearly fixed, however, the angular rate varied in particular time intervals. They divided this stage into 3 substages bounded by chrons 21 (48 Ma), 18 (43 Ma), 13 (37 Ma), and 8 (28 Ma). A best fit angular rate was found for each of these substages by holding the best fit pole for the stage fixed. For Pacific-Farallon motion between chrons 8 and 0 (28-0 Ma), Engebretson et al. used the poles of Wilson et al. (1984).

As part of a national geologic survey of the Exclusive Economic Zone (EEZ) of the United States, the USGS, in cooperation with the Institute of Oceanographic Sciences (IOS) of the United Kingdom, initiated Program EEZ-SCAN in April 1984. That year, aboard the MV FARNELLA, GLORIA (Geological Long-Range Inclined ASDIC) was used to map the EEZ off California, Oregon, and Washington. The results of this survey were presented in EEZ-SCAN 84 Scientific Staff (1986). Seismic reflection (airgun), bathymetric, and magnetic data were collected as well as the GLORIA side-scan sonar data throughout the EEZ-SCAN survey. The residual magnetic anomaly data were calculated by subtracting from the measured total-field value the IGRF updated to 1979.

Atwater (1989) updated her 1970 tectonic history of the northeast Pacific and western North America. In examining Pacific-North American plate motions, Atwater stated that the first break in the Farallon plate occurred at about 55 Ma creating the new Vancouver plate to the north. She located the new Farallon-Vancouver plate boundary between the Pioneer and Murray fracture zones. The trace of the migrating triple junction between the Pacific, Farallon, and Vancouver plates is a set of "curving toothlike disjunctures in anomalies 19-13." She felt that because a narrow neck had developed in the Farallon plate in this general area as the Pacific-Farallon spreading center approached the North American trench, it was the logical location for a break to occur. Further breaks occurred abruptly between the Pioneer and Murray fracture zones in the middle of anomaly 10 (30 Ma). She named two small plates, the Monterey and Arguello plates (Severinghaus and Atwater, 1989), due to two separate sets of rates and directions. Atwater suggested that these microplates were at least partially coupled to the North American plate since the northwest-southeast direction of their motion resembles the motion of the Pacific past North America. From isochron identifications and the position of Davidson seamount, Atwater agreed with Lonsdale's (1988)

interpretation of a dead ridge just after chron 6 (19 Ma) in the northern Monterey plate.

Although the original PIONEER records were thought to be lost, they were being stored by Art Raff who generously made them available for this project so that they could be digitized and analyzed with modern techniques.

II. DATA REDUCTION METHODS

The Raff-Mason PIONEER survey consisted of 11 separate cruises, PIONEER 1 through PIONEER 11, from August 1955 to October 1956--a total of 185 survey days. A twelfth cruise, aboard the REHOBOTH for five days in March 1956, was also acquired with the Raff-Mason data, and it partially fills a gap in the PIONEER data from 42°N to 43.5°N. Ship track plots for the complete Raff-Mason data set are shown in Figures 3 and 4. This entire data set, from 32°N to 52°N, was digitized and processed according to the data reduction methods stated below. However, only the southern half of the data, from 32°N to 41°N, was utilized for this study.

The Digitizing Process

The lengthy initial phase of this study was digitization of the original Esterline-Angus magnetic records. Figure 5, displaying a photograph of these antique data records, shows their uniqueness, quality, complexity, and great variability. An example of clean, clear-cut data is shown in Figure 5a, while Figure 5b shows data quality of the opposite extremity, abstruse data. The data were digitized with a Complot Series 7000 Digitizer using incremental switch stream mode (the digitizer automatically read points at a constant rate). The data were picked with a maximum of one minute between digitized points. The length of record that could be digitized at any one time was limited by the width of the digitizing table. This digitizing interval varied from 24 hours to 10 minutes of record depending on the particular survey day. For the majority of the records this interval was approximately 10 hours (survey time defined the x-axis). A day, therefore, was generally divided into three files, more if there were complications. A total of 624 raw magnetic files were created for the 190 survey days.

The Editing Process

Modification of the raw digitized files was required for a number of reasons. Initially the files were edited to compensate for the arcuate coordinate system of the Esterline-Angus records; the arc of the pen recording the signal defined the y-axis. Only the Varian records from the REHOBOTH survey had normal rectangular coordinates. Furthermore, units had to be converted from millimeters, the output unit of the digitizer, to decimal hours for the x-axis and nanoteslas (nT) for the y-axis. However, the most annoying problem when digitizing the records was the offsets that were created when the magnetic signal went off the edge of the paper. These offsets, generally a constant value of 500 nT, had to be eliminated to produce a continuous record. Throughout surveys PIONEER 4 and PIONEER 5, however, the recorded offsets randomly varied by multiples of 50 nT between the range of 50 to 500 nT. These offsets were slightly more difficult to deal with. So, three separate editing programs were required to manage these various problems: the first dealt with the majority of the surveys with the arcuate coordinate system and a constant offset value; the second dealt with surveys PIONEER 4 and 5, with the arcuate coordinate system but variable offsets; and the third program was for the REHOBOTH survey, with a constant offset value of 600 nT and a rectangular coordinate system.

At this juncture in the process, the files were merged to produce one file per day for more efficient handling. Additional editing was then required according to which magnetometer was used to collect the data. Calibrations indicated that each magnetometer sensor had individual specifications that needed to be applied to the reading to obtain the absolute field. For the Mark I Head, 19,850 nT were added to the reading to obtain the absolute field, while for the Mark II Head, 19,900 nT were added to the reading, then it was multiplied by the factor 1.049824035 to obtain the absolute field.

To test the quality of the editing process, the modified files were plotted to check if a smooth, continuous curve was produced. Any problems, e.g., minor discontinuities where offsets were eliminated, incorrect offset values, glitches due to digitizer failure, etc., were then addressed and corrected. For many of the surveys, the arc of the pen recording the signal became slightly off the arc of the Esterline-Angus record paper. This misalignment caused time, on the order of a minute, to repeat or to display a small gap in numerous places. The time overlap was eliminated for the data to merge properly into the required format for later analysis.

The Merging Process

Concurrently with the magnetic digitizing process, the navigation and bathymetry from the original log books were input into the computer and files were created for each survey day. Bathymetry data were separated from the navigation to create a bathymetry data set. These two sets of files were checked against the log books, and the navigation was plotted at a large scale for a visual check. Obvious errors were corrected. However, a formidable problem with the navigation occurred due to the course changes. The log books state the ship maneuvered exactly 90° turns at very specific times, however, they did not include navigational fixes for the times of these course changes. The only fixes that were recorded in the logs were at 15 or 30 minute intervals in between the course changes. Hence, the corners of the ship tracks were usually cut off and rounded. An interpolation program, designed to interpolate the correct fix for the course change at the given course change time, was then utilized to correct the navigation for these errors, and a much more accurate track plot was created.

Thus, three data sets were created individually: navigation, bathymetry, and magnetics. These data were reformatted to Hawaii Institute of Geophysics (HIG) ASCII event format, the layout required to merge the files to MGD77 format, the

standard marine geophysical data format of the National Geophysical Data Center (NGDC). The bathymetry files, originally in time and fathoms, were modified to time and two-way travel time. These files were then run through the program BATHCOR to create files with time, two-way travel time, corrected depth in meters and Matthews zone. The magnetic files were run through a computer program for the removal of the Definitive Geomagnetic Reference Field (DGRF). The program used the 1955 DGRF for the 1955 data and a weighted combination of the 1955 and 1960 DGRF's for the 1956 data. A listing of the total magnetic field and the residual magnetics was output from the program.

Following the modification of each of these three data sets, the HIG ASCII files were merged to create 12 comprehensive MGD77 files: one for each of the PIONEER surveys and one for the REHOBOTH survey. Once the merging procedure was completed, the magnetics of the entire data set were plotted along track. At this point, a geographical division was made in the data set from the area plot, and only the files within the study area were thereafter processed and analyzed. The complete digital data set will be made available at the NGDC.

Gaps in the magnetic data were filled as best as possible with available data from the NGDC. Additional data from the National Oceanic and Atmospheric Administration (NOAA), the United States Geological Survey (USGS), the United States Coast and Geodetic Survey (USCGS), and Scripps Institution of Oceanography (SIO), were included. The foremost supplemental cruises included the 1984 USGS GLORIA survey on the MV FARNELLA, and the 1970 NOAA California Continental Margin Project data of Theberge (1971). These two cruises primarily covered the same area as the Raff-Mason data, except that they surveyed closer to the coast (up on the continental shelf). Also employed in the study were: data described in Lattimore et al. (1968) covering the area west of the Raff-Mason data from 35° to 39°N (referred to in this study as the 1965 USCGS data); a 1972 NOAA cruise covering the northernmost

portion of the study area; and six different SIO cruises, from the years 1961 to 1977; each adding a single trackline to the data deficient southwest corner of the study area. Figure 7 displays the east-west trending magnetic anomaly profiles plotted along track.

The Contouring Process

Due to the tremendous data density, the residual magnetics were contoured by a computer program from the GMT system by Paul Wessel and Walter H. F. Smith of Lamont-Doherty Geological Observatory. This software package can not only contour and image in two or three dimensions, but also plot tracklines and gridded data locations, and analyze cross-over errors.

The first step to a final magnetic anomaly contour plot was an analysis of the ship track cross-overs. Wessel (1989) describes the cross-over programs developed for the GMT system. Both internal cross-overs (within a particular cruise) and external cross-overs (between two different cruises) were determined. The mean value of the cross-over error (COE), the difference between the magnetic values that are located at the same position, and its standard deviation were calculated for each of the cruises and cruise pairs. The cruise with the lowest internal COE standard deviation (15 nT) was considered the most reliable cruise (as long as it had sufficient internal cross-overs). This cruise turned out to be the USGS FARNELLA survey. This is not surprising because it is the most recent survey with the most up-to-date technology and navigation. The mean external COE value of the other cruises with respect to the USGS survey was used as a determination for its correction value for standardization. Thus, each cruise was corrected and subsequently standardized with respect to the USGS data. Sixty-nine nT were added to the Raff-Mason data in order for the mean external COE with the USGS data to be minimized. Likewise, 32 nT were added to the 1970 NOAA data and 65 nT were added to the 1965 USCGS data. This standardization was done for the contour maps only. The data for the NGDC and for

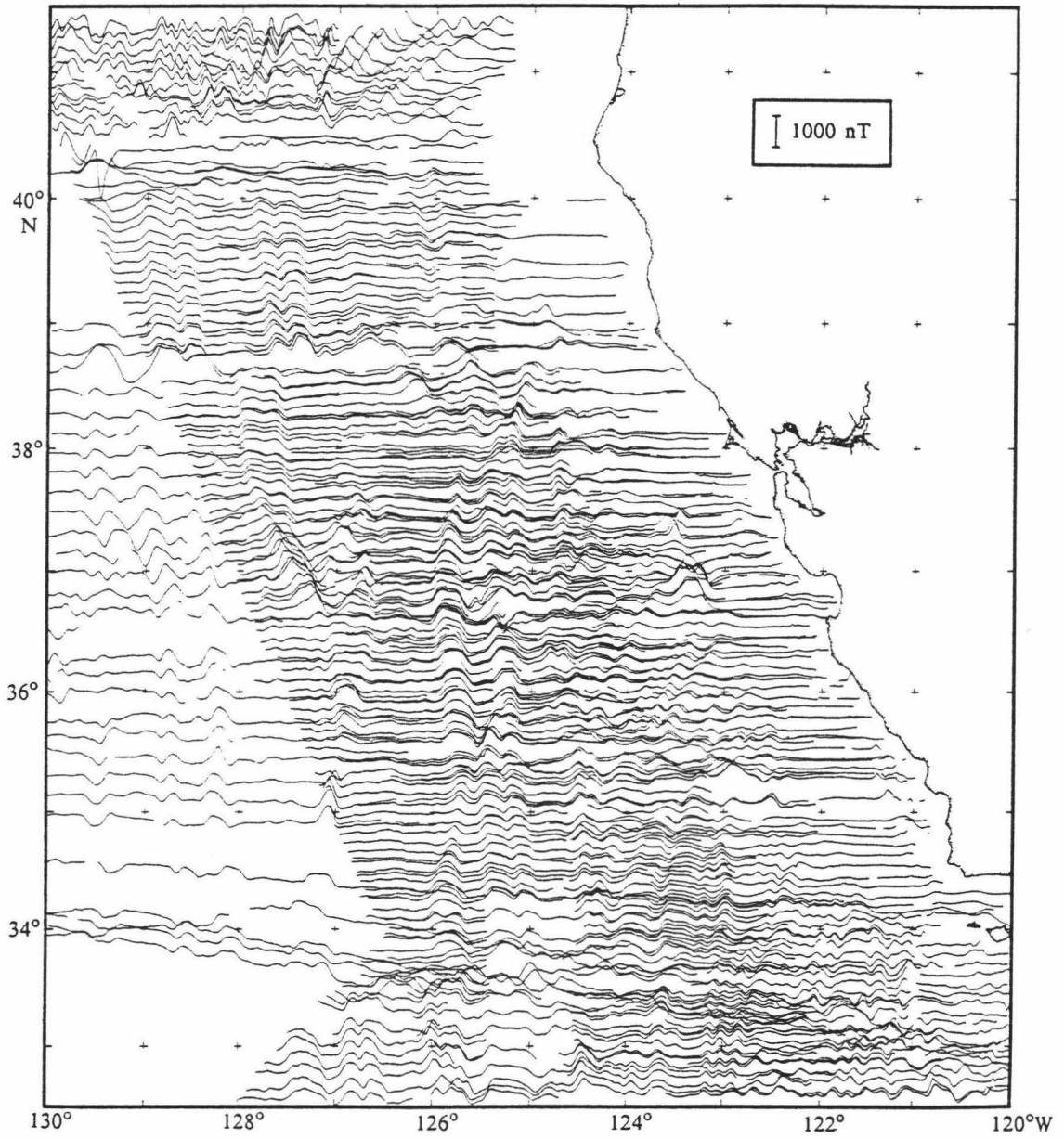


Fig. 7. Magnetic anomaly profiles, projected north-south, of the entire data set, including the Raff-Mason, USGS, NOAA, and USCGS surveys, and SIO tracklines.

the magnetic profiles were left at their original values. The sparse tracklines of the SIO and Navy data produced very large external COE standard deviations and were considered too unconstrained, and hence, unreliable. These cruises were not standardized or used in the contouring process.

Two contour maps were produced. The first was a combination of all the dependable data including the Raff-Mason, USGS, NOAA, and USCGS surveys. The data were gridded into one minute grids. The location and distribution of these gridded data points are shown in Figure 8. The data points were then fitted to a minimum curvature surface approximating "the shape adopted by a thin plate flexed to pass through the data points" (Smith and Wessel, 1989), analogous to elastic plate flexure. Tension was added to the elastic plate flexure equation to eliminate extraneous inflection points, and thus not require it to pass through all data points. This surface was then contoured at 100 nT intervals (Figure 9).

A second contour plot was constructed using a unique combination of data. The PIONEER survey data, which had the greatest density, comprised the majority of the data used for this new data set. Additional USGS, 1970 NOAA, and 1965 USCGS data were used to fill in the data gaps to the west and east of the Raff-Mason data set. These data were initially gridded and contoured with one minute grids, but the data distribution favored one minute (E-W direction) by two minute (N-S direction) grids; the general azimuth of the ship tracks concentrated the data in an east-west direction relative to a north-south direction. The contours of the one by two minute gridded data were more continuous and elongated than the one by one gridded contours, which tended to be chopped up into circular pieces. Figure 10 displays the location and distribution of the one by two minute gridded data points. Figure 11 is a color contour map of the one by two minute gridded residual magnetic data with a 50 nT contour interval. This data set, based primarily on the corrected Raff-Mason data, produced a clearer, more cohesive anomaly map compared to that produced by

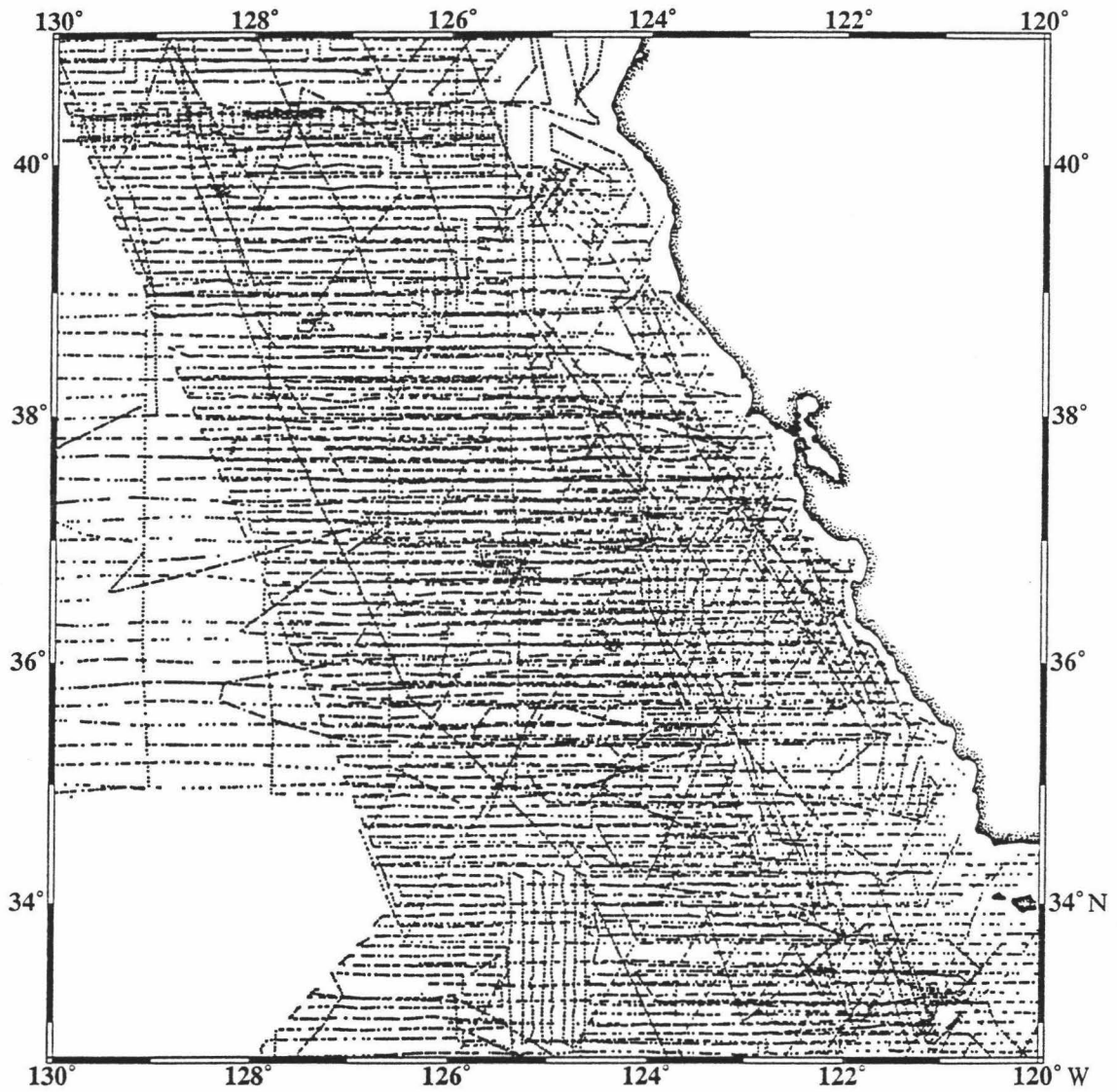


Fig. 8. Location and distribution of 1 minute by 1 minute gridded data points for the entire data set, including the Raff-Mason, USGS, NOAA, and USCGS surveys.



Fig. 9. Magnetic anomaly map of the entire data set gridded at 1 minute by 1 minute intervals. Contour interval is 100 nT. Positive anomalies (greater than -100 nT) are shaded.

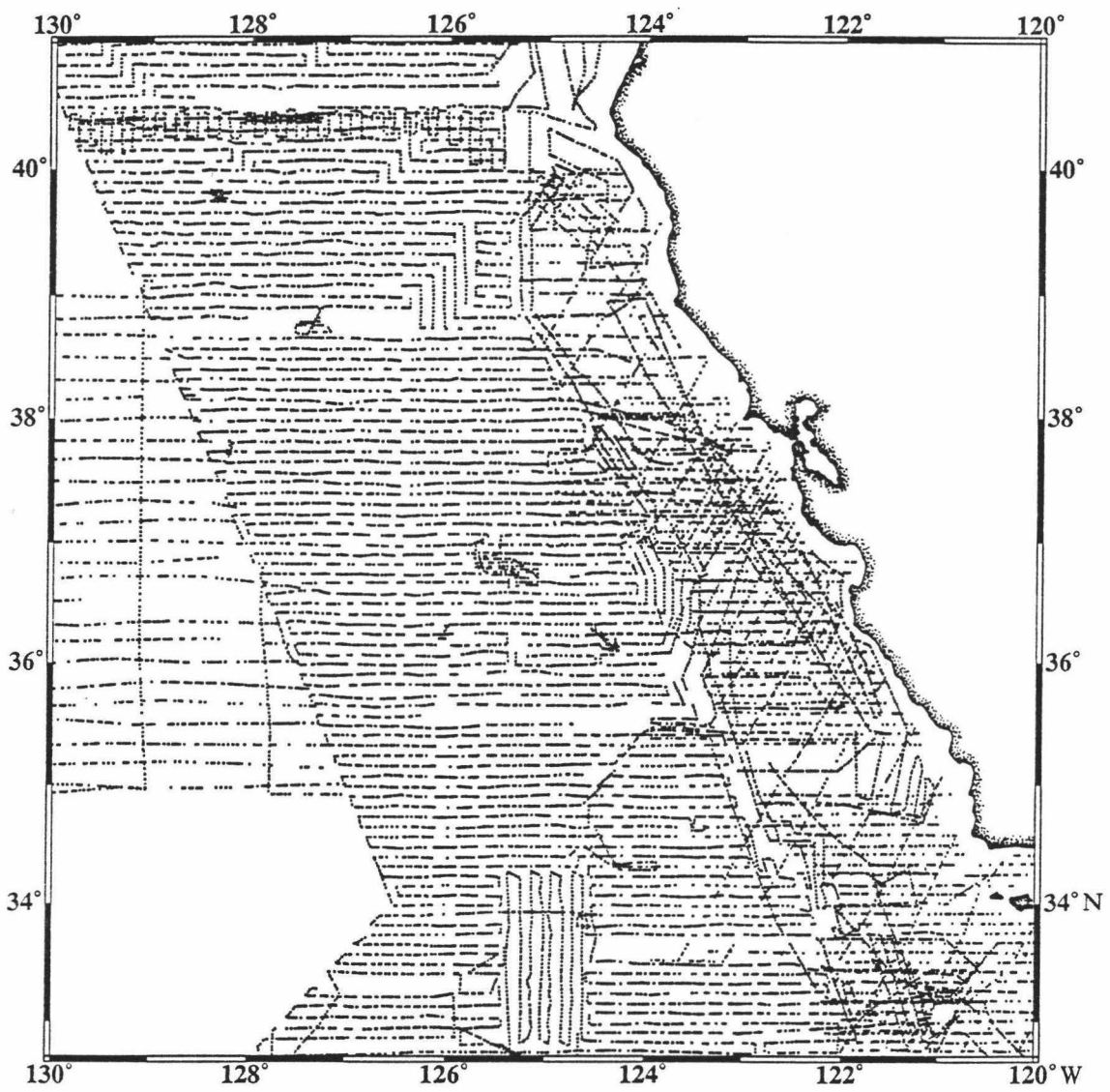


Fig. 10. Location and distribution of 1 minute by 2 minute gridded data points for the definitive data set: a combination of Raff-Mason, USGS, and NOAA data.

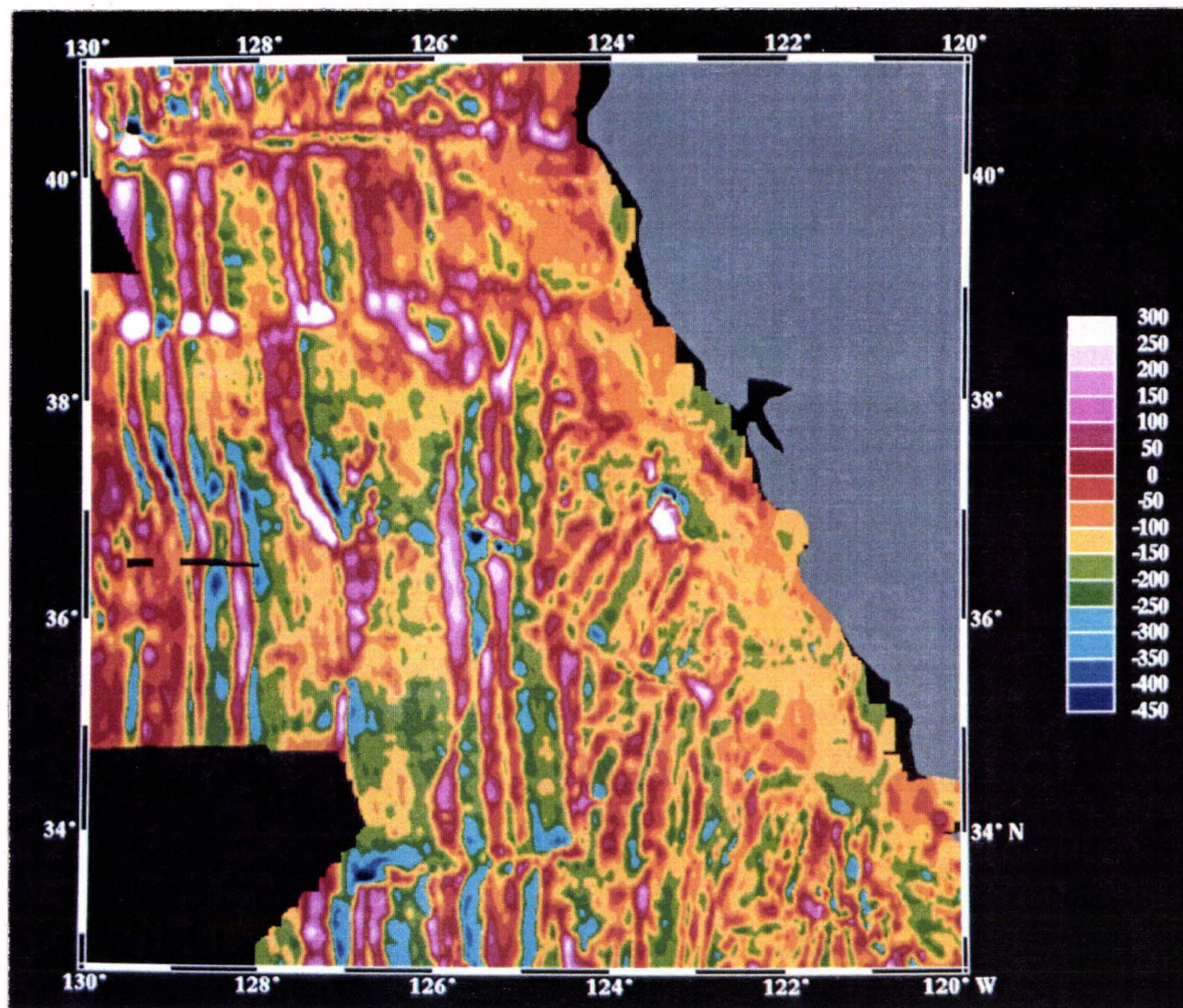


Fig. 11. Color contour anomaly map of the definitive data set. The contour interval is 50 nT.

combining all available data. For this reason, the above data were chosen as the definitive data set and were utilized in all ensuing analyses. It is interesting to note that the final residual magnetic map (Figure 11), has anomaly amplitudes approximately 100 nT less than the original Raff-Mason contour maps. This is due to my removal of the appropriate DGRFs whereas Raff and Mason subtracted a linear approximation to the regional field.

Lastly, the southernmost tip of the Raff-Mason data set is not used in this study. Therefore, in order to complete the publication of the entire Raff-Mason data from 32°N to 41°N, this southwest portion of the data is shown in Figure 12.

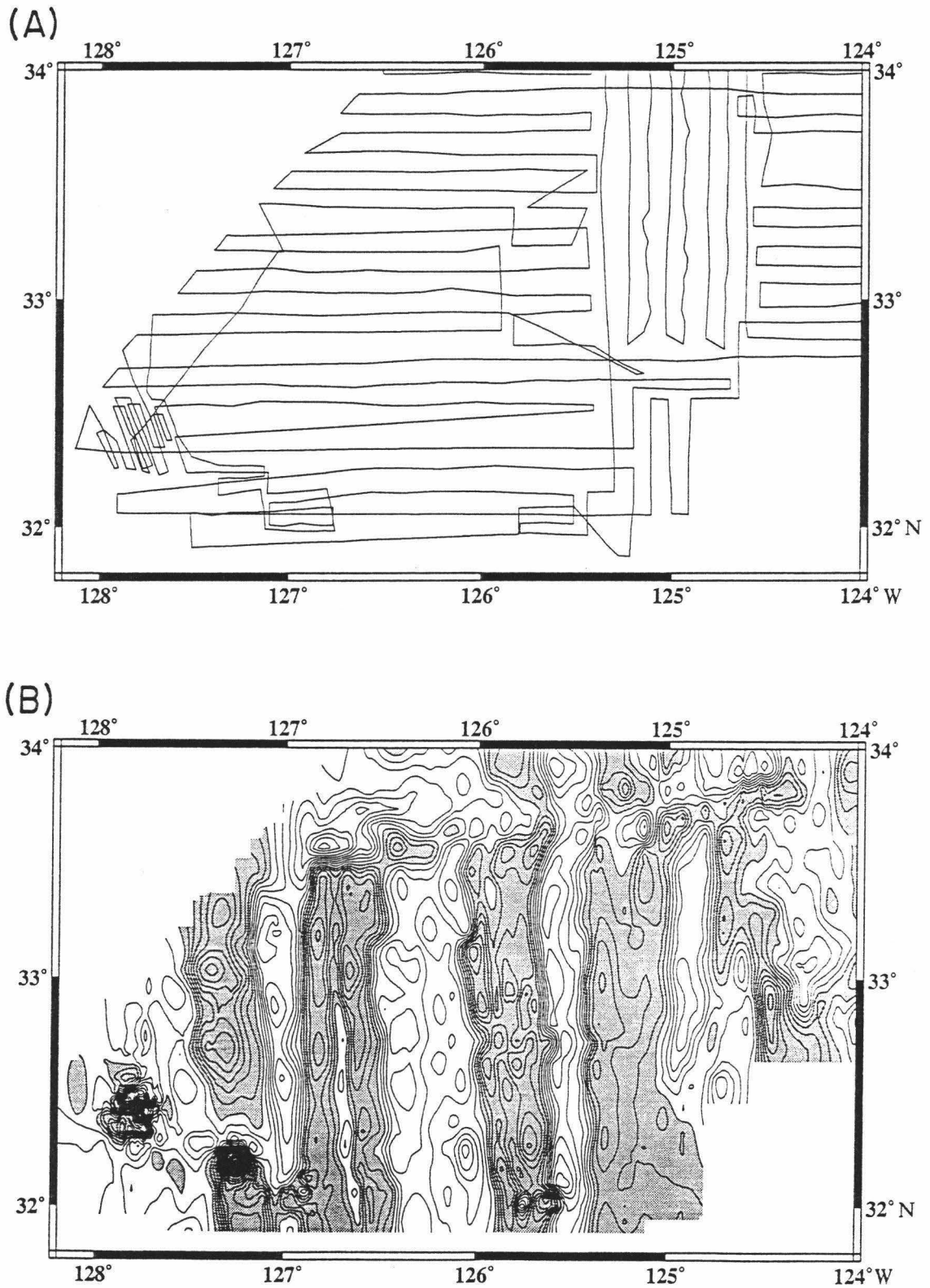


Fig. 12. Southernmost portion of the Raff-Mason data. (a) Shiptracks for the data. (b) Magnetic anomaly map contoured at 50 nT intervals. Positive anomalies (greater than -100 nT) are shaded. For reference, chron 10 begins at about 126°W.

III. ANALYTICAL METHODS

Analysis of the magnetic data was initiated by reinterpretation of the anomalies and resolution of the dominant fracture zones and pseudofaults using the definitive residual magnetic contour map (Figure 11) and magnetic anomaly profiles (Figure 7). USGS GLORIA side scan imagery (EEZ-SCAN 84 Scientific Staff, 1986) and bathymetry data (Chase et al., 1981) were beneficial in distinguishing the effects of seamounts, the continental margin, irregular basement, etc., from the true magnetic signal of the oceanic crust formed by seafloor spreading. To strengthen the interpretation, the magnetic anomaly data were modelled with the MAGBATH program (Hey et al., 1986) which generates synthetic magnetic anomalies using the observed orientation of the magnetic stripes, bathymetry, and the magnetic polarity time scale of Kent and Gradstein (1986) used throughout this study (Figure 13). The final interpretation of the magnetic data is shown in Figure 14. The -100 nT contour was determined to best display the normal and reversed polarity magnetics equally. The low amplitude northeast trending stripes were particularly well delineated with this contour. However, in a few areas south of the Pioneer FZ around the high amplitude chrons 12 and 13, the 0 nT contour was considered to more closely represent the normal/reverse magnetic boundary. Only normal anomalies (chosen here to be anomalies with values greater than -100 nT) with an amplitude greater than 100 nT are shaded. This amplitude discrimination was done to differentiate the strong seafloor spreading magnetic signal from minor fluctuations.

The principal analytical technique was a computer graphic program that produces mercator projections of predicted isochron patterns for two-plate spreading on a sphere. This program, developed and first utilized by Hey and Wilson (1982), has been extensively used in the Juan de Fuca region to decipher its tectonic history (Hey and Wilson, 1982; Wilson et al., 1984; Wilson, 1988), as well as to study the Eocene

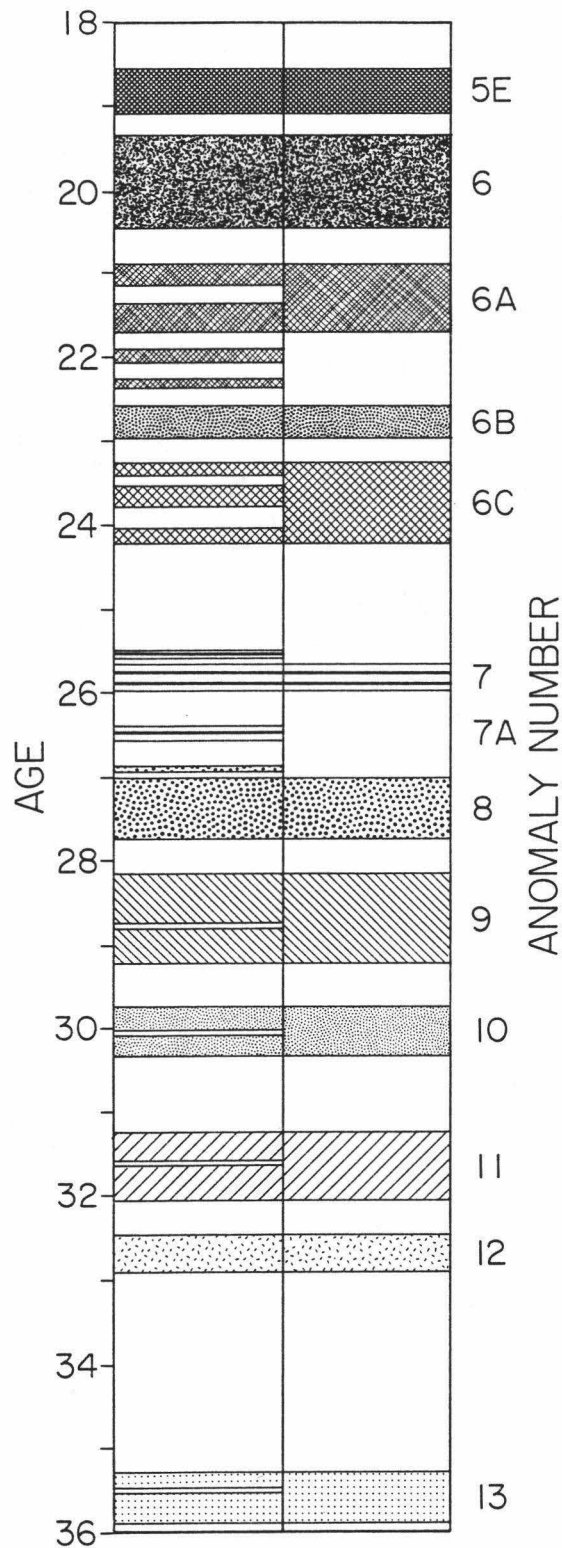


Fig. 13. Magnetic polarity time scale utilized in this study. The left side is from Kent and Gradstein (1986) and the right side is the simplified time scale used for forward modelling.

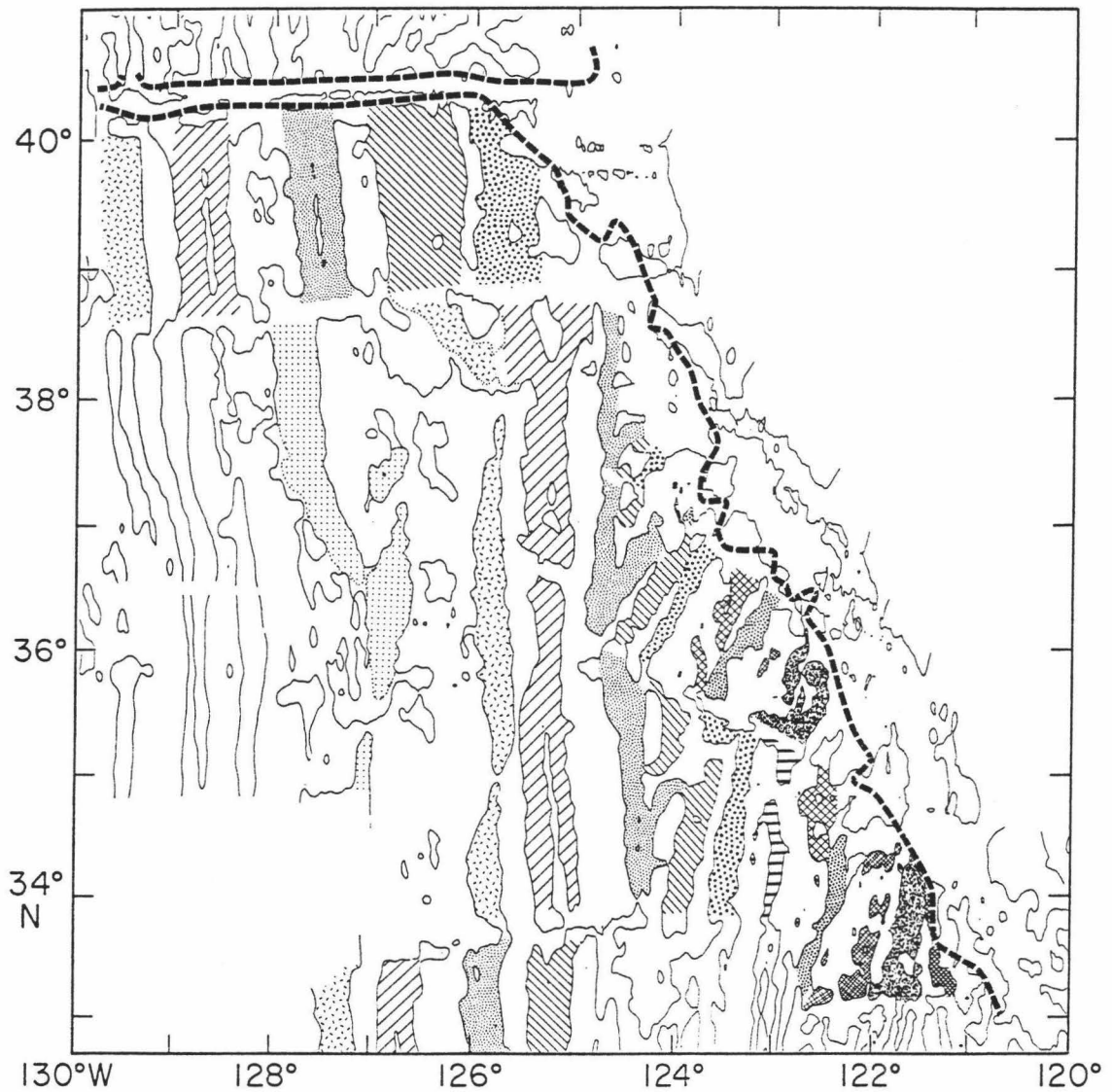


Fig. 14. Magnetic anomaly interpretation. The -100 nT contour was considered to best summarize the magnetic anomaly pattern (solid contour), however, in areas south of the Pioneer FZ near chrons 12 and 13, the 0 nT contour (dotted contour) corresponded more closely to the reversal boundary. Only positive anomalies (greater than -100 nT) with an amplitude greater than 100 nT are shaded. Refer to Figure 13 to correlate shadings and anomaly identifications.

reorganization of the Pacific-Farallon spreading center north of the Mendocino FZ by Caress et al. (1988). For this project, the program was employed to test ideas about the tectonic evolution of the Pacific-Farallon spreading system between the Murray and Mendocino fracture zones as it approached the North American trench. The program, with a specified starting plate boundary configuration, connects the ridges, approximated as a succession of arbitrarily oriented great circle segments, to transform faults, simulated as small circles about the rotation pole, and advances through time using the given stage rotation poles of relative motion and other parameters that change the ridge configuration. Isochrons, generated on each plate at specified times, usually anomaly-bounding reversals or convenient time increments, are represented as sequences of uniformly spaced points originating along the ridges moving incrementally by the given finite rotations to their final positions. The rotation pole coordinate system is used for the entire system to ease computation, resulting in rotations incurring equal but opposite shifts to the two plates. Thus, for symmetric spreading, the ridge is fixed in these coordinates. For further details regarding this program see Wilson et al. (1984).

The object of this analytical technique is to fit the synthetic isochron model to the observed isochron pattern as accurately as possible. Rotation poles, starting configuration, and propagation parameters, including rates, angle changes, and the initiation of new propagators, are varied until an acceptable agreement to all available data is achieved simultaneously. Limitations of the program resulted in several problems. Namely, the program could only model the spreading of two plates at any single time. Tectonic complexities such as overlapping spreading centers, duelling propagators, and microplates, could not be emulated. In the region between the Murray and Mendocino fracture zones, the Farallon plate broke up into numerous smaller plates as the Pacific-Farallon spreading center approached North America. As a result, the spreading of each new plate system had to be modelled separately, each

producing a separate set of model parameters. The pieces were then 'pasted' together for each time reconstruction.

For the stage pole sequence, the most difficult parameter to obtain, I began with poles from Wilson (1988), adjusting them from the Harland et al. (1982) time scale, utilized by Wilson, to the Kent and Gradstein (1986) scale. However, these poles generally did not fit the data because they represent Vancouver plate motion north of the Pioneer FZ (Menard, 1978) and not the motion of the more southern Farallon plate. These poles were adjusted by trial and error until a series of stage poles were found that produced a set of synthetic isochrons which agreed with the data in areas where no rift propagation had occurred. For stage poles between chrons 13 and 10, the Wilson (1988) pole for this time interval was adjusted slightly. However, after chron 10 when the Farallon plate broke up, the stage poles were completely different. For the region between the Pioneer and Mendocino fracture zones (Pacific-Vancouver relative plate motion), the Wilson (1988) pole was utilized until just before chron 8 (27.95 Ma) at which time a new pole was used.

The angular rates for the rotation poles were estimated by modelling isochron sequences unaffected by ridge jumps, and the location of the pole was determined by matching fracture zone trends. The southern fracture zone of each piece of lithosphere was considered to govern the location of its rotation pole. For example, the pole locations for Pacific-Farallon spreading from chrons 13 to 10 were generally determined by the trend of the Murray FZ, while for the Pacific-Vancouver relative motion, the trend of the Pioneer FZ was used. The difference between relative motions between the Pacific-Farallon and Pacific-Vancouver spreading directions caused some tension and compression along the Pioneer transform fault. The details of the passage of the RFF (ridge-fault-fault) triple junction along the Pioneer transform fault and the corresponding plate motions are discussed below. For each of the microplates after chron 10, the southern fracture zone trends were utilized causing

some misfit in the northern fracture zones which has been interpreted to be compression or extension accordingly. The poles used, although concurring with the magnetics, probably have large uncertainties but are adequate for the tectonic analysis.

Once a satisfactory sequence of rotation poles was established, the initial configuration of each ridge was determined. The version of the program used in this study, unfortunately, has the singular option of keeping the ridge fixed in the coordinate system. Thus, the starting configurations do not correspond to the present location of the particular starting time isochron, but to a location determined by the total rotation of that chron from the starting time to the ending time of that portion of the model. A more convenient method would have been to keep the Pacific plate fixed and have the spreading ridge move away at the specified rotation rate and have the Farallon plate move away at twice that rate (similar to Wilson, 1988). Rift propagation parameters were determined by iterative trial and error using the forward modelling program to match the observed pseudofault pattern. The angle of the pseudofault depends on the ratio of spreading rate to propagation rate. In the program, the propagation rate is specified as the rate of change of the distance from the ridge tip to the rotation pole. Bends in the pseudofaults were produced by changing the spreading rate/propagation rate ratio. Although this program can simulate asymmetric spreading, for simplicity and lack of data (the Farallon plate, Vancouver plate, and microplates have been subducted), symmetric spreading was assumed. Tables 1 through 5 list the parameters used as input for the final version of the model. Figure 15 shows a summary of the model by presenting a stepwise evolution of the ridge geometry. A series of time reconstructions for the model, corresponding to the times in Figure 15, is shown in Figures 17a through 17x. The final configuration of the model, the present day situation (0 Ma), is shown in Figure 22.

TABLE 1. Model Parameters for Pacific-Farallon Spreading

Time Interval ^a	Rotation Poles		
	°N	°E	deg/Ma ^b
36.00-35.30	76.5	-140.0	0.95
35.30-33.40	76.5	-150.0	0.55
33.40-32.90	77.5	-160.0	0.55
32.90-32.25	77.5	-160.0	0.85
32.25-30.33	72.5	-125.0	0.75

Time ^a	Ridge Locations (North End, South End)			
	°N	°E	°N	°E
36.00	38.88	-125.05	37.98	-124.95
36.00	38.075	-124.215	34.055	-123.71
36.00	34.18	-124.27	33.83	-124.24
34.75	38.86	-125.185	38.82	-125.15
33.42	33.87	-124.406	33.82	-124.40
30.34	38.874	-124.82	37.44	-124.75

PR Number	Time Interval ^a	Propagation Rate (deg/m.y. ^c)	(km/m.y. ^c)
1	36.00-35.40	2.20	244
1	35.40-34.70	0.70	78
1	34.70-34.25	1.20	133
1	34.25-32.90	0.50	56
1	32.90-32.30 ^d	1.50	167
2	35.85-35.53	-3.80	-422
3	35.53-35.30	2.00	222
3	35.30-34.50	0.60	67
4	34.75-32.30 ^d	-0.32	-36
5	33.50-32.82 ^d	0.70	78
6	33.42-31.80	1.15	128
6	31.80-30.80	1.00	111
6	30.80-30.66 ^d	1.50	167
7	31.90-31.40	1.50	167
7	31.40-30.60 ^e	0.80	89
8	31.30-30.33	-2.08	-231

PR Number	Time ^a	Propagation Angle Change ^f
2	35.75	18.0
5	33.50	-25.0
1	32.70	-10.0
7	31.45	-11.5

^aAll times in Ma.

^bAngular velocity half rates.

^cPositive propagation rates are northward.

^dApproximate time that propagator intersects another propagator and stops.

^eApproximate time that propagator intersects transform fault.

^fPositive rotations are counterclockwise.

TABLE 2. Model Parameters for Pacific-Vancouver Spreading

Time Interval ^a	Rotation Poles		
	°N	°E	deg/Ma ^b
33.00-32.50	76.5	-144.0	1.20
32.50-30.30	76.5	-144.0	0.90
30.30-29.70	76.5	-144.0	1.05
29.70-29.20	76.5	-144.0	0.90
29.20-27.95	76.5	-144.0	1.00
27.95-25.00 ^c	76.5	-130.0	1.00

Time ^a	Ridge Locations (North End, South End)			
	°N	°E	°N	°E
33.00	40.46	-123.80	38.93	-123.55
27.95	38.975	-123.85	38.925	-123.849

PR Number	Time Interval ^a	Propagation Rate (deg/m.y. ^d)	(km/m.y. ^d)
14	27.95-27.80 ^e	10.0	1110

^aAll times in Ma.

^bAngular velocity half rates.

^cArbitrary time for Pacific-Vancouver spreading termination.

^dPositive propagation rates are northward.

^eApproximate time that propagator intersects transform fault.

TABLE 3. Model Parameters for Pacific-Arguello Spreading

Time Interval ^a	Rotation Poles		
	°N	°E	deg/Ma ^b
30.33-30.00	72.5	-125.0	0.50
30.00-28.50	72.5	-125.0	0.40
28.50-27.00	70.0	-120.0	0.40
27.00-25.50	70.0	-110.0	0.50
25.50-23.00	70.0	-110.0	0.25
23.00-22.50	70.0	-110.0	0.50
22.50-20.25	72.5	-130.0	0.50
20.25-19.10	72.5	-130.0	0.60
19.10-16.00 ^c	72.5	-130.0	0.30

Time ^a	Ridge Locations (North End, South End)			
	°N	°E	°N	°E
30.33	36.15	-120.55	33.82	-120.17
30.05	34.30	-120.178	34.25	-120.19
26.90	35.474	-120.08	35.423	-120.084
24.10	33.87	-120.335	33.82	-120.36
21.45	33.22	-120.665	33.17	-120.68
19.80	33.22	-120.683	33.17	-120.68

PR Number	Time Interval ^a	Propagation Rate	
		(deg/m.y. ^d)	(km/m.y. ^d)
12	30.05-29.40	1.00	111
12	29.40-27.0 ^e	0.20	22
13	30.05-29.18 ^e	-0.50	-56
15	26.90-25.50	-0.50	-56
15	25.50-23.94	-0.30	-33
15	23.94-22.60	-0.25	-28
17	24.10-23.94 ^f	2.50	278
18	24.10-23.00	-0.25	-28
18	23.00-22.32	-0.45	50
19	22.60-21.9 ^e	1.20	133
20	21.45-20.0 ^e	1.00	111
21	19.80-18.5 ^e	1.00	111

^aAll times in Ma.

^bAngular velocity half rates.

^cArbitrary time for Pacific-Arguello spreading termination.

^dPositive propagation rates are northward.

^eApproximate time that propagator intersects transform fault.

^fApproximate time that propagator intersects another propagator and stops.

TABLE 4. Model Parameters for Pacific-Monterey Spreading

Time Interval ^a	Rotation Poles		
	°N	°E	deg/Ma ^b
30.33-29.60	60.0	-96.0	0.50
29.60-24.15	60.0	-96.0	0.32
24.15-22.50	60.0	-96.0	0.50
22.50-19.00 ^c	60.0	-96.0	0.30

Time ^a	Ridge Locations (North End, South End)			
	°N	°E	°N	°E
30.33	36.506	-122.62	35.006	-122.78
30.05	35.289	-122.725	35.239	-122.759
25.50	36.375	-122.311	36.335	-122.338

PR Number	Time Interval ^a	Propagation Rate (deg/m.y. ^d) (km/m.y. ^d)	
11	30.05-28.67 ^e	0.80	89
16	25.50-25.17 ^e	-3.50	389

^aAll times in Ma.

^bAngular velocity half rates.

^cPacific-Monterey spreading termination leaving dead ridge.

^dPositive propagation rates are northward.

^eApproximate time that propagator intersects transform fault.

TABLE 5. Model Parameters for Pacific-Reyes Spreading

Time Interval ^a	Rotation Poles		
	°N	°E	deg/Ma ^b
30.33-29.75	60.0	-90.0	0.35
29.75-24.25	60.0	-90.0	0.17
24.25-20.45 ^c	60.0	-90.0	0.25

Time ^a	Ridge Locations (North End, South End)			
	°N	°E	°N	°E
30.33	38.302	-123.687	36.856	-123.59
30.05	36.914	-123.58	36.864	-123.61

PR Number	Time Interval ^a	Propagation Rate	
		(deg/m.y. ^d)	(km/m.y. ^d)
9	30.33-29.75	0.08	9
9	29.75-24.25	0.04	4
9	24.25-20.45 ^c	0.06	7
10	30.05-29.10	0.35	39
10	29.10-20.45 ^c	0.08	9

^aAll times in Ma.

^bAngular velocity half rates.

^cArbitrary time for Pacific-Reyes spreading termination.

^dPositive propagation rates are northward.

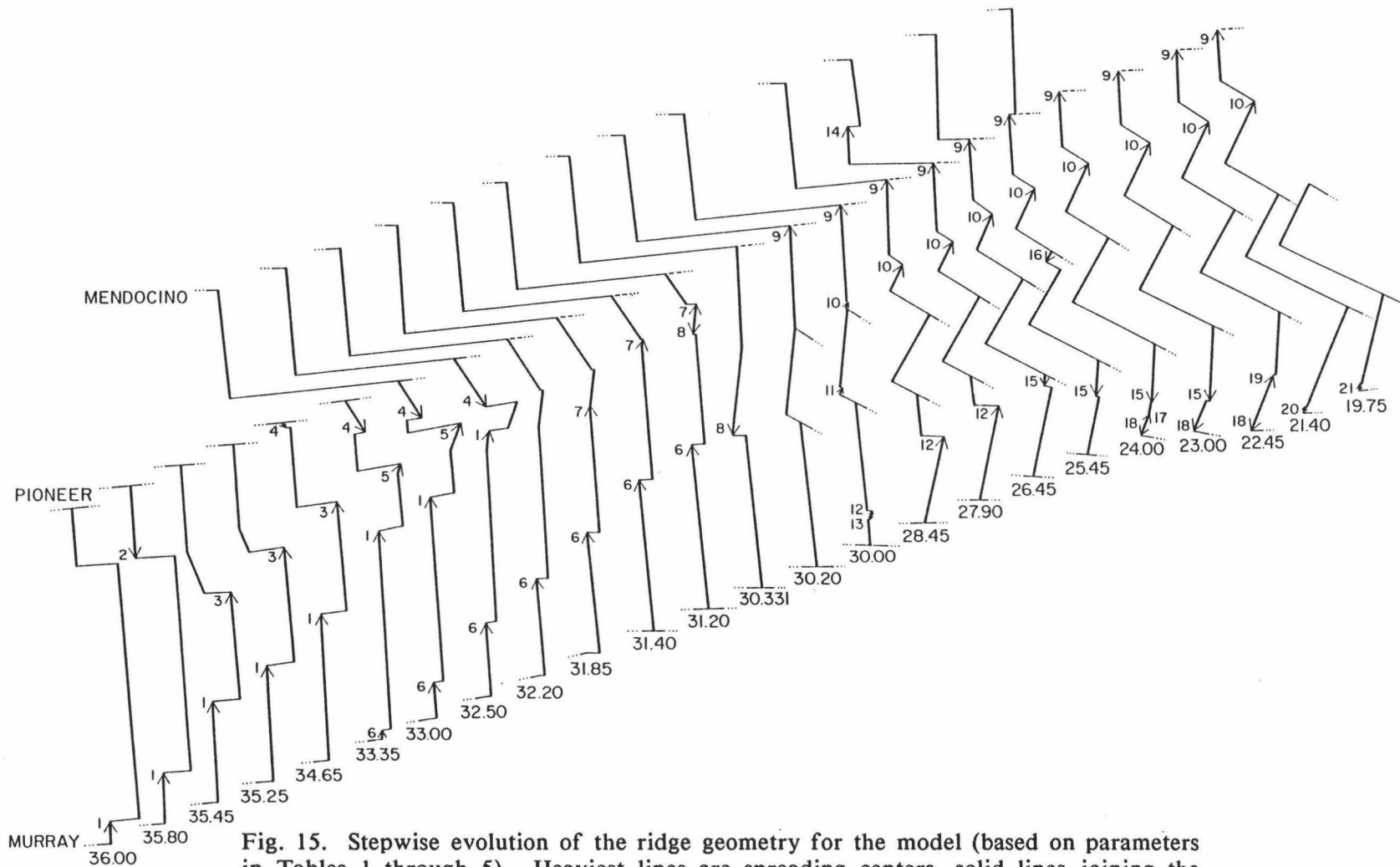


Fig. 15. Stepwise evolution of the ridge geometry for the model (based on parameters in Tables 1 through 5). Heaviest lines are spreading centers, solid lines joining the spreading centers are transform faults. Propagation episodes are numbered as in Tables 1 through 5. The dashed lines represent extensional sections of the Pioneer transform. Continuation of active transforms beyond the ridges is indicated by three dots.

IV. THE MODEL

The model for the tectonic evolution of the area between the Murray and Mendocino fracture zones was started just before chron 13, at 36 Ma, corresponding to the age of the oldest seafloor within the area constrained by the Raff-Mason data. At that time, the Farallon plate had already broken into at least two large plates, the Vancouver plate to the north and the Farallon to the south (Menard, 1978; Rosa and Molnar, 1988). This break was completed by chron 21, approximately 48 Ma (Atwater, 1989). The location of the Vancouver-Farallon plate boundary is questionable. Originally, it was placed at the Murray transform fault by Menard (1978), but Atwater (1989) has argued that the boundary was south of the Pioneer by about 1.5 to 2 degrees, defined by a set of "curving toothlike disjunctures" which was the trace of the RFF triple junction. Nevertheless, for simplicity and consistency with spreading rates determined from the Raff-Mason data, I have followed Rosa and Molnar (1988) and have treated the Pioneer transform as the boundary. Thus, from chrons 13 to 10 (approximately 36 to 30.3 Ma), there were two individual plates within the study area spreading with the Pacific plate, the Vancouver and the Farallon, whose spreading center systems were modelled separately. A cartoon of the plate boundary configuration at 36 Ma, just prior to chron 13, is shown in Figure 16.

The initial configuration of the Pacific-Farallon spreading system (Figure 17a) has three ridge segments, with the southern one propagating to the north (PR 1). Table 1 lists the model parameters for the Pacific-Farallon portion of the model. Near the beginning of chron 13 (35.85 Ma), the northern segment began to propagate south (PR 2; Figure 17b). This propagator may or may not have existed prior to chron 13, where it becomes apparent on the contour map (Figures 11 and 14). At 35.75 Ma, this southward propagator (PR 2) rotated 18° counterclockwise (a positive angle change) and formed the arresting bend in chron 13 (Figure 18a). It continued to propagate

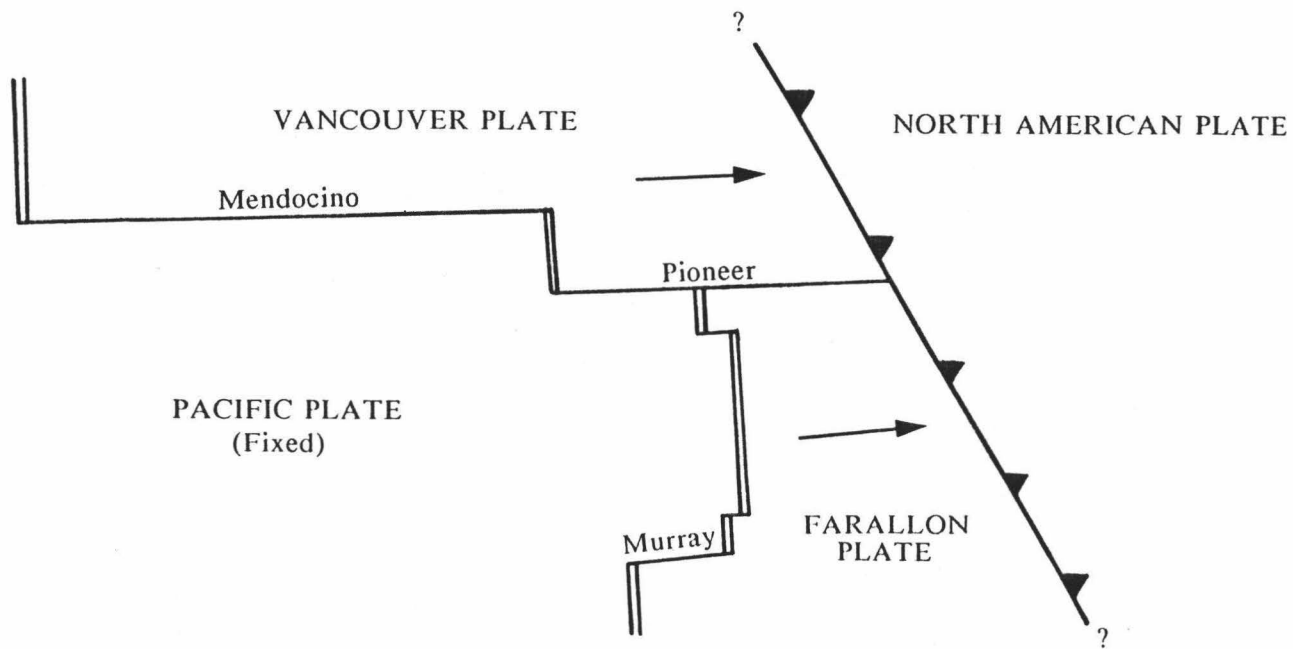
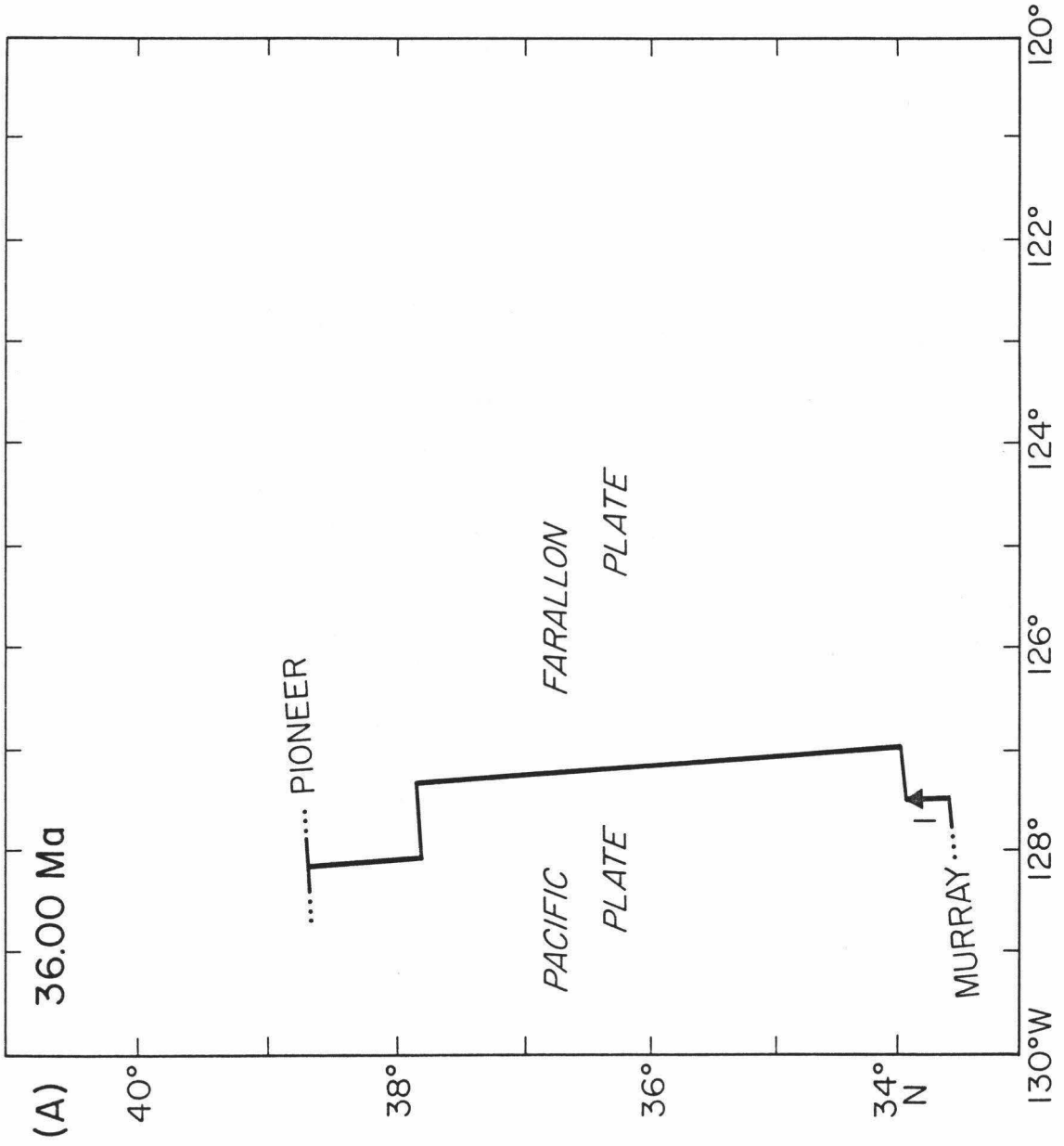
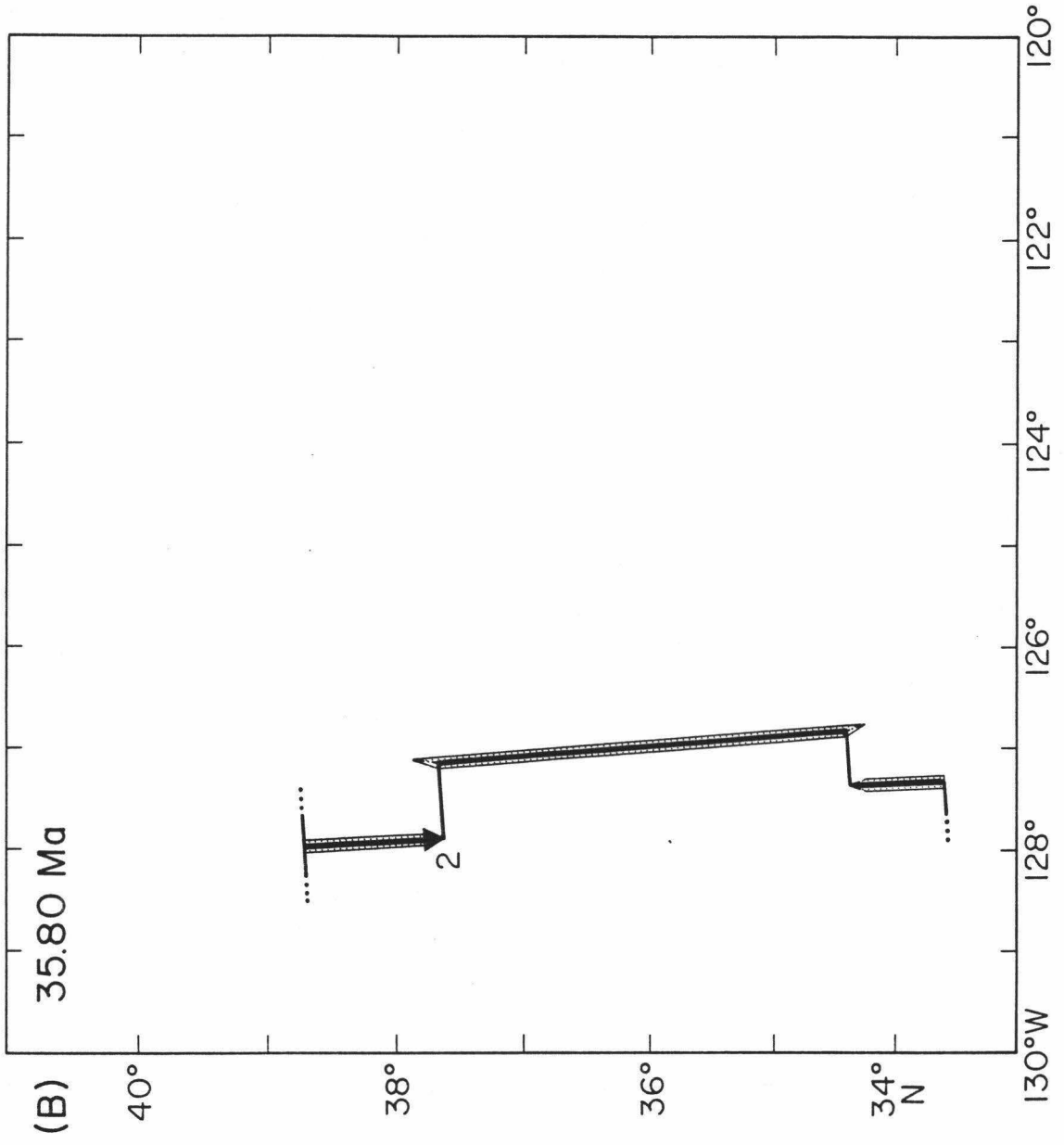
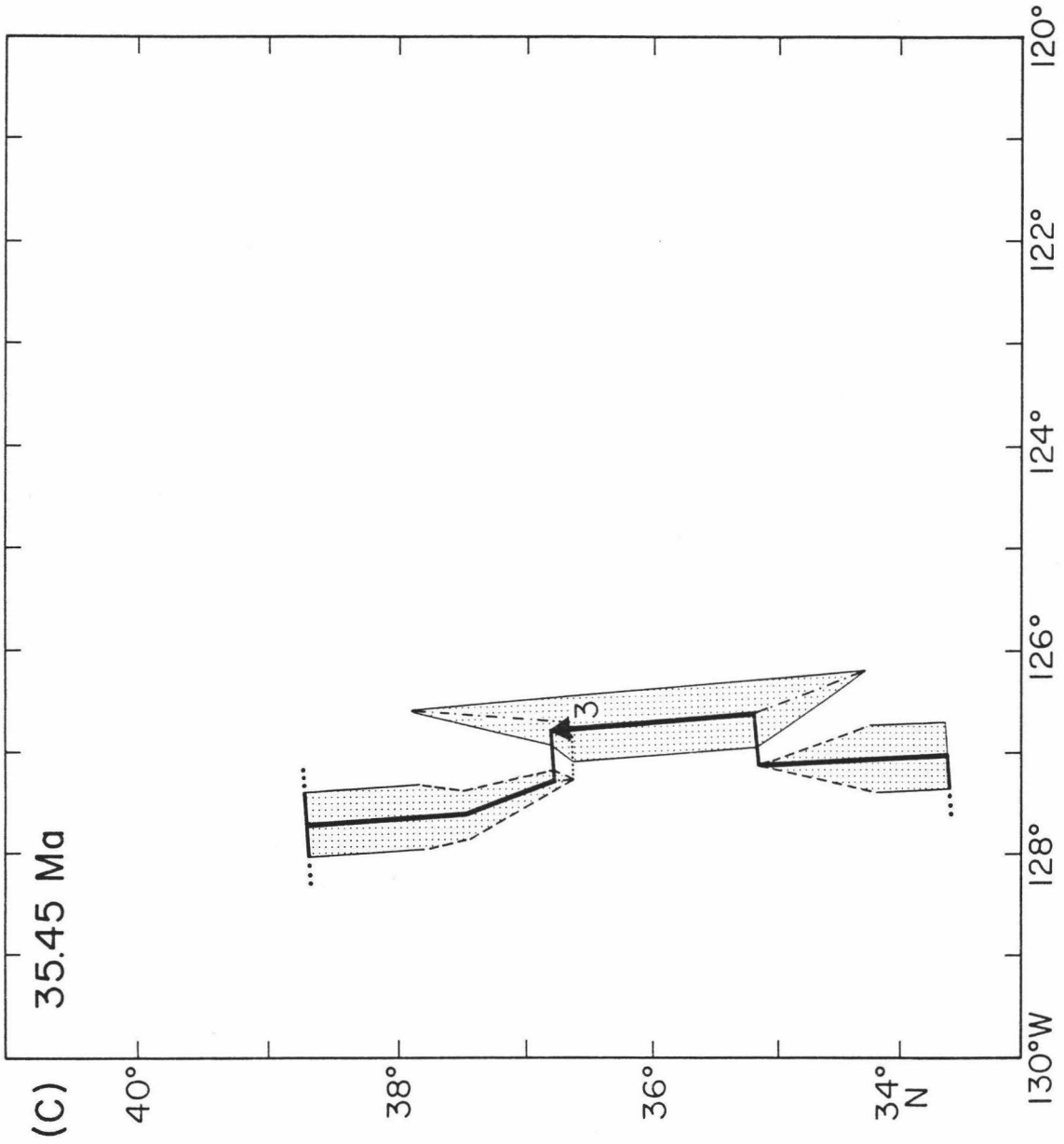


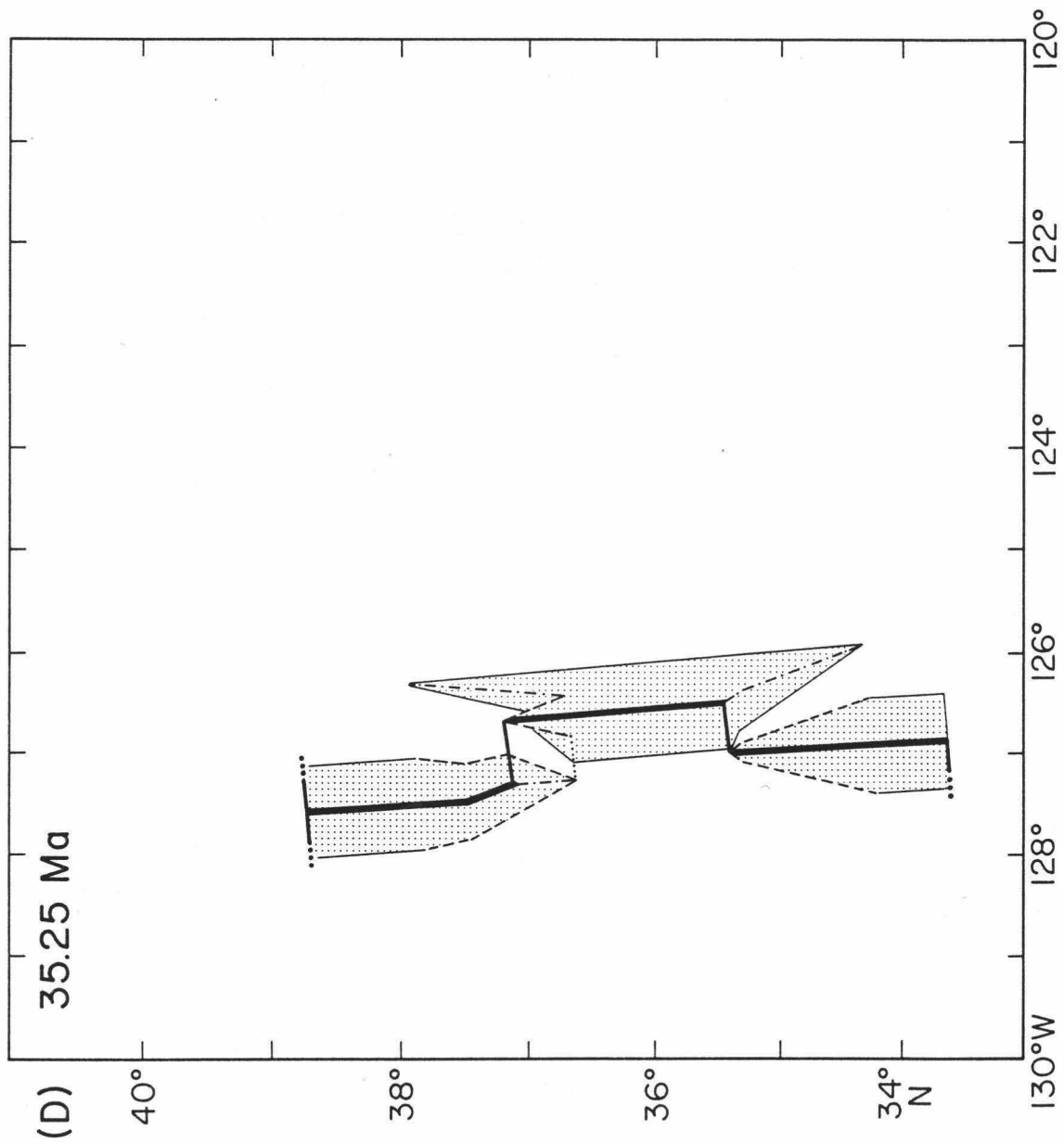
Fig. 16. Cartoon of the plate boundary configuration at 36 Ma, just prior to chron 13. Solid lines are active transform faults, spreading centers are shown by solid, double lines, and subduction is indicated by the sawtoothed line. Arrows represent approximate plate motion with respect to the Pacific plate which is arbitrarily held fixed.

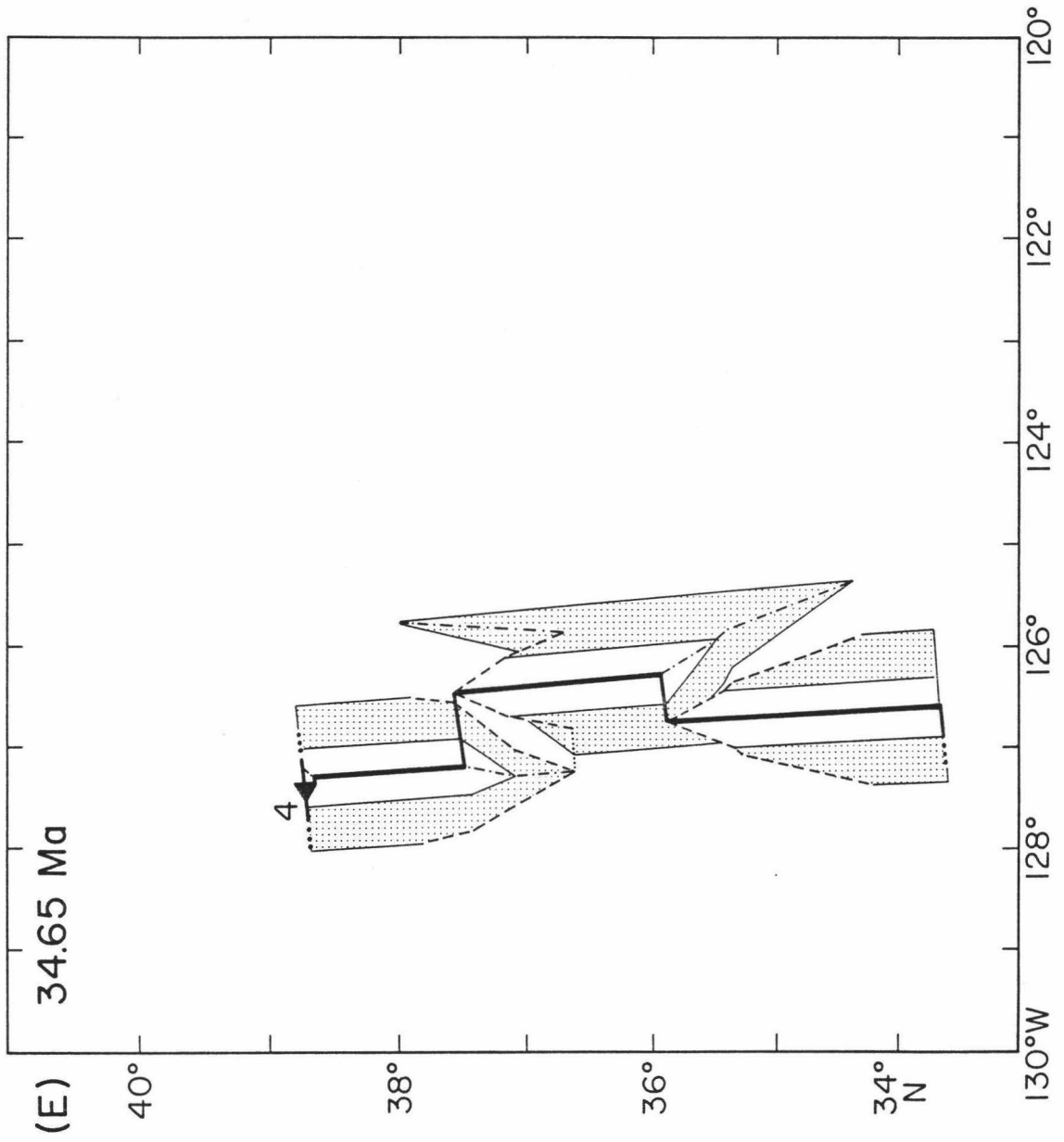
Fig. 17. Step-by-step evolution of the model. Heaviest lines are spreading centers, heavy lines joining spreading centers are transform faults, light lines are fracture zones, dashed lines are pseudofaults, dot-dashed lines are failed rifts, short dashed lines are abandoned transforms, and light dotted lines are transferred lithosphere boundaries. Continuation of active transforms beyond the ridges is indicated by three heavy dots. For Figures 15f through 15l, the region north of the long dashed horizontal line (extension of the Pioneer transform fault) experienced shortening. Heavy dashed lines represent extensional sections of the Pioneer transform. Reconstructions were assembled at the present day coordinates with the Pacific plate fixed. The current North American continental margin is shown (thickest dashed line) after 30.33 Ma for reference only. It approximates the 3000 m bathymetric contour (Chase et al., 1981). Isochrons are shaded according to Figure 13. Initiation of new propagation episodes are indicated by solid arrows; they are numbered according to Tables 1 through 5. Plate labels are in italics.

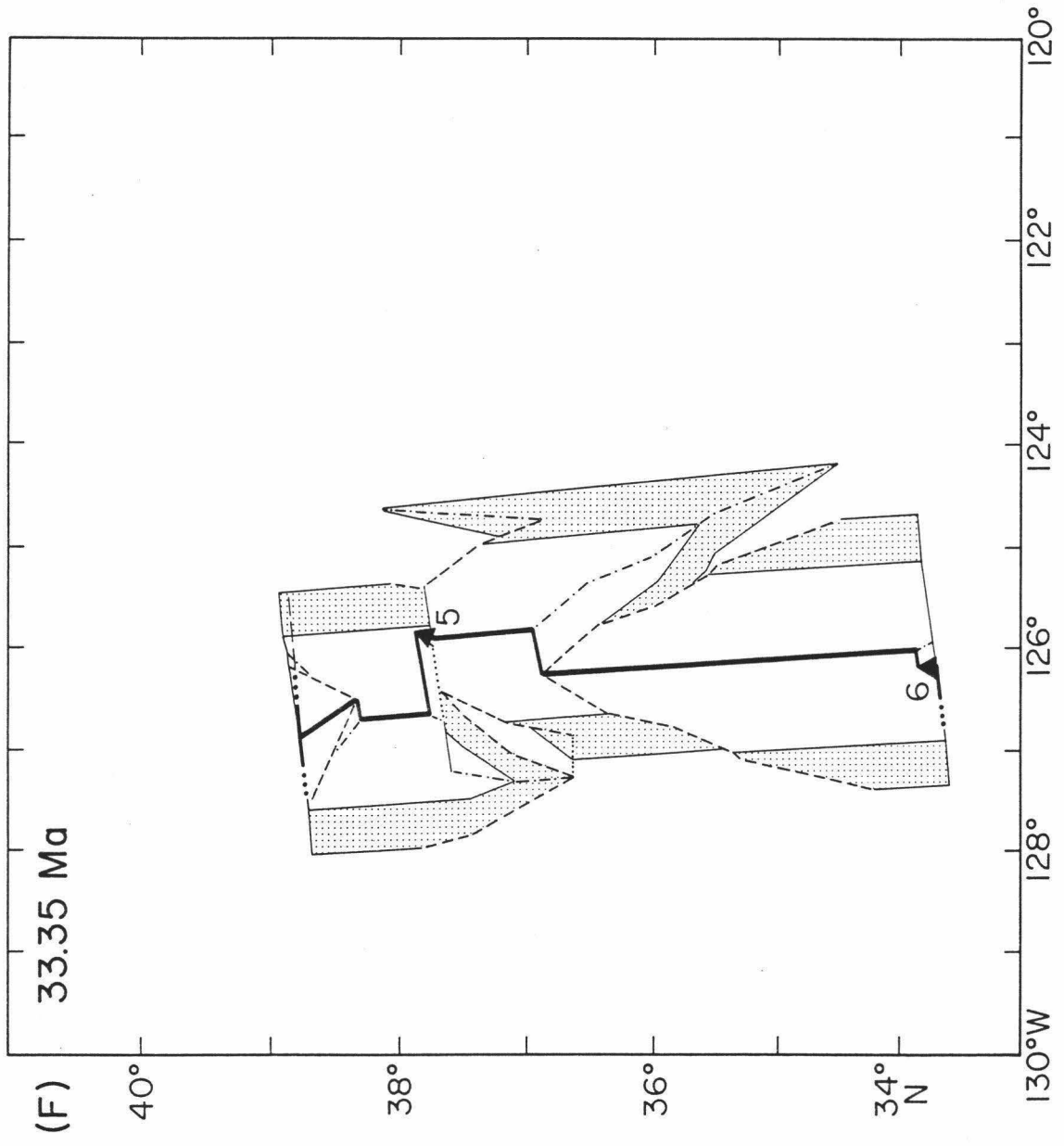


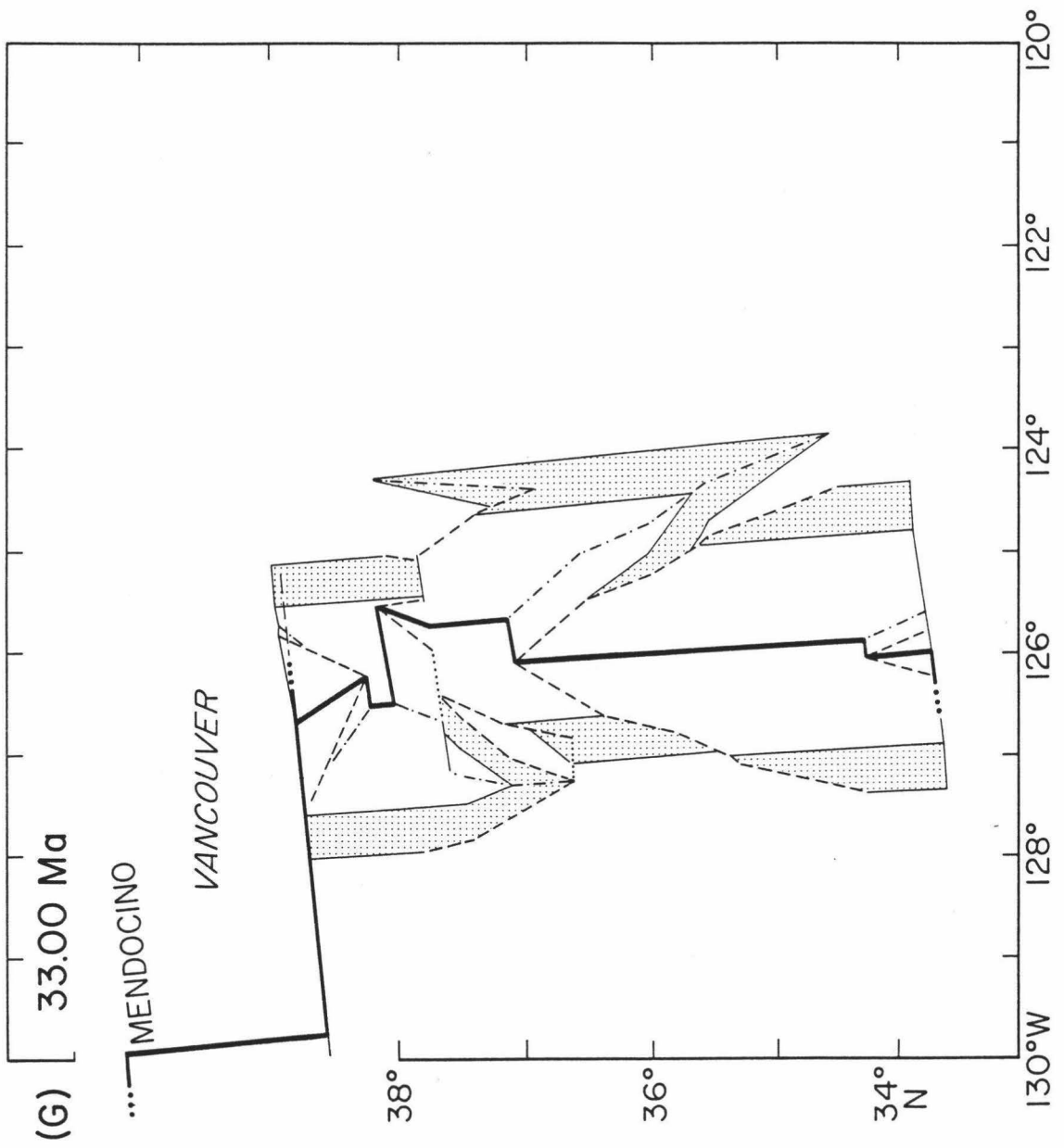


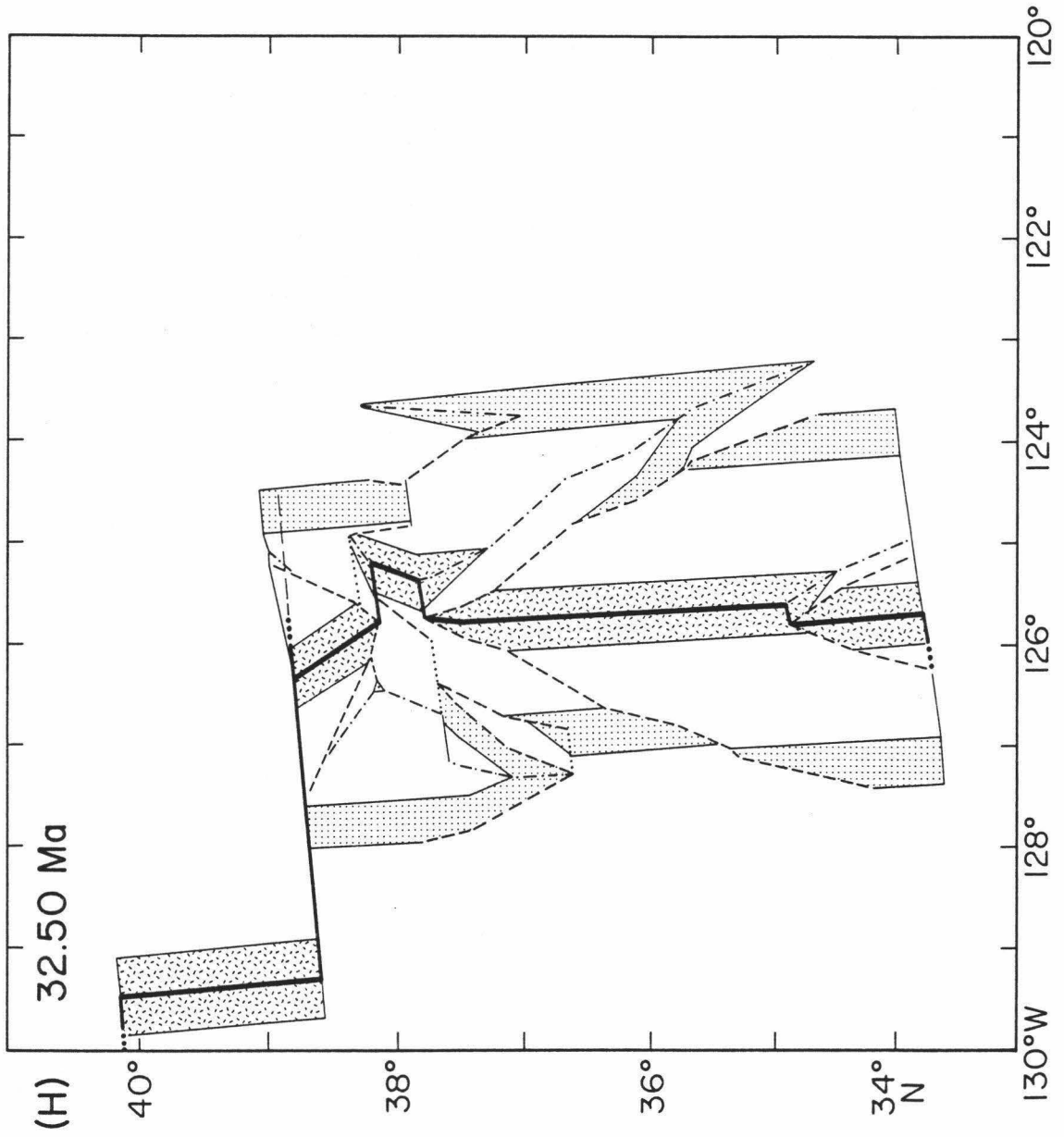


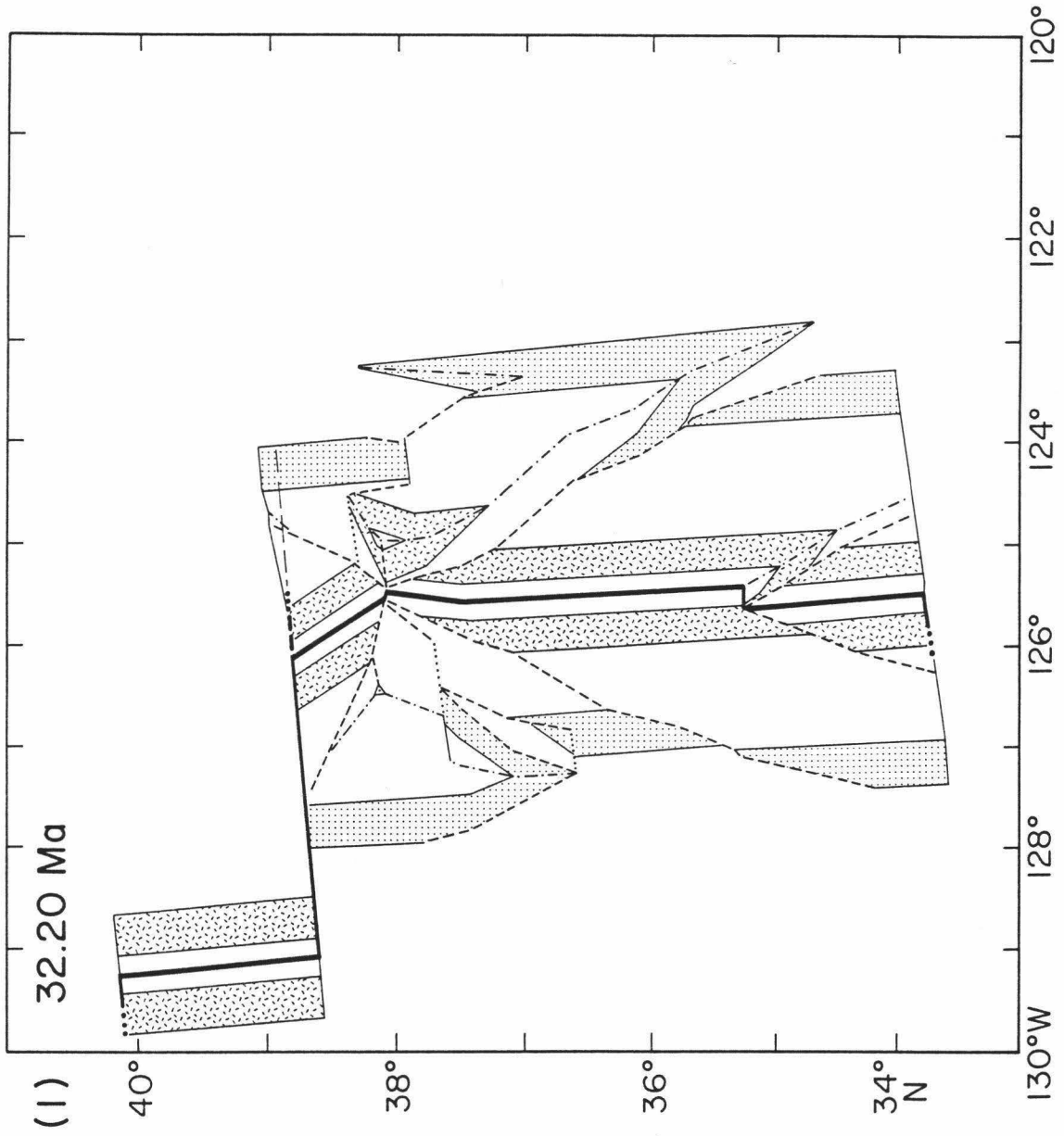


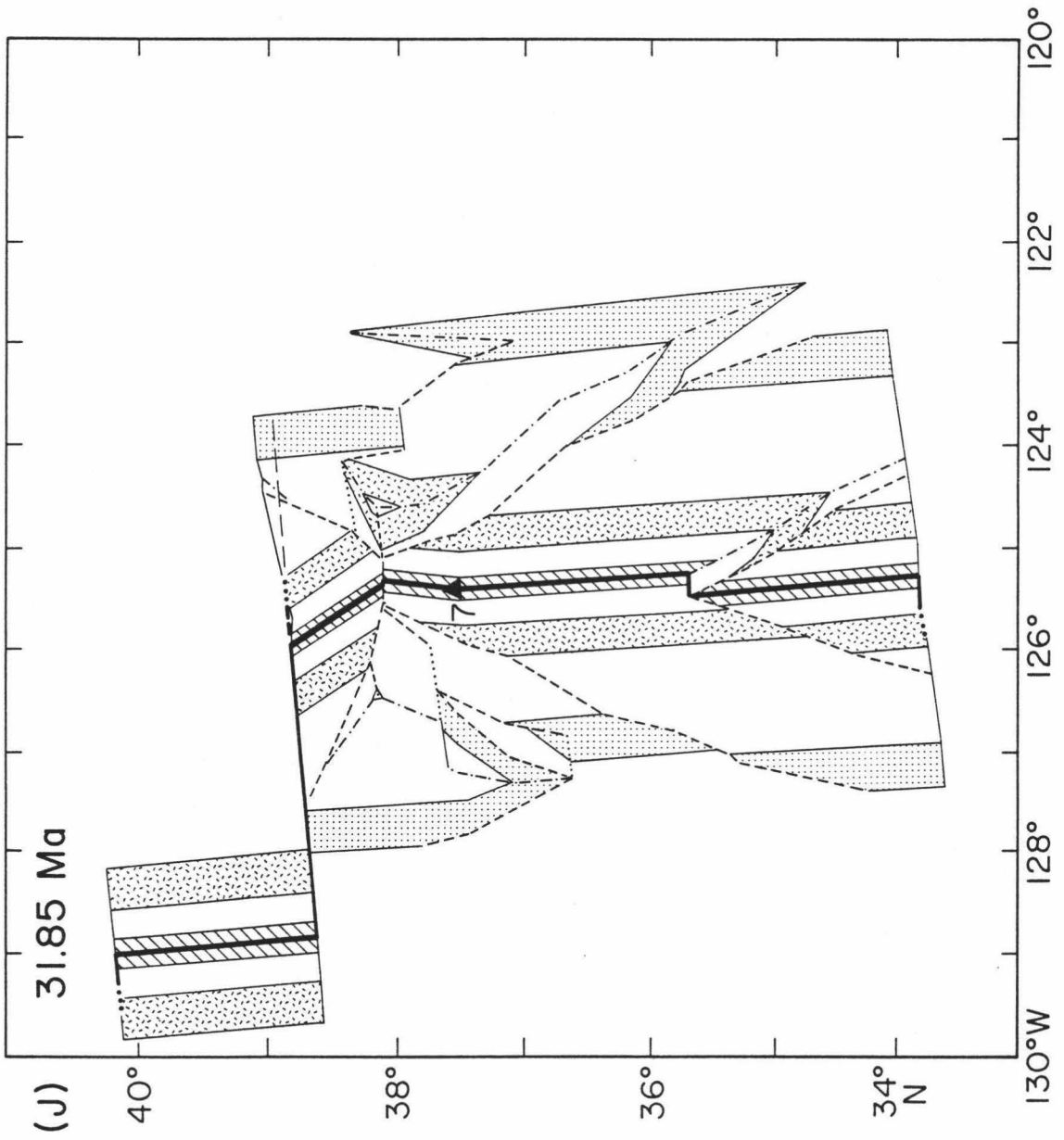


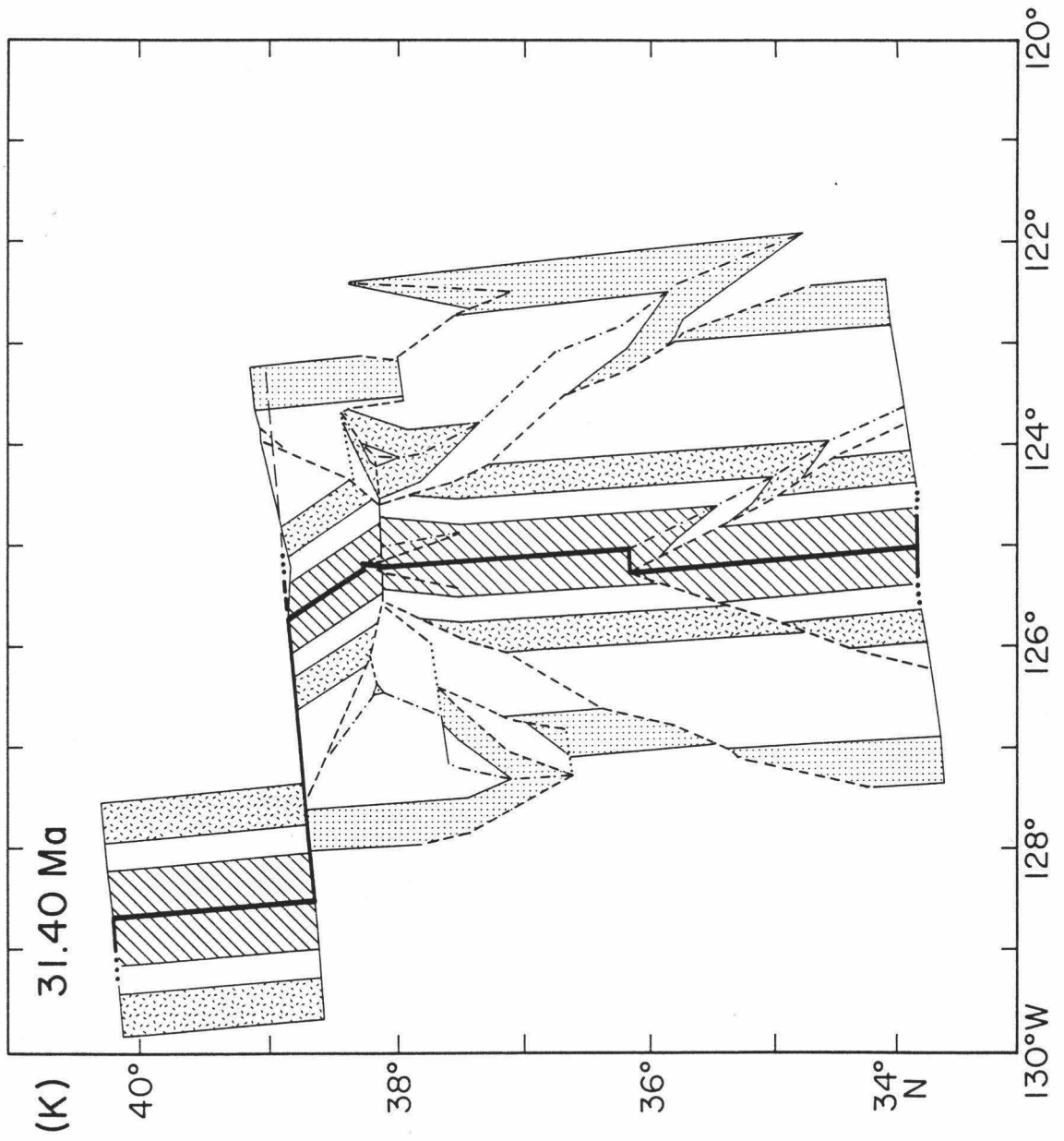


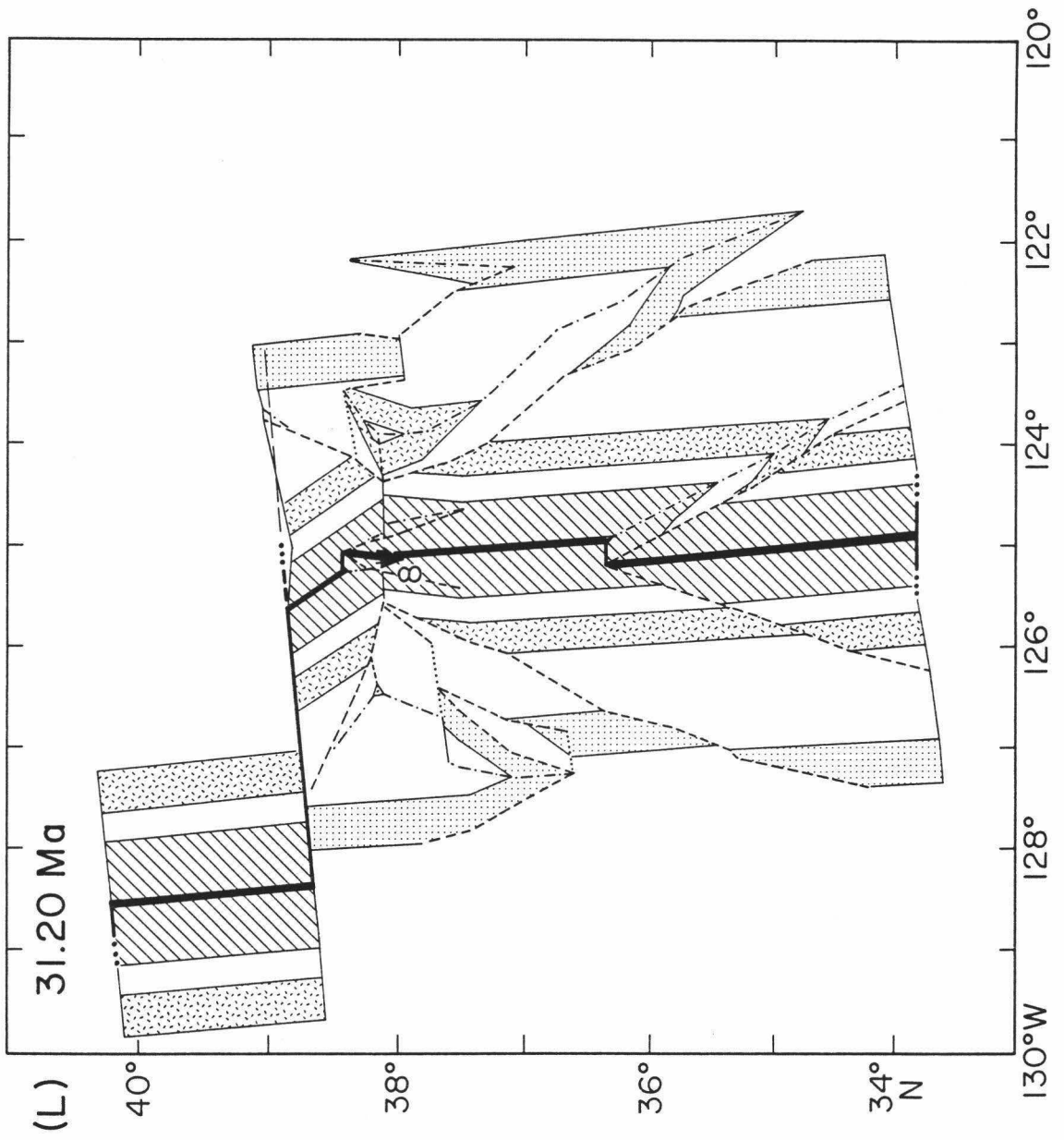


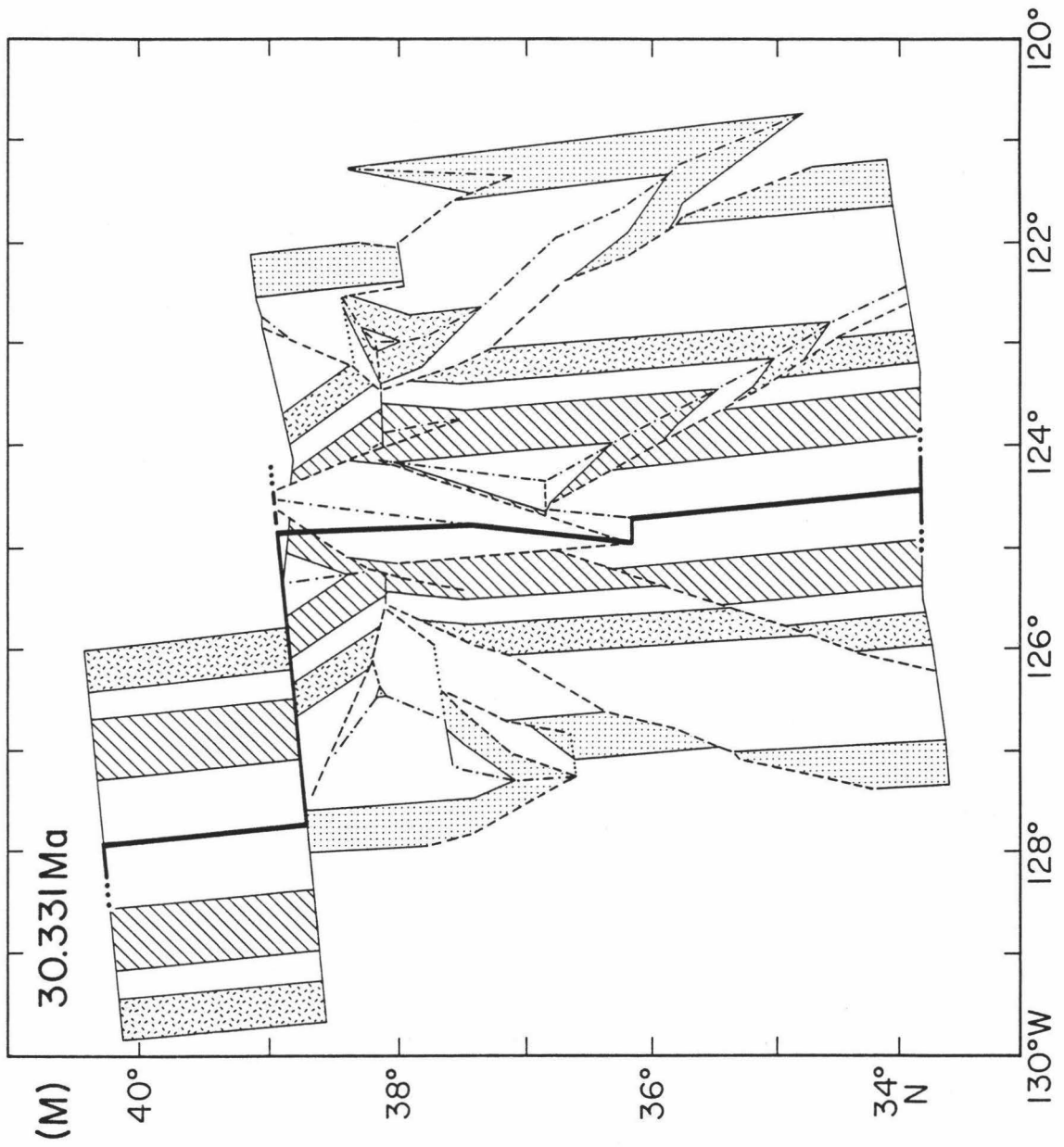


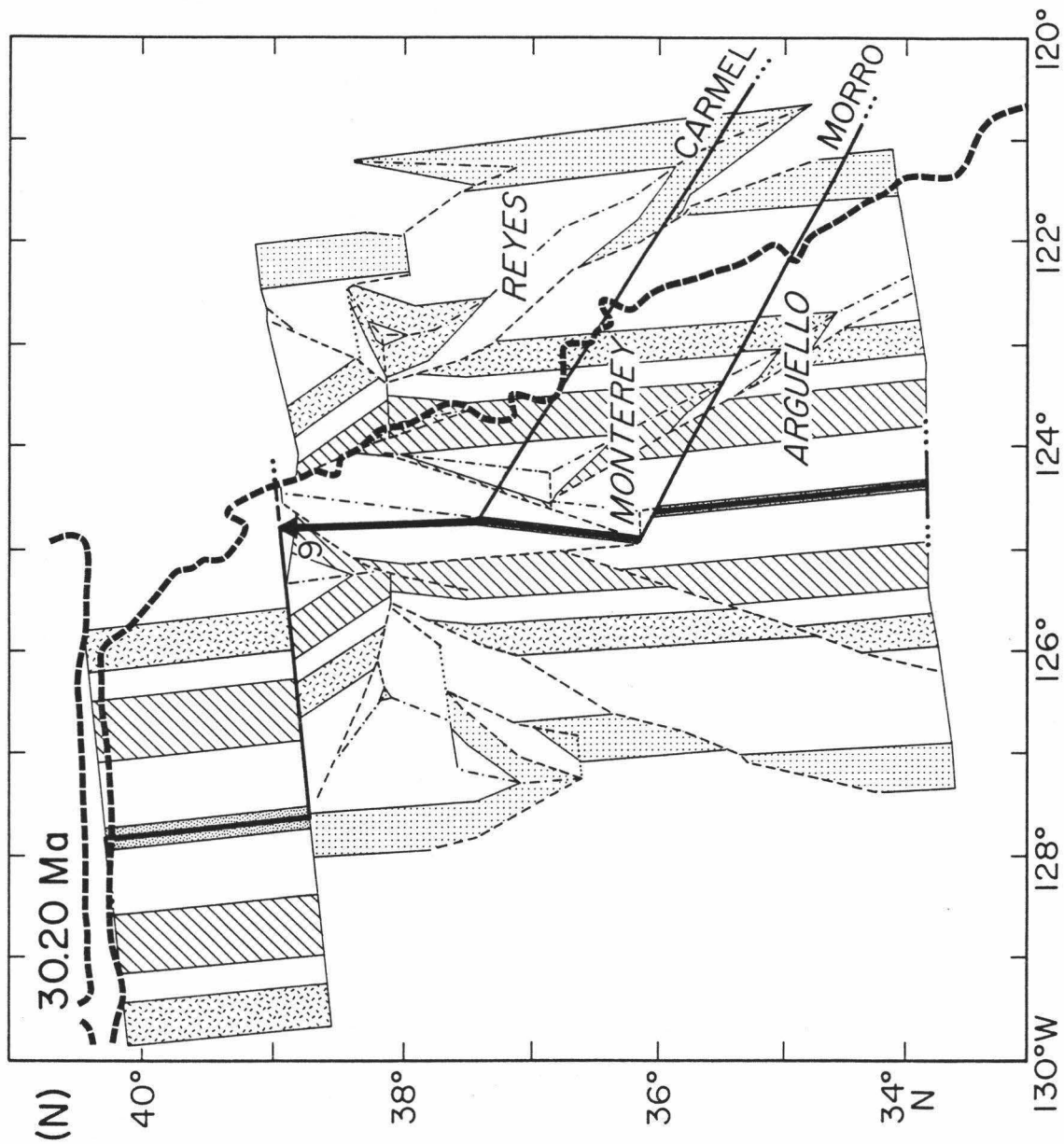


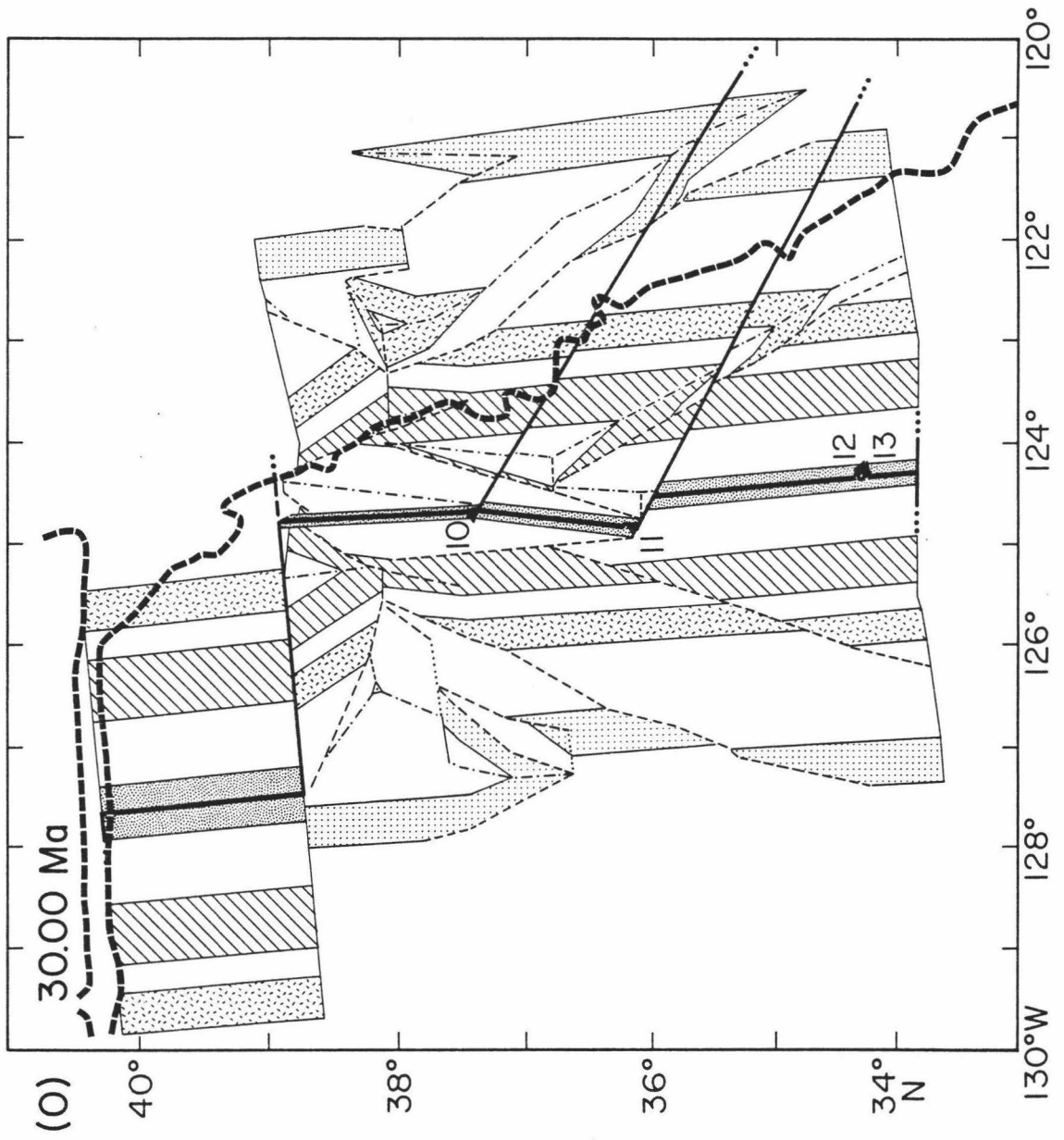


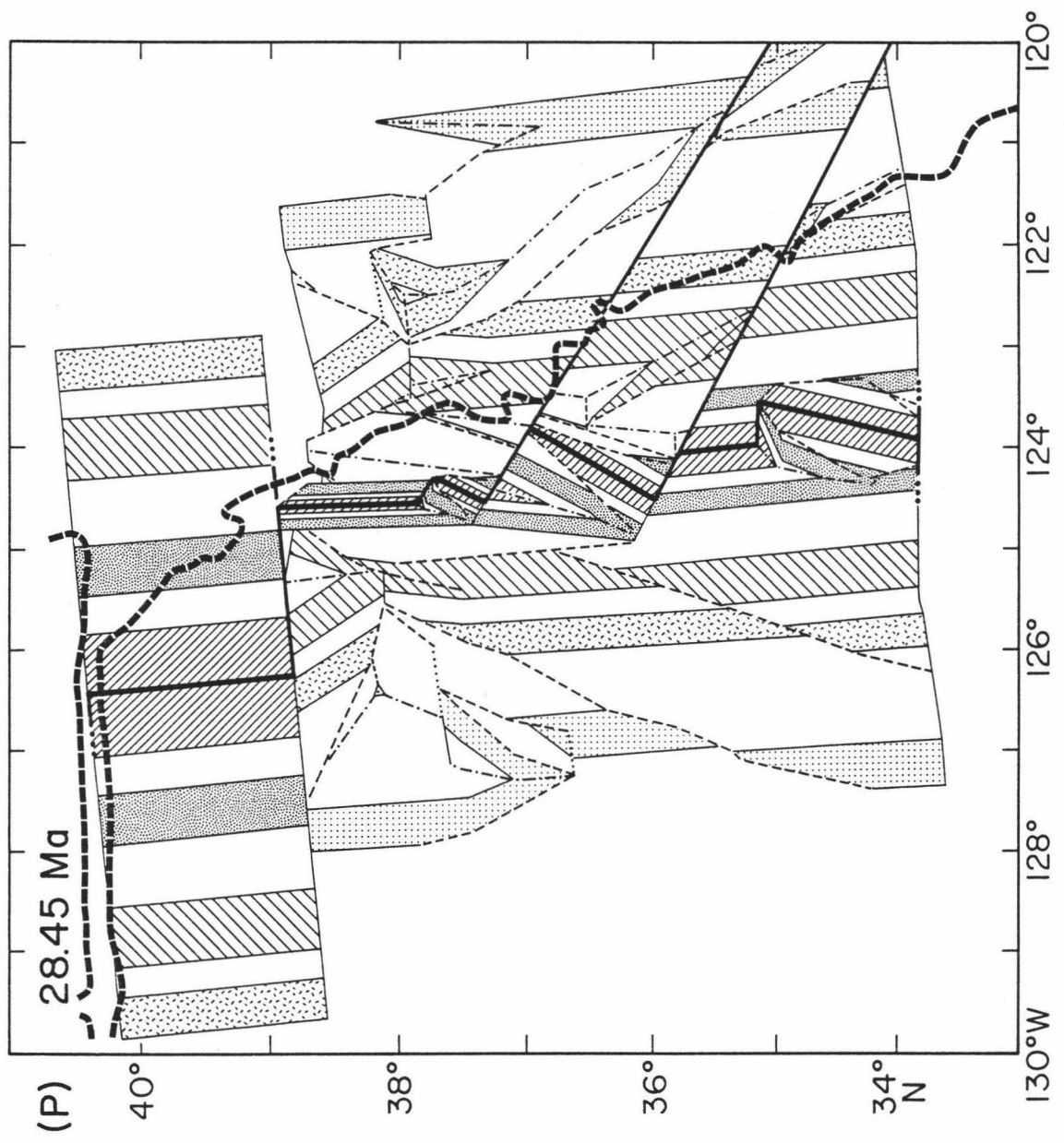


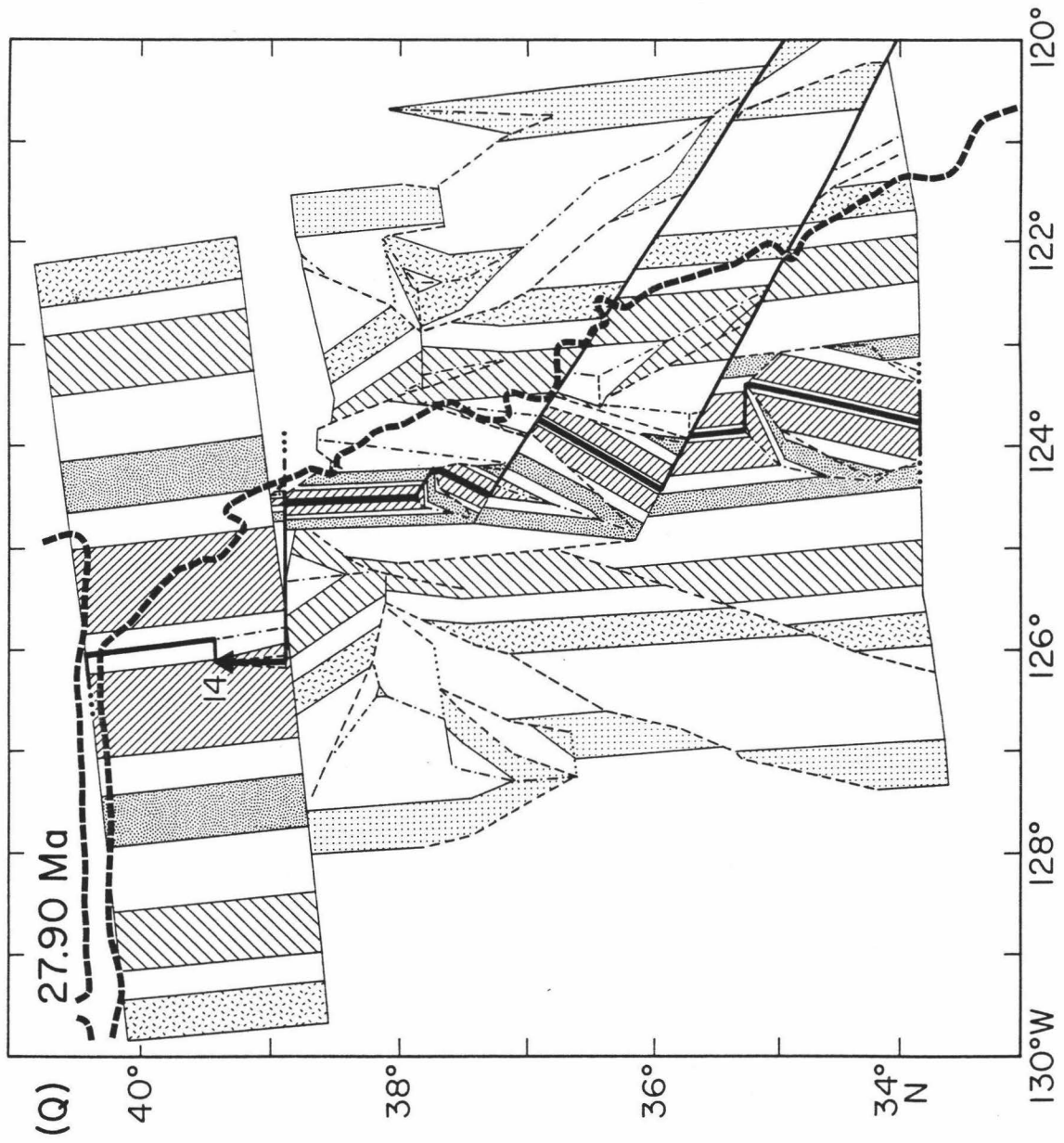


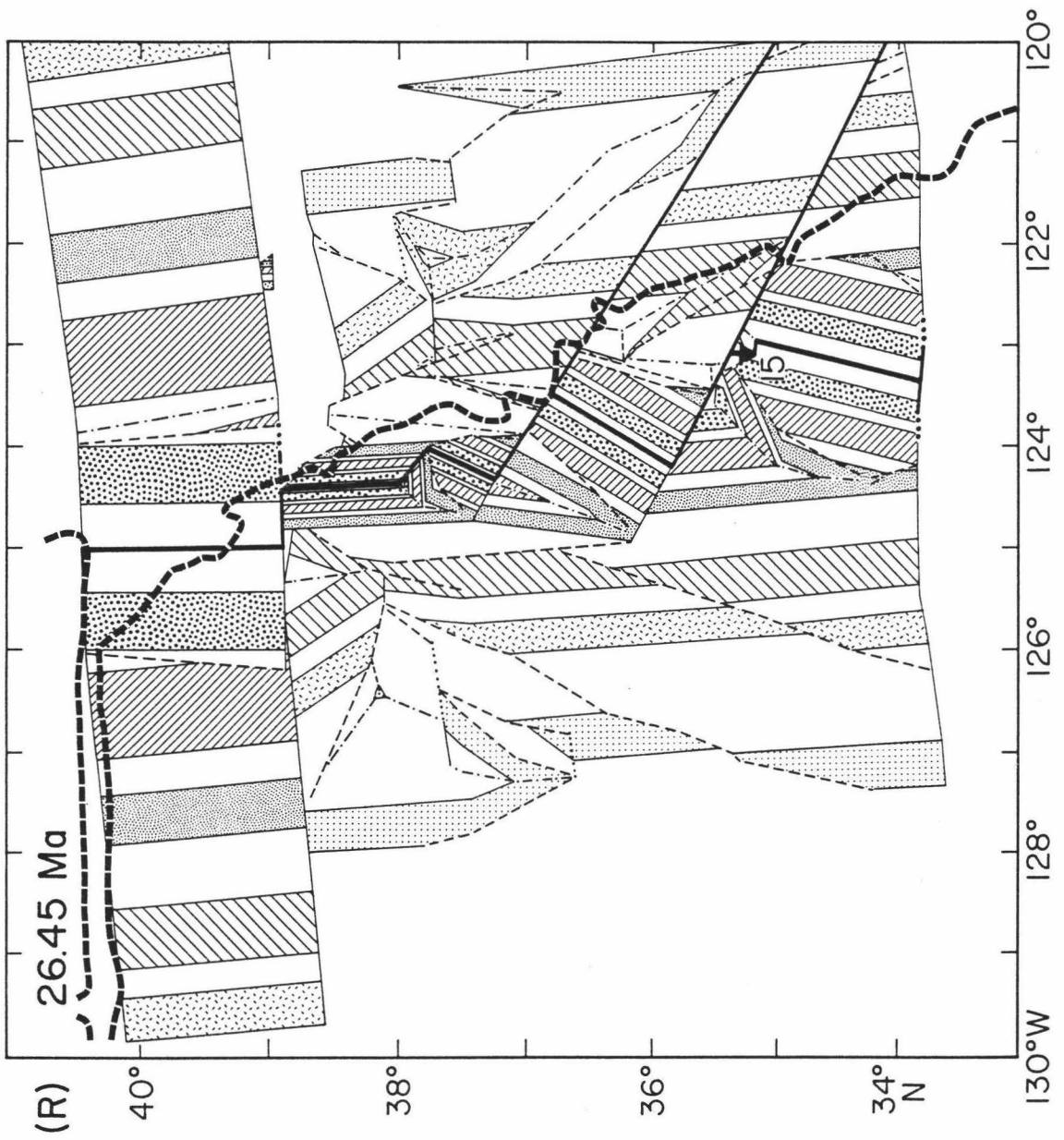


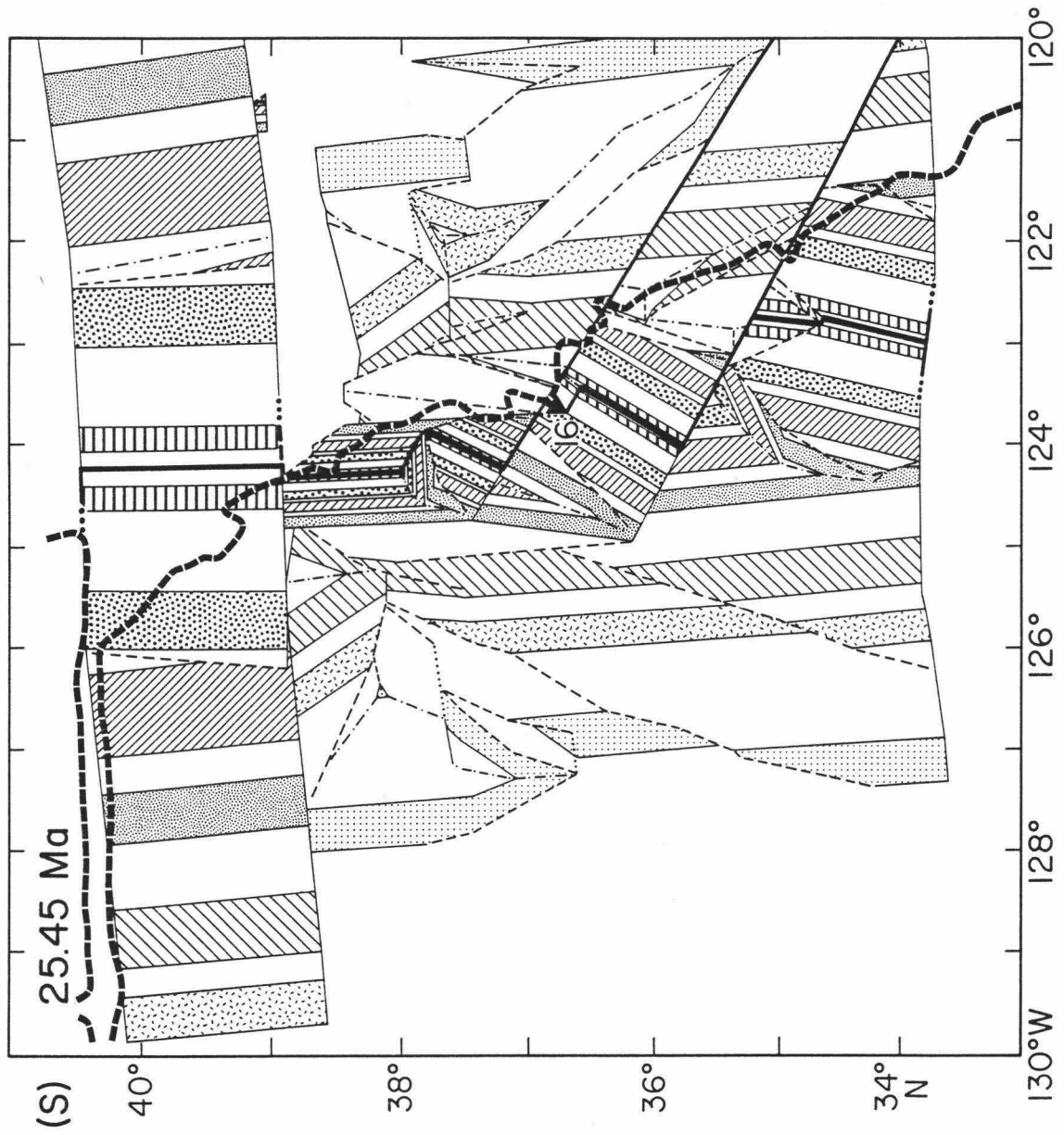


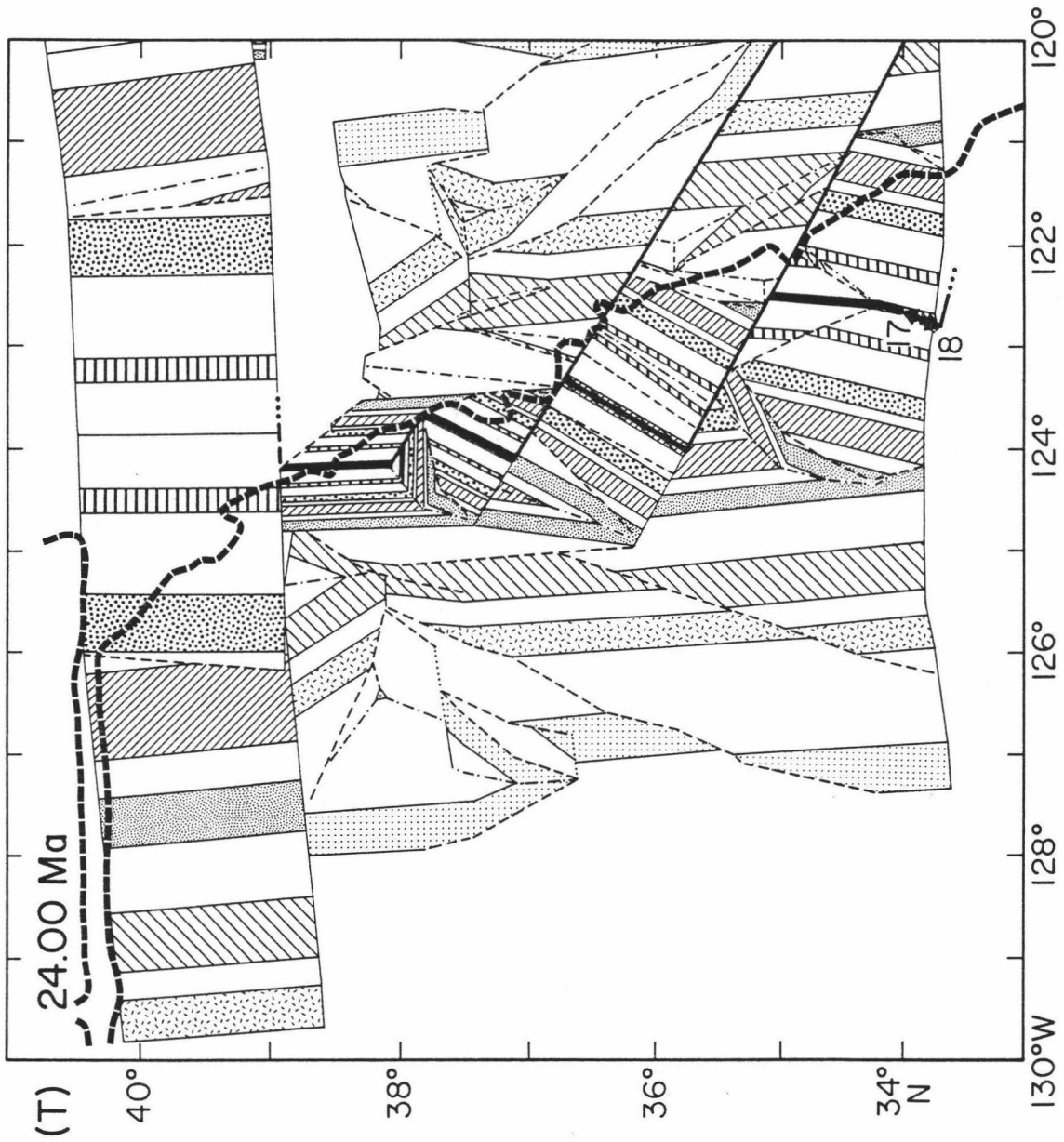


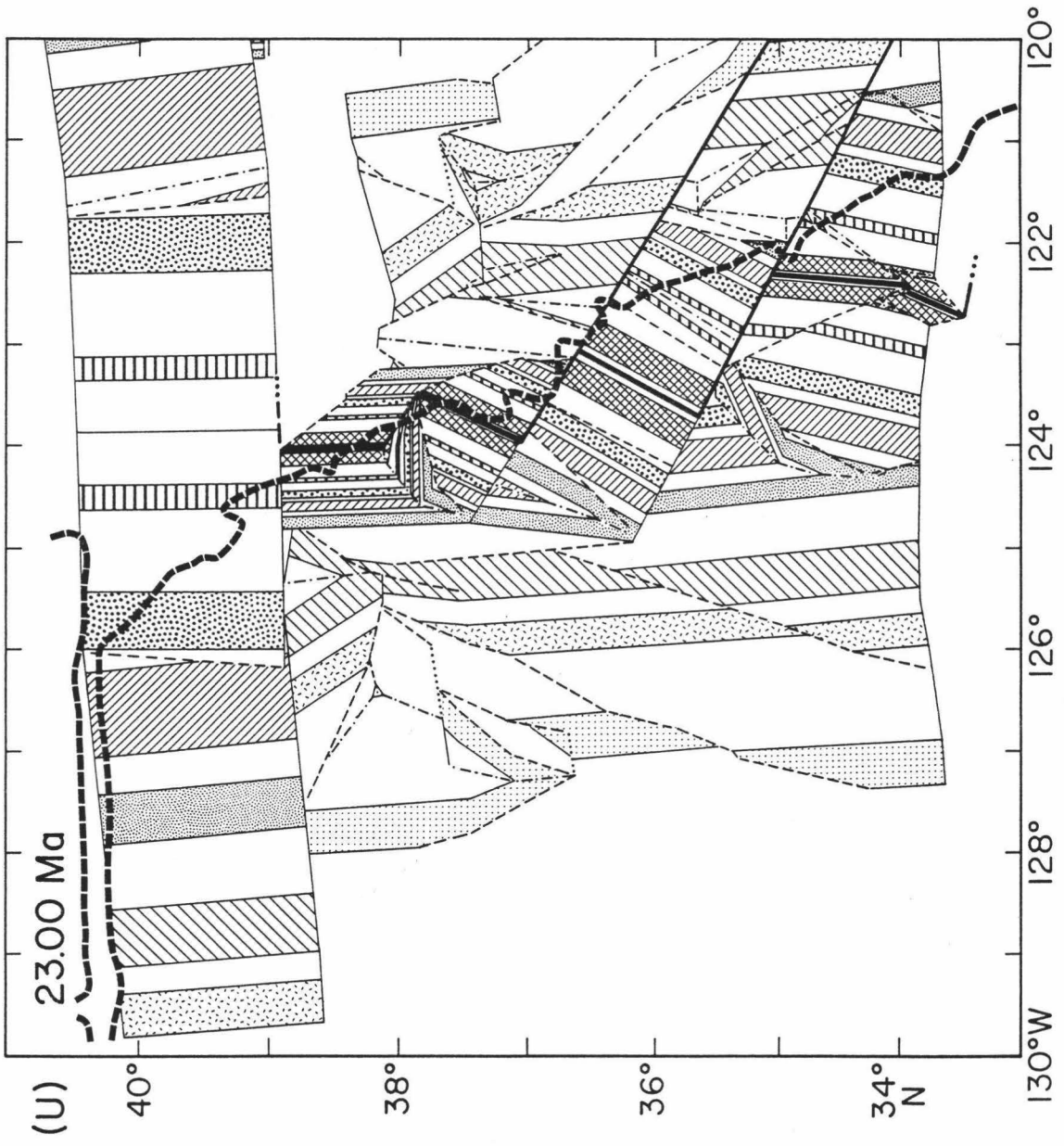


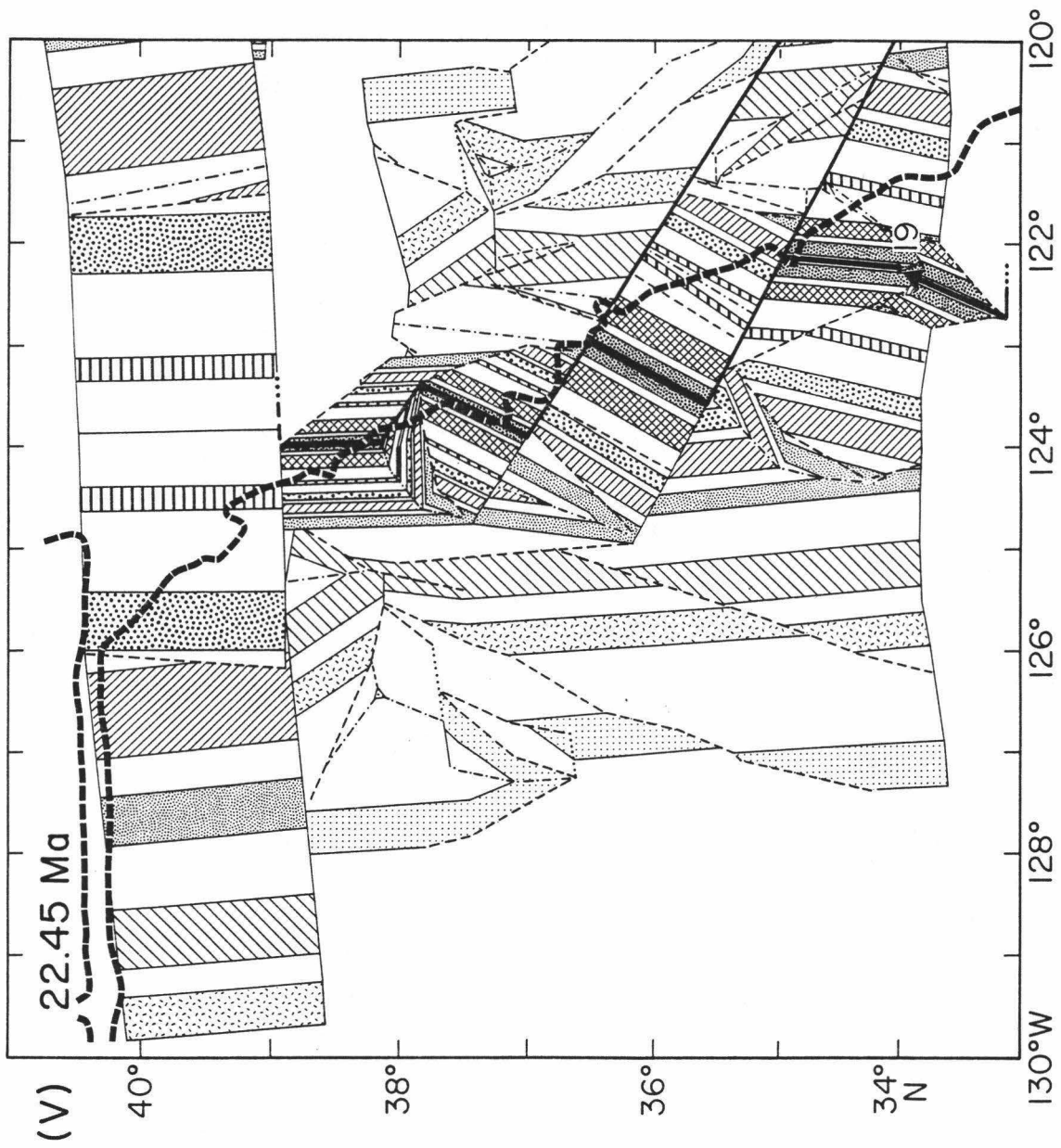


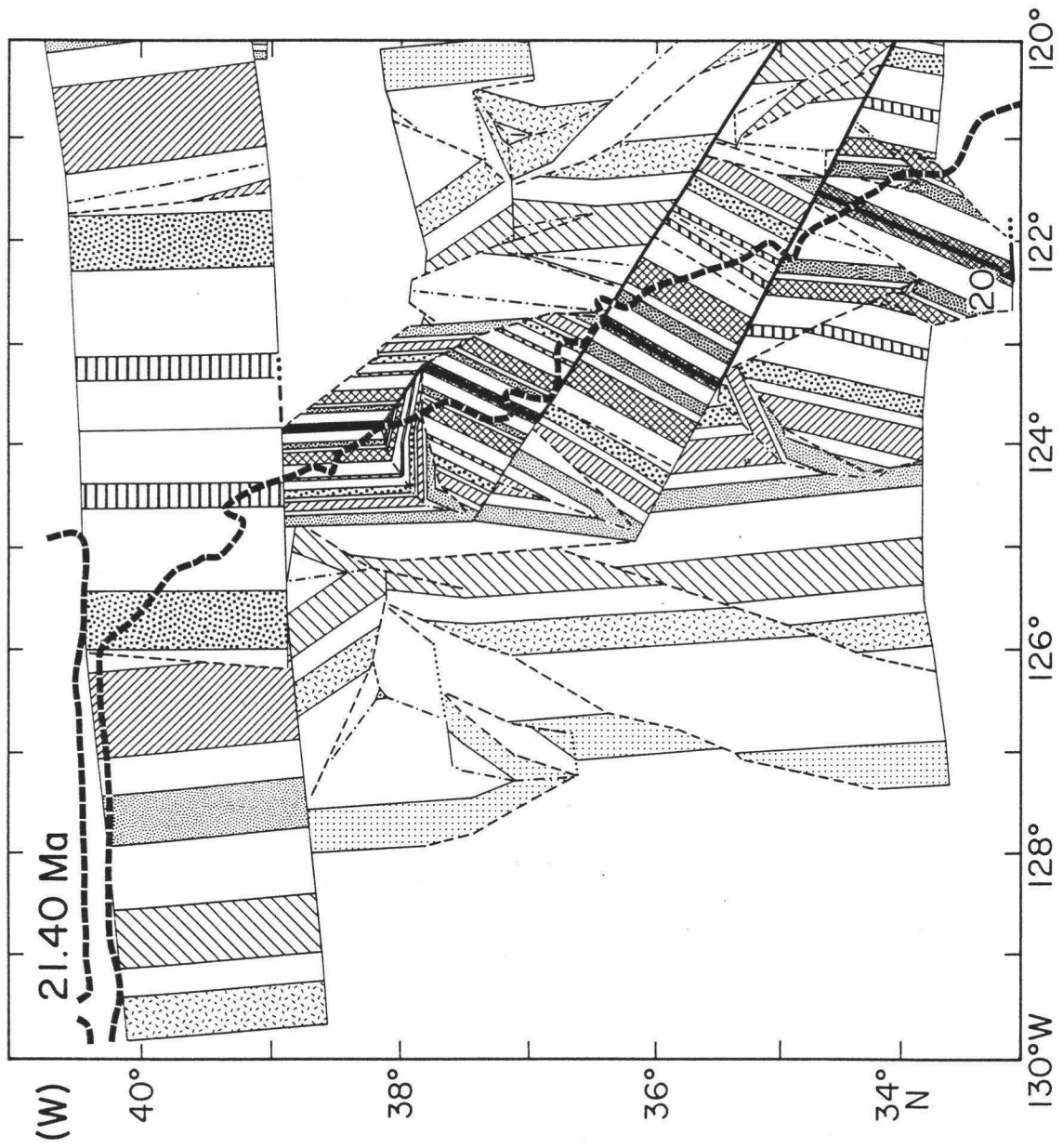


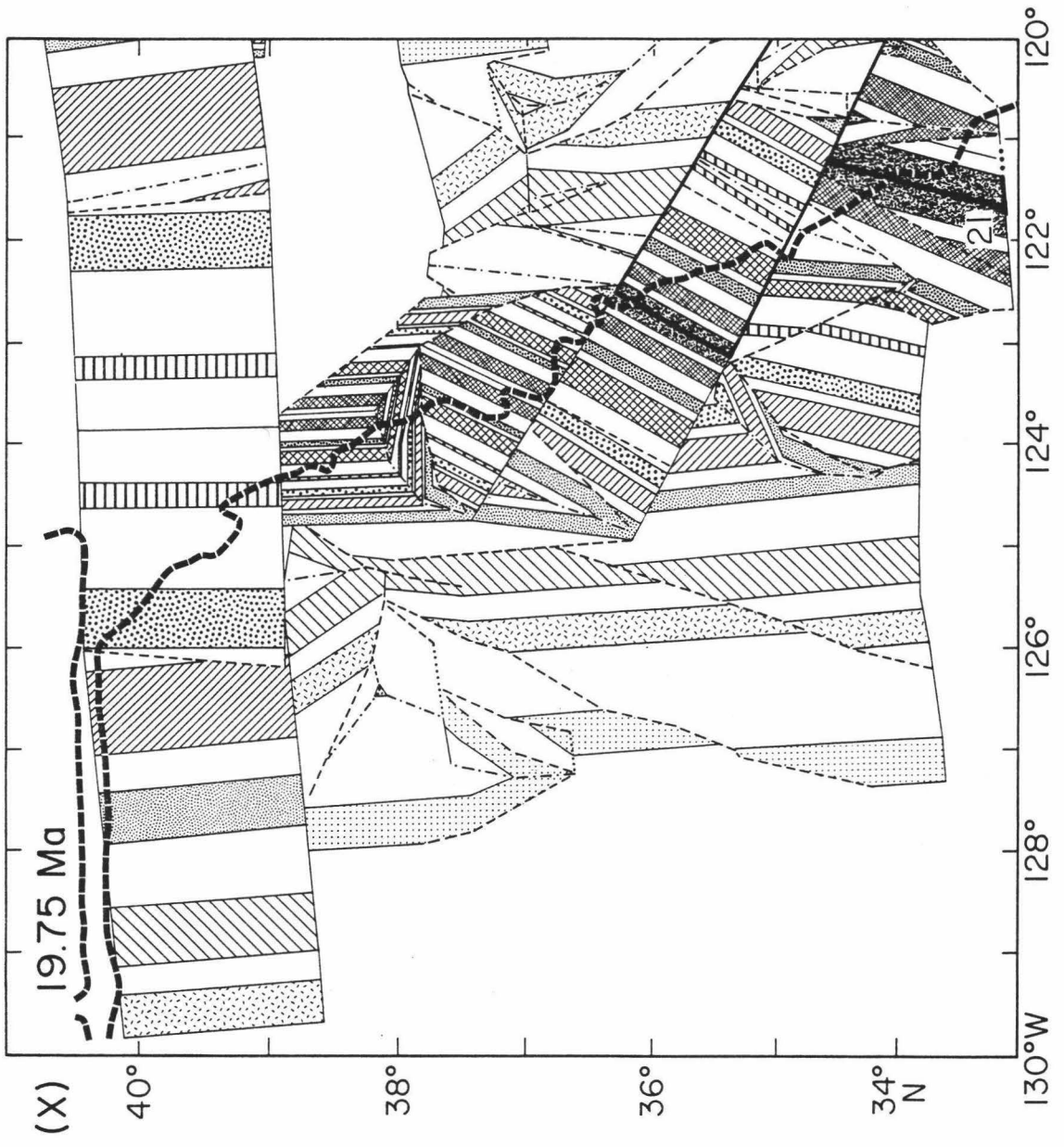












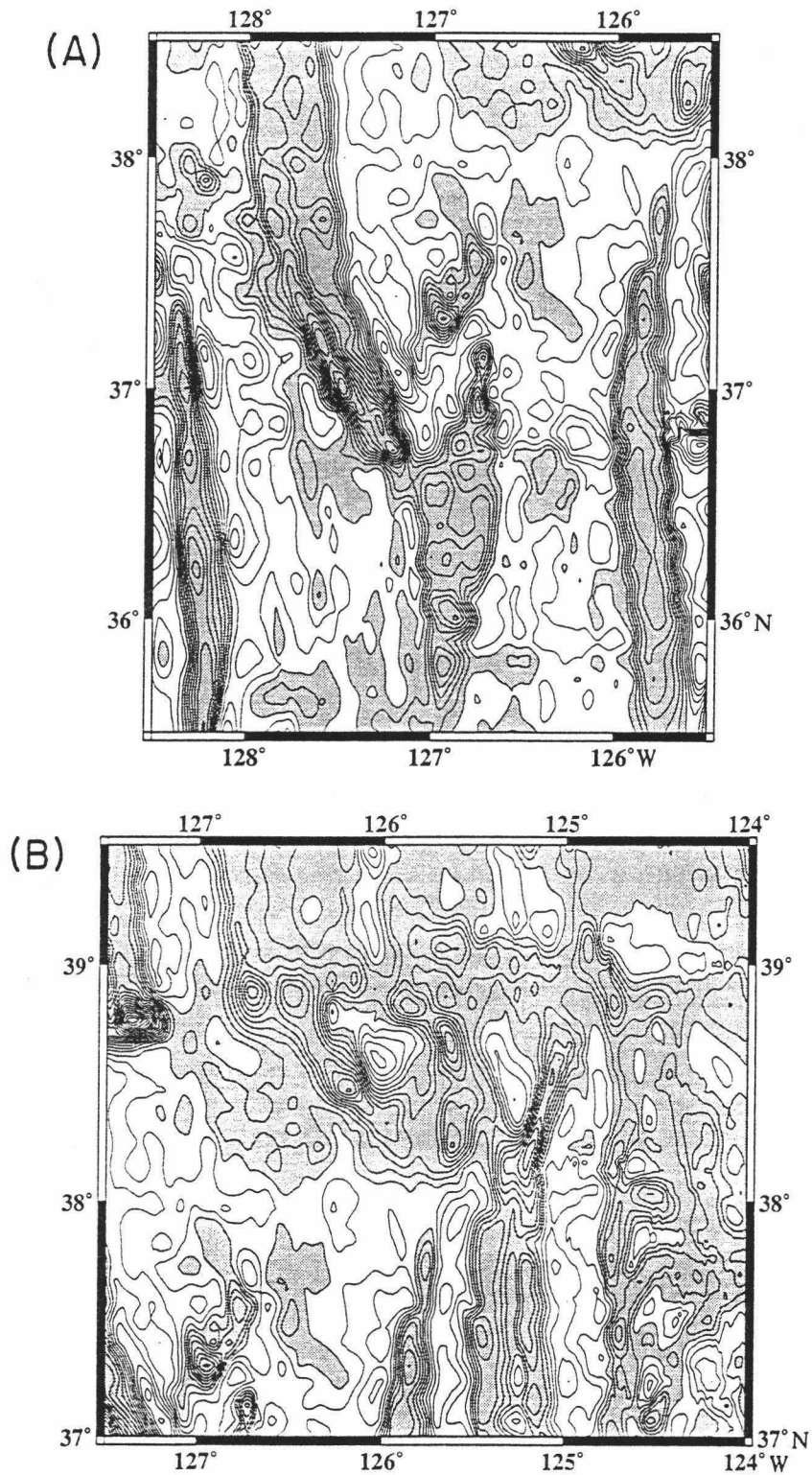
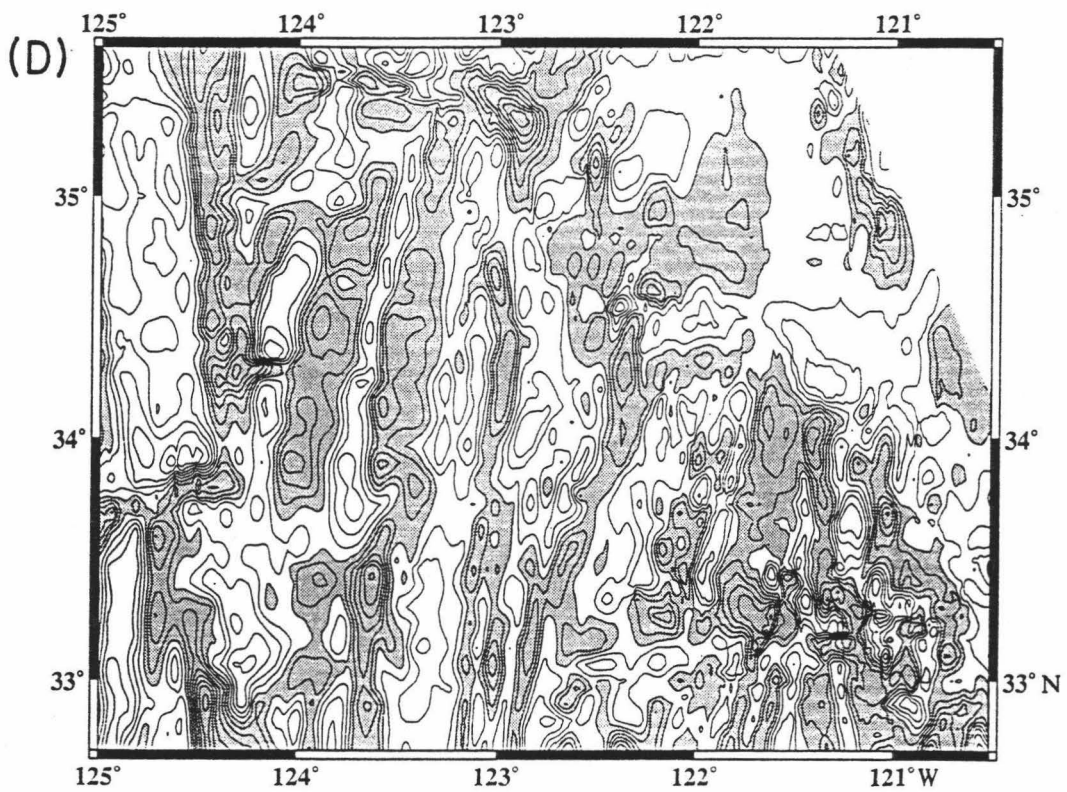
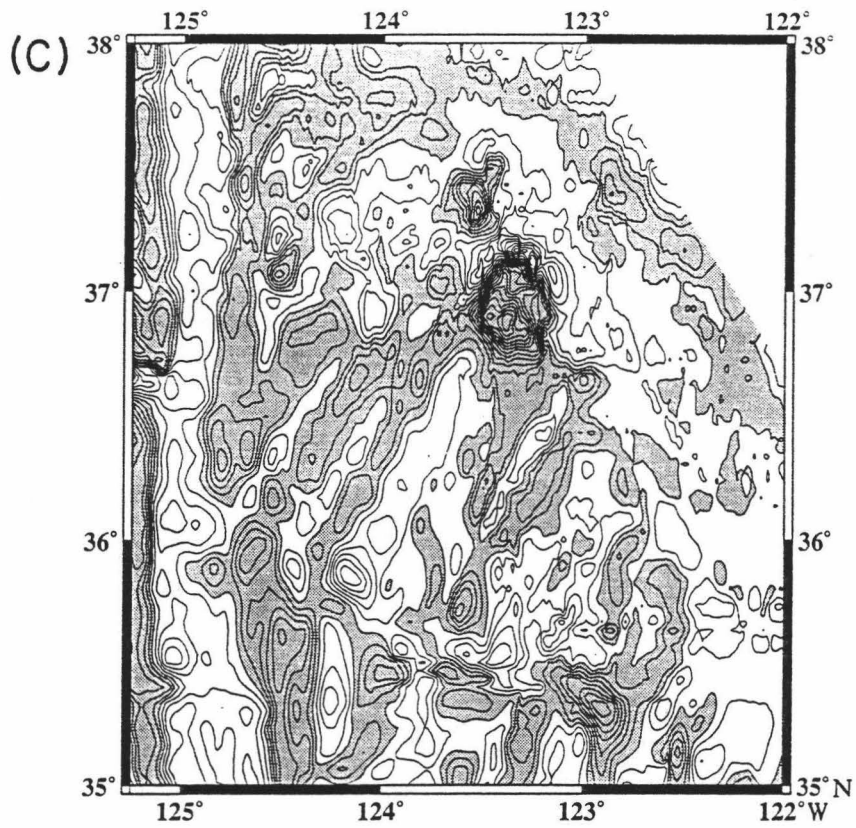


Fig. 18. Detailed magnetic anomaly contour maps for complex areas. Contour interval is 50 nT. Positive anomalies (greater than -100 nT) are shaded. For reference: (a) chron 13 begins approximately at 128°W on the northern border; (b) chron 12 begins at about 126°W on the southern border; (c) chron 10 begins at about 124.7°W; and (d) chron 10 begins at approximately 124.7°W on the northern border.



southeast until approximately 35.53 Ma when propagation ceased. About this time, the corresponding failing rift rejuvenated and began to propagate northward (PR 3; Figure 17c). This propagator's failed rift formed the general V-shaped appearance of chron 13 at 37°N, 127°W (Figure 18a). At 35.4 Ma, the propagation rate of PR 3 slowed down considerably, fanning out the failed rift (Figures 17d and 18a). The piece of lithosphere between the inner pseudofault (the pseudofault located between the propagating rift and the failed rift) of PR 2 and the inner pseudofault of PR 3 was transferred twice to the opposite plate. It originated on the Pacific plate, was subsequently transferred to the Farallon by PR 2, then was again transferred by PR 3 back to the Pacific plate. The complex pattern of chron 13 (Figure 18a) was completed when PR 3 terminated at 34.5 Ma and a transform fault was formed. There is a slight disagreement between the model and the data in the area of PR 3's failed rift. The reason may be that the tectonic history was more complicated than a single propagating and failed rift. The magnetic pattern may also have been disrupted by younger intrusions. Evidence in the USGS seismic profiles (EEZ-SCAN, 84 Scientific Staff, 1986) suggests uplifted young sediments in the region around 37.2°N, 127°W. A detailed seismic survey of this area is required to completely resolve its history.

At 35.4 Ma, the propagation of the most southern ridge segment (PR 1) also slowed down to form a minor kink in the pseudofaults (Figure 17d). Near the end of chron 13 (35.3 Ma), the Farallon rotation pole shifted slightly to the west by 10° and the angular rate slowed substantially, forming another small kink in PR 1's pseudofaults. These propagation rate changes and pole change may or may not have occurred simultaneously; the data are inadequate to actually differentiate the timing of these events. Prior to the 35.3 Ma pole location change, it appears that the Pacific-Farallon and Pacific-Vancouver relative plate motions were basically parallel, although the average Pacific-Vancouver spreading half rate was approximately 15 km/m.y. faster than the average Pacific-Farallon spreading half rate. However, after this pole

shift, the spreading direction for the Pacific-Farallon ridge was slightly more NE-SW than the spreading direction above the Pioneer transform. This difference forced the RFF triple junction to adjust slowly to the south contracting the Pacific-Farallon ridge slightly and also caused minor tension and compression in the Pioneer transform fault to the west and east of the triple junction, respectively.

At 34.7 Ma, PR 1's propagation rate increased. It slowed once more to form another small bend in its pseudofaults at 34.25 Ma, only to speed up again at 32.9 Ma. At about 32.7 Ma, PR 1 rotated clockwise by 10° (Figure 17h). This series of propagation rate changes and angle changes were postulated to correlate the oblique truncation of anomalies 13 and 12 to a single pseudofault which remains on the Pacific plate (Figures 11 and 14). Changes in spreading rates could also have formed bends in the pseudofaults, however, the spreading rates, determined from undisturbed magnetic chrons, could not alone account for the trend of the pseudofault.

The first new ridge for the system was introduced at 34.75 Ma. This new southward propagator (PR 4), located on the southern side of the Pioneer transform fault, was at an oblique angle to the spreading direction (Figure 17e). This extreme oblique spreading seems unlikely, however, it is necessary for the formation of chrons 12 and 11 as discussed below. Alternatively, these oblique stripes may have been formed by a tectonic feature similar to the extensional transform zone in the Manus Basin (Taylor et al., 1986). Just south of the Pioneer FZ between chrons 13 and 12, exists an extra wide piece of reversed polarity crust (Figures 11 and 14). In order to avoid the formation of normal polarity seafloor in this region, a new propagator (PR 5) was initiated at 33.5 Ma (Figure 17f) at a small angle to the current spreading direction. This angle change was necessary so that all the positively magnetized crust formed, specifically chron 12, was transferred to the Farallon plate (Figure 17i). PR 5 was not just an angle change in PR 3; there was a one million year period between the termination of PR 3 and the initiation of PR 5 when normal spreading occurred and a

transform fault and fracture zone developed. PR 4 and PR 5 propagated towards each other south and north respectively, and created a set of negatively magnetized failed rifts which form most of this expanse of reversed polarity seafloor. Presumably, other explanations for the wide negative seafloor are also possible. The failed rifts intersected when the two propagators met at approximately 32.82 Ma (Figures 17g and 17h). This intersection resulted in an abandoned transform fault due to the propagating/failed rift offsets before the two collided. PR 4 continued southward after the collision (Figure 17h) only to be terminated upon impact with PR 1 at about 32.3 Ma (Figure 17i), forming another failed rift-failed rift-abandoned transform (FR-FR-AT) triple junction-like feature on the Farallon plate.

A new propagator, producer of the very prominent outer pseudofault offsetting chrons 12 and 11 on the Pacific plate (Figures 11 and 14), was launched at 33.42 Ma as a tiny ridge segment just north of the Murray transform fault (Figure 17f). This new propagating rift, PR 6, decreased the offset across the Murray transform fault by approximately 16 km. PR 6 continued steadily northward with only minor adjustments in propagation rate to match minute changes in the pseudofault trend (Figures 17g through 17l).

The magnetics data just south of the Pioneer FZ between 125 and 126.5°W, exhibiting a highly complex pattern (Figure 18b), are interpreted to be chrons 12 and 11 at an oblique angle to the corresponding chrons south of 38°N. These chrons have been modelled as having been produced by PR 4 which is inclined to the ridges to the south, as indicated above. There is also a V-shaped feature in chron 11 (Figure 18b) providing further complication. I have interpreted this feature to be a failed rift formed by a northward propagator. However, in order to allow sufficient time for chron 11 to develop prior to the rift failure, propagator PR 1 must be stopped, slowing it down does not permit enough time passage. Hence, I have terminated PR 1 at the time of its impact with PR 4 (Figure 17i). The actual probability of both propagators

terminating at once is uncertain, but it is necessary in this model to closely match the data. Northward propagation was then initiated at the bend PR 1 took at 32.7 Ma (Figure 17j). This new propagator (PR 7), which thinned chron 11 slightly, continued northward through the tiny transform fault formed after the intersection of PR 1 and PR 4 (Figure 17k). This disrupted any evidence of a depression or deep formed by the collision of the two propagators. At about the same time (31.45 Ma), PR 7 rotated clockwise by 11.5° (Figure 17k). The new trend, slightly oblique to the spreading direction, initiated the future orientation of chron 10 for the Pacific-Monterey spreading center discussed below. PR 7 continued to propagate northward, slowing down at 31.4 Ma (Figure 17l), until it terminated at the Pioneer transform fault at 30.6 Ma, forming the failed rift feature in chron 11 (Figures 17m and 18b). Once again there is a slight disagreement between the data and the model for chron 11. Seismic profiles show uplifted, disturbed sediments and an overall high in the basement at the locality. This may indicate an igneous intrusion. A complete seismic survey would be beneficial in determining the exact tectonic history of this very complex area.

Southward propagation began at the bend formed by PR 7 at 31.3 Ma (Figure 17l). This fairly fast propagator (PR 8) cut off PR 6 at approximately 30.66 Ma, forming a FR-FR-AT junction on the Farallon plate (Figure 17m). PR 8 continued south until it stopped propagating with the initiation of new poles and microplates at 30.33 Ma (Figure 17m). PR 8 established the NNE-SSW trend for the ridge between 36 and 37.5°N at the beginning of chron 10, however, the northernmost portion of the ridge required a north-south orientation (Figures 11, 14 and 18c). Reorientation of the northern ridge segment could have been achieved several ways. For simplicity, I inserted a ridge jump at 30.34 Ma (Figure 17m), just prior to the activation of the new rotation poles. This ridge jump may have been accomplished by a series of small jumps over a short period of time, or a fast southward propagator from the Pioneer

transform could have also been the mechanism for reorientation. Lack of data limits the resolution of any one particular ridge reorientation method.

North of the Pioneer FZ, for Pacific-Vancouver plate motion south of the Mendocino FZ, the model was started at 33 Ma, just before chron 12. This time concurs with the oldest seafloor in the area within the PIONEER survey limits. It is assumed, however, for analysis of the Pioneer transform fault, that the plate motion was similar prior to this time, back to at least 36 Ma. The starting configuration for this spreading system, a single ridge, is shown in Figure 17g. Spreading continued moderately fast (approximately 65 km/m.y. half rate) with only minor changes in the rate. Small errors in the time scale may be responsible for the multiple rate changes. Model parameters for the Pacific-Vancouver spreading are listed in Table 2.

At 32.25 Ma, the rotation pole for Pacific-Farallon spreading shifted significantly to the east and a bend in the Murray FZ formed by the approximately 9° clockwise rotation of the spreading direction from ENE-WSW to more directly east-west (Figure 17i). The piece of Farallon plate lithosphere between the Murray and Pioneer transforms began to move in the new direction. Meanwhile, the Pacific-Vancouver ridge retained its ENE-WSW spreading direction until roughly 27.95 Ma, when it also rotated clockwise by about 6°. During the delay in time between the reorientation of the spreading centers north and south of the Pioneer, approximately 32.25 to 27.95 Ma, the Pioneer transform fault was in compression west of the triple junction and in tension ("leaky" according to Menard and Atwater (1969)) east of the triple junction. The triple junction adjusted to accommodate the changes in plate motion by slowly migrating to the north and slightly elongating the Pacific-Farallon ridge until a new east-west transform fault fractured through at 27.95 Ma.

A similar, but not quite parallel, situation was found by Caress et al. (1988) for the Eocene reorganization of the Pacific-Farallon spreading center north of the Mendocino FZ. When a clockwise rotation of the direction of spreading occurred at

about chron 24 time, 55 Ma, the piece of Farallon plate lying between the left-lateral Mendocino offset and the right-lateral Surveyor transform fault was constrained to move in the old spreading direction by the Mendocino. This caused the Surveyor to become "leaky" until a new Mendocino transform fault was fractured through in the new east-west trend, evoking the spreading center reorientation to "close up" the Surveyor transform fault.

Modelled spreading rates for the Farallon plate south of the Murray transform fault indicate that this piece of lithosphere had probably separated from the portion of Farallon plate north of the Murray transform by approximately 31.5 Ma. This is demonstrated in Figure 15 as the difference in ridge and transform fault geometry between 31.85 and 31.4 Ma. Prior to this time the active transform is only to the west side of the Pacific-Farallon ridge/Murray transform intersection. After 31.5 Ma, this intersection turns into a RFF triple junction with active transform faults on both sides of the ridge.

A major reorganization of the Pacific-Farallon spreading center system occurred at the beginning of chron 10 (30.33 Ma). At this time, changes in plate motions caused transforms to fracture through to the trench generating new rotation poles. The section of Farallon plate between the Murray and Pioneer transform faults broke into at least two, probably three, independent pieces, each with its own new rotation pole relative to the Pacific plate (Figure 17n). The evidence for these new microplates is seen clearly in the three-dimensional representation of the magnetic data (Figure 19). There is a definite contrast between the older, high amplitude, north-south trending stripes and the lower amplitude, northeast-southwest trending stripes.

The southernmost of these new microplates is the Arguello (Severinghaus and Atwater, 1989). The Pacific-Arguello rotation poles (listed in Table 3) were governed by the trend of the Murray FZ, thus, the spreading direction remained generally east-west. However, the plate north of the Arguello, the Monterey (Severinghaus and

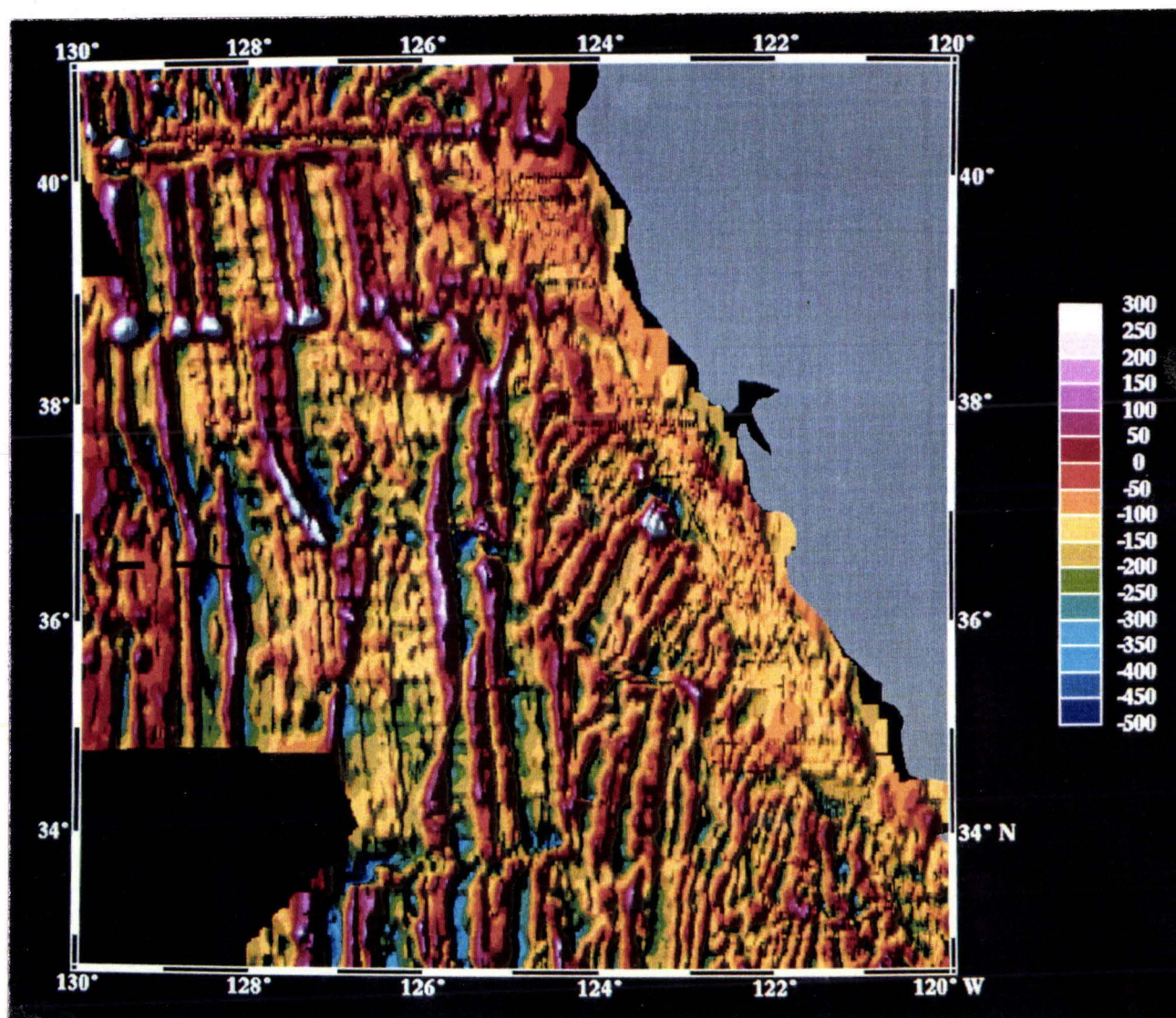


Fig. 19. Three-dimensional color shaded relief magnetic anomaly plot. Contour interval is 50 nT. Illumination direction and angle are 300°, 60° elevation.

Atwater, 1989), had a spreading direction that was clearly NW-SE. Its controlling fracture zone, the Morro (Severinghaus and Atwater, 1989), although clearly visible in the magnetic data, is not very distinct in the bathymetry (Figure 20). Thick blankets of sediments, the Delgada and Monterey deep-sea fans, cover most of the oceanic basement east of 126°W including the terminations of the Pioneer and Murray fracture zones. However, close to the continental shelf, there is an elongated ridge-type feature along the fracture zone trend near 35.2°N, 122.5°W (Figure 20). Also, at the fracture zone/continental margin intersection, there is a promontory along the continental slope directed towards the fracture zone trend. Different trends in plate motions across the Morro transform fault predicts approximately 50 percent shortening of the Arguello plate by compression. This plate, however, has been subducted, thus no evidence remains. This large component of compression existing across the Morro transform probably generated the disrupted bathymetry along the fracture zone trend, evident in the seismic profiles from the USGS FARNELLA survey (EEZ-SCAN 84 Scientific Staff, 1986).

The northern portion of Severinghaus and Atwater's (1989) Monterey plate appears to have had much slower spreading rates relative to the Pacific plate than its southern counterpart (a half rate spreading difference of approximately 8 km/m.y.). Therefore, I have treated this northernmost section as an individual plate, the Reyes plate. The plate boundary between the Monterey and Reyes microplates was the NW-SE trending Carmel transform (Figure 17n). The Carmel FZ inclines slightly more north-south than the more southern Morro transform fault (Figure 18c). Thus, the Pacific-Reyes rotation pole is not quite copolar with the Pacific-Monterey pole, and is about 6° farther east. The model parameters for the Monterey and Reyes plates, including the rotation poles, are listed in Tables 4 and 5. There is a slight component of compression across the Carmel transform fault due to the fact that these poles are not located at identical positions. The basement in this region is very rugged and

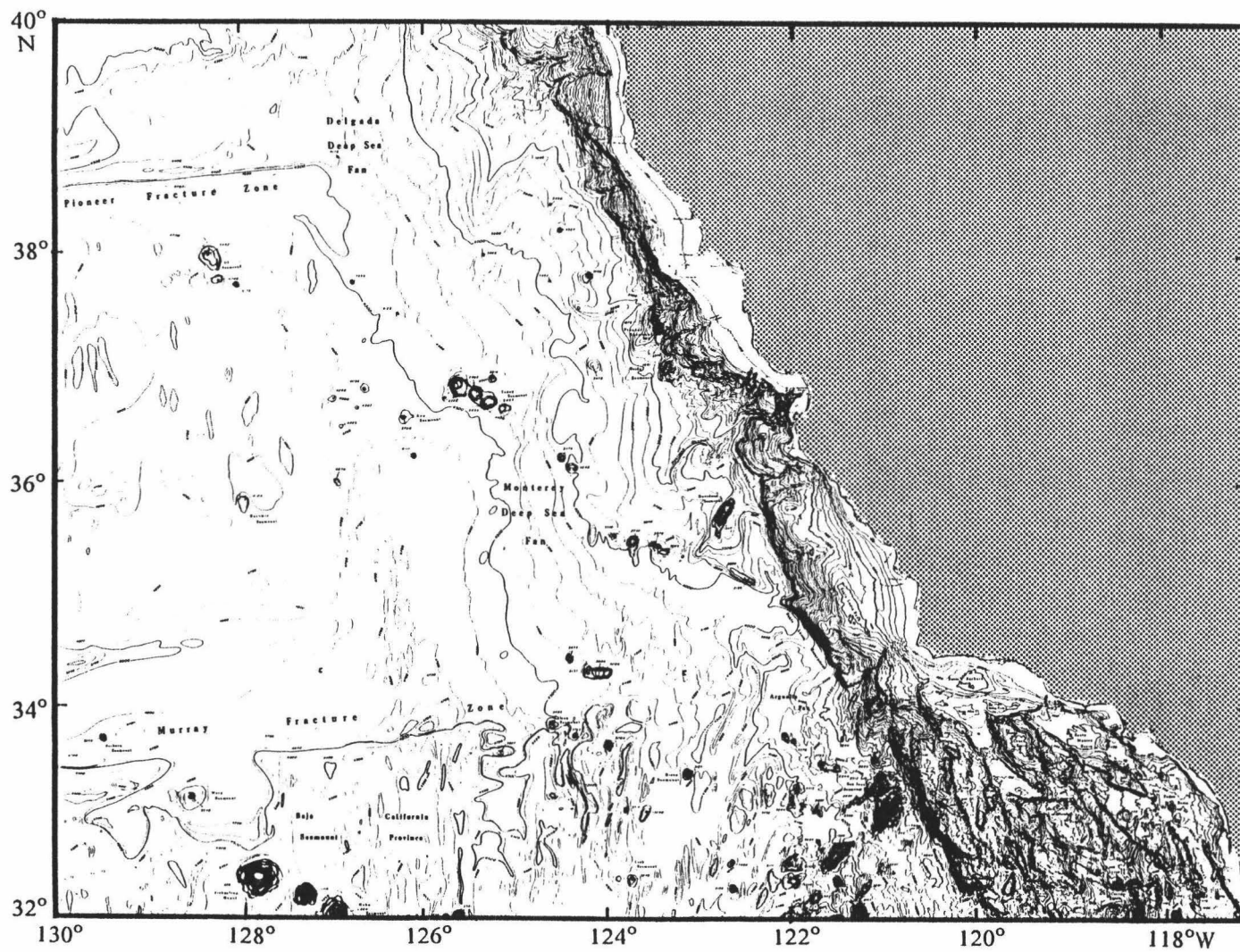


Fig. 20. Bathymetry of the survey area (modified from Chase et al., 1981). Contour interval is 100 m.

anomalous, consistent with the model. A cartoon of the plate boundary configuration at the time of the reorganization, the beginning of chron 10, is shown in Figure 21.

With the initiation of these new transform faults, the northernmost portion of the southern Pacific-Farallon ridge segment was severed by the Morro transform. This generated an instantaneous failed rift and formed, along with the old Pacific-Farallon transform, a FR-FR-AT junction on the Monterey plate (Figure 17n).

The oblique direction of spreading for the Reyes plate relative to the Pacific was at an angle to the old spreading direction for the Pacific-Farallon ridge. This difference caused the "leaky" Pioneer (Vancouver-Reyes) transform to open even wider. To minimize the opening and maintain the triple junction configuration, the northern tip of the Pacific-Reyes ridge is assumed to have propagated northward slowly to fill in the gap. This propagator (PR 9) began just as the Reyes plate was formed and continued until its demise with only a small interruption at the 27.95 Ma Pacific-Vancouver relative plate motion change (Figures 17n through 17w).

As spreading for each of these new microplates progressed, the ridges reoriented to accommodate the new spreading directions developed, especially for the Monterey and Reyes plate spreading systems. This was accomplished by a series of propagating rifts starting at approximately 30.05 Ma (Figure 17o). PR 10 executed the reorientation for the Reyes plate with a 28° clockwise rotation. This propagation produced a characteristic V-shaped failed rift on the Pacific plate (Figure 18c). A distinct bend (almost 90°) in the transferred chron 10 (Figure 18c) was formed by a decrease in propagation rate at about 29.1 Ma (Figure 17p). East of the failed rift on the Pacific plate, there appear to be double magnetic stripes (Figures 18c and 19). These stripes have been modelled as anomalies 9 and 8 (Figure 17r). Chron 7 was considered to be too brief to be distinct in the magnetic pattern formed by very slow spreading. The quality of the data restricts absolute identification, but it seems that east of these stripes there is a negatively magnetized strip of crust, then some minor positive

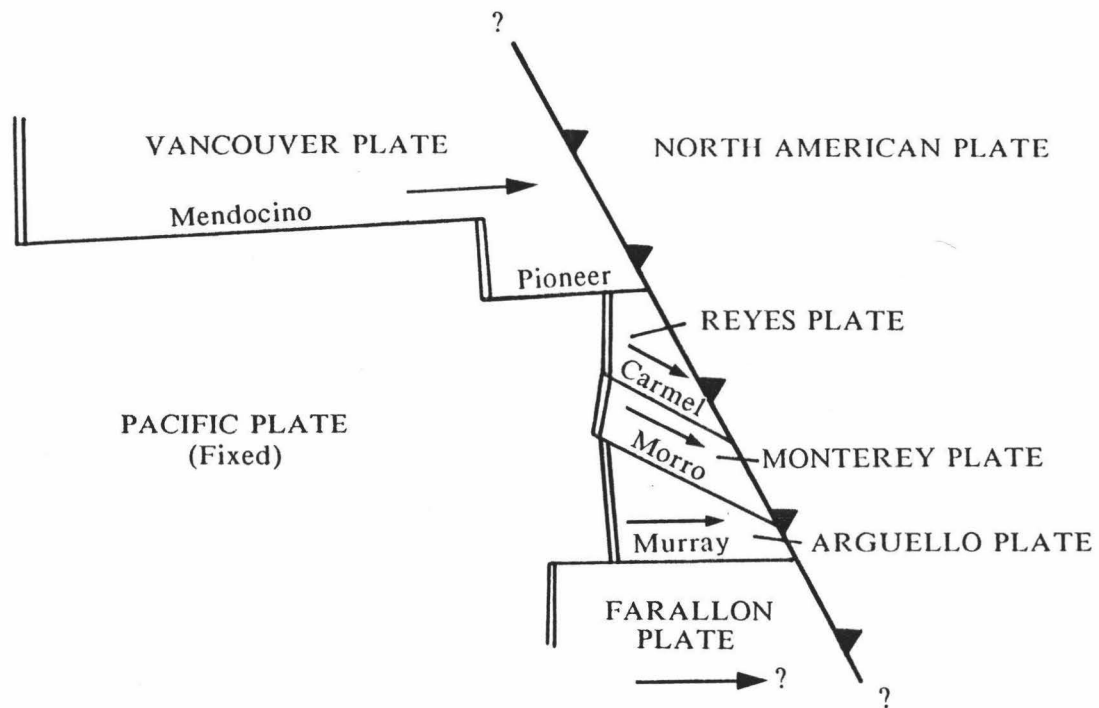


Fig. 21. Cartoon of the plate boundary configuration at time of the major reorganization, at the beginning of chron 10. Same explanation as in Figure 16.

material which could be chron 6C (Figures 18c and 19). After the "slowing down" of PR 10, transferred lithosphere between the inner pseudofault and the failed rift was oriented roughly east-west. This corresponds to what I believe is an east-west trend in the magnetics for this area (Figure 11). The northern section of the plate retained its north-south orientation by oblique spreading or perhaps another microplate existed. This north-south direction is weakly discernible in the data (Figure 11).

Reorganization of the Pacific-Monterey spreading center was accomplished by northward propagator PR 11. It began at about 30.05 Ma as a tiny extra ridge segment oriented NE-SW just north of the Morro transform fault (Figure 17o). PR 11 caused the formation of the failed rift in chron 10 (Figure 17p), whose V-shaped form is distinct in the data (Figure 18c).

The Pacific-Arguello spreading center system also reoriented to a NNE-SSW direction by the propagation of PR 12 and PR 13. At about 30.05 Ma, a small sliver of the ridge rotated slightly clockwise, about 0.4 degrees north of the Murray transform fault. Presently, this location corresponds to a seamount, however, the age of the seamount is unknown and it may or may not have been responsible for this disturbance of the ridge. This new small ridge segment propagated both north and south, PR 12 and PR 13, respectively (Figure 17o). The propagation rate of PR 12 slowed considerably at about 29.4 Ma (similar to the situation of PR 10) to form the NE-SW discordance (PR 12's inner pseudofault) in the magnetic data (Figure 18d; Figure 17p). Just south of the Morro FZ, between 123 and 124°W, several seamounts also disrupt the magnetic pattern (Figure 20). The seamount trend does not parallel the Morro FZ. The southward propagator, PR 13, terminated at the Murray transform fault (Figure 17p).

The Pacific-Arguello rotation pole shifted gradually 15° to the east over the time interval between 30.33 and 22.5 Ma forming a slight bend in the Murray FZ as the spreading direction rotated from basically east-west to ESE-WNW (Figures 17o through

17t). This bend is suggested in the bathymetry (Figure 20) and is supported by the magnetic data (Figure 18d). At approximately 27.95 Ma, new plate motions caused the Pacific-Vancouver pole to move to the east prompting a reorganization of the Pacific-Vancouver ridge and the fracturing of a new east-west Pioneer transform fault (Figure 17q). The new transform severed the tip of the Pacific-Reyes ridge (PR 9) and transferred it to the Vancouver plate. At the new triple junction location just slightly south of the previous one, PR 9 continued to propagate. A very fast northward propagator (PR 14), originating near the Pioneer transform, reoriented the spreading center to north-south, in agreement with the new east-west spreading direction (Figure 17q). Contemporaneously, PR 14 functioned as an eliminator of reversely magnetized seafloor from the Pacific plate. The reversed anomaly between chrons 9 and 8 is abnormally thin (Figures 11 and 14). That is to say, without PR 14, the spreading rate would have had to have been reduced in half for a short period of time then doubled again at the beginning of chron 8. This doesn't seem likely. Instead, PR 14 is proposed to have transferred half of the reversed anomaly to the Farallon plate. However, within the resolution of the data, this tremendously fast propagation episode could have been a discrete or instantaneous ridge jump.

Spreading continued between the Pacific plate and the microplates with generally NE-SW spreading centers until about 26.9 Ma. At this time a southward propagator (PR 15) originated at the Morro transform fault and provided a new north-south orientation for a segment of the Pacific-Arguello ridge (Figure 17r). PR 15 cut off the northward propagating PR 12 just prior to its intersection with the Morro.

At about 25.5 Ma, a relatively fast propagator began at the Carmel transform fault which transferred chrons 7A and 7 to the Farallon plate (PR 16; Figure 17s). This transfer is postulated because chron 6C is definitely the next positive anomaly seen today on the Pacific plate next to chron 8 (Figures 18c and 19). However, this transfer was only necessary with a failed rift model for chron 10. Atwater (1989),

using different anomaly identifications, suggested another method for ridge reorientation discussed in the next section.

At 25 Ma, I arbitrarily terminated the Pacific-Vancouver spreading between the Pioneer and Mendocino fracture zones. The youngest identifiable anomaly is chron 8 (26.86 Ma), thus, by 25 Ma, the entire ridge should have been overridden by the trench.

The next reorganizing event began at 24.1 Ma for the Pacific-Arguello ridge. At the Murray transform fault, two propagating rifts were generated: one northward at a fast rate (PR 17) and a slow one to the south (PR 18). This tiny new ridge segment reoriented the existing spreading center to a NE-SW trend (Figure 17*t*). PR 17 quickly propagated to the north and was extinguished by PR 15 on its southward journey (Figure 17*u*). PR 18 drove the Murray transform fault southward, offsetting the main trend of the fracture zone with a pseudofault. The break in the Murray FZ is obvious in the magnetic data (Figures 11, 14, and 18*d*). The termination of a fracture zone by rift propagation also occurred north of the Mendocino FZ with the elimination of the Surveyor (Shih and Molnar, 1975), Sedna, and Sila fracture zones (Wilson, 1988). At the time of the initiation of PR 18, the spreading rate difference between the Pacific-Farallon (remaining portion of the Farallon plate south of the Murray transform) and Pacific-Arguello spreading systems had caused the Pacific-Farallon ridge to migrate east past the Pacific-Arguello ridge, resulting in the Murray being active only on the eastern side of the Pacific-Arguello spreading center. This is indicated in the ridge/transform geometry summary (Figure 15).

PR 15 continued southward after terminating PR 17 until 22.6 Ma, when propagation switched directions and the rejuvenated "doomed" ridge began to propagate towards the north (PR 19; Figure 17*v*). This allowed the new NE-SW trending ridge to increase in length; by about 22 Ma, the entire active Pacific-Arguello ridge had

obtained this new orientation. The magnetic lineations formed at this time (chrons 6AA and 6A) trend NE-SW for their entire length (Figure 18d).

At approximately 22.5 Ma, the Pacific-Arguello rotation pole shifted for the last time to form the very linear, east-west trending segment of Murray FZ which terminates at the continental margin near 33.2°N. The fragment of Pacific plate formed during this spreading interval has a fan-like appearance with the chrons narrowing to the north (Figure 18d). Although this pattern suggests a nearby pole, this would have caused the Murray transform to be arcuate. Instead, the fracture zone is straight (Figures 11, 14, and 18d). Thus, another method of ridge reorientation is preferred. The data are consistent with a series of propagating rifts generating the reorganization of the Pacific-Arguello ridge from a NE-SW orientation to north-south. Two northward propagators were sufficient to achieve the reorganization. The first, at approximately 21.45 Ma (PR 20), rotated the ridge counterclockwise by about 8° (Figure 17w). The second propagator (PR 21), initiated at about 19.8 Ma, completed the reorganization with a rotation of 18° (Figure 17x).

At 20.45 Ma (the beginning of chron 6), the Pacific-Reyes spreading was arbitrarily terminated. From the magnetic data (the last identifiable anomaly is chron 6C), it is assumed that the entire ridge had been overridden by the North American trench by this time. Moreover, the spreading of the Pacific-Arguello ridge was terminated at 16 Ma for the same reason; the last identifiable magnetic anomaly in this particular area is chron 5E (18.56 Ma). Magnetic lineations (Figures 11, 14, and 18b), plus the location and orientation of Davidson Seamount (Chase et al., 1981), suggest that Pacific-Monterey spreading terminated at roughly 19 Ma (Lonsdale, 1988; Atwater, 1989; Severinghaus and Atwater, 1989). The elongated seamount is the trace of the dead ridge. Therefore, a piece of the Monterey plate remains to the east of Davidson Seamount.

The final configuration (0 Ma) of the model is shown in Figure 22. The part of the model east of the present day continental margin has been deleted so that the remainder corresponds to what exists today. A few prominent magnetic anomalies (chrons 12 through 9) have been added to the final model configuration south of the Murray FZ to show its sense of offset. Figure 23 shows the magnetic data interpretation at the same scale as the model superimposed with fracture zones and pseudofaults. Figures 22 and 23 can be compared directly to show the agreement between the model and the data.

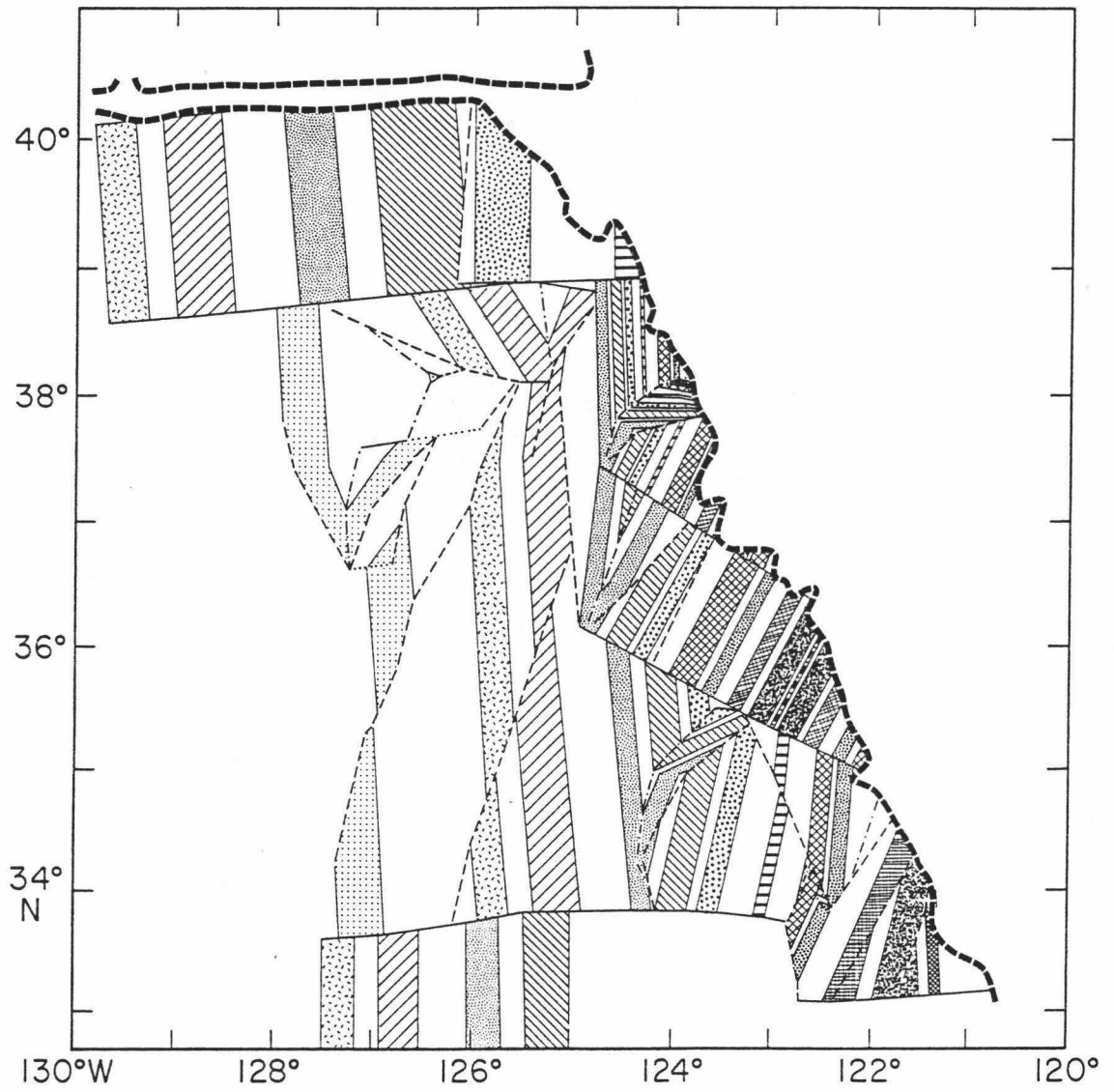


Fig. 22. Final configuration (present day) of the model. Same explanation as in Figure 17.

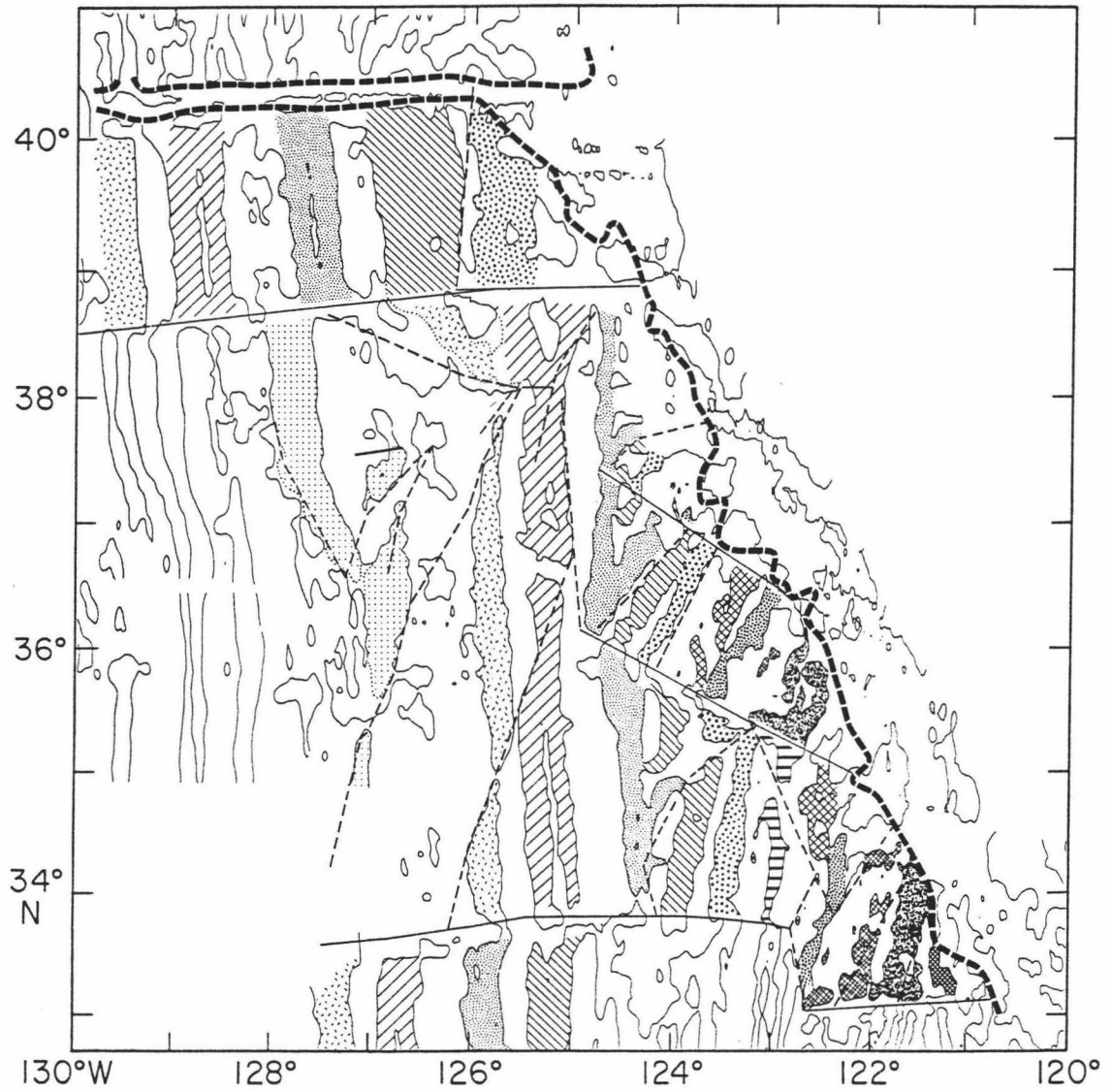


Fig. 23. Magnetic anomaly interpretation superimposed with fracture zones (solid lines) and pseudofaults (dashed lines) presented at the same scale as the final model configuration. Other symbols same as Figure 14.

V. DISCUSSION

The tectonic evolution model presented here (Figures 17 and 22) shows excellent agreement with the magnetic anomaly interpretation (Figure 23). The trends of the Pioneer and Murray fracture zones, the termination of the Murray FZ, the oblique offsets in chrons 13, 12, and 11, and the distinctive *V*-shaped features in chrons 11 (just south of the Pioneer) and 10 (in each microplate), have been particularly well matched. However, it is important to remember that agreement between the model and the data indicates only possibilities and not actualities, as with any forward modelling application. Ruling out unsuccessful models supplies a great deal of the information we learn. The slight misfits of the model, namely chron 13 at 37°N and chron 11 at 38.3°N, occur at localities with extremely complex magnetic patterns and indicate that we can at least rule out simple tectonic histories for these areas.

In the reconstructions, chron 13 was formed by a southward propagator (PR 2) that eventually failed; its failing rift subsequently rejuvenated to propagate northward (PR 3; Figures 17*b* through 17*e*). The strong curvature of the propagating rift tip (PR 2) just before it failed is similar to the failed rift curvature at Galapagos 95.5°W, the Cobb offset on the Juan de Fuca ridge, and certain microplates, in particular, the Easter microplate. The failing rift rejuvenation is, in a simplistic way, an example of duelling propagation. However, I think the two propagators (PR 2 and PR 3) did not "spar" with each other in the true sense of duelling propagation, but in fact, propagated in sequence, one after the other. If these two propagators did overlap and duel, one might expect the magnetic pattern to only display the western pseudofault and failed rift (of the overlapped portion) of the southward propagator (PR 2). The overlapped part of PR 3 would have probably been rafted away on the Farallon plate. However, today we see a more classic failed rift pattern associated with the later northward

propagation indicating that the northward propagation occurred after the southward propagation. The precise tectonic history of this locality, nevertheless, is still unclear.

Another minor problem with the model occurs between the Vancouver and Reyes plates. The large difference in relative motions between Pacific-Reyes plates and Pacific-Vancouver predicts east-west trending extension east of the Pioneer triple junction. This extension augments the tension, previously discussed, that was already present in the Pioneer transform fault due to the Pacific-Farallon pole change at 32.25 Ma (at least until 27.95 Ma). The majority of the extension probably occurred after that portion of lithosphere had been subducted by the North American trench. With this in mind, one might expect to see some kind of east-west structure in the continental structure onshore. However, all the structure east of the San Andreas fault has a general northwest-southeast azimuth parallel to the continental margin.

There is a second possibility, however, for the Pioneer FZ orientation. If Wilson's (1988) pole for the time interval of 30 to 27 Ma had been used after the 27.95 Ma pole change, the section of the fracture zone created after the 27.95 Ma pole change would have trended NW-SE instead of east-west. This orientation would have minimized the east-west trending extension east of the Pioneer triple junction. Unfortunately, there is not enough evidence in the magnetics or bathymetry to substantiate this NW-SE trend; thus, a basic east-west bearing was favored because it caused the Pioneer FZ to intersect the continental margin at Point Arena.

There are several differences between my model and Atwater's (1989) model for the formation of the microplates from the fragmentation of the Farallon plate and the resulting ridge reorientation. The first difference is that Severinghaus and Atwater (1989) only defined two microplates: the Arguello and the Monterey. I think that the spreading rate difference between the southern and northern portions of the Monterey plate is sufficient evidence to break the plate in two along the fracture zone offsetting the magnetic stripes. I have called this new northern plate the Reyes plate and its

fracture zone, the Carmel. Another difference between this model and Atwater's is different anomaly identifications for this area. The V-shaped features at 34.7°N, 124.3°W; 36.5°N, 124.5°W; and 37.7°N, 124.7°W; have here been interpreted as failed rifts, formed during chron 10 (Figures 18c and 18d). At the middle of chron 10 (30.05 Ma), three northward propagators (PR 10, PR 11, and PR 12) were initiated to reorient the spreading segments to the new spreading direction and to form these failed rifts. For each of the microplates, the adjacent northeast trending stripe has been identified as chron 9, with chron 8 just to the east of chron 9. Details of the magnetic patterns are shown in Figures 18c and 18d. For the Pacific-Monterey spreading segment, the model transferred chrons 7A and 7 from the Pacific plate to the Monterey plate by propagator PR 16 because chron 6C is the next positive anomaly seen today on the Pacific plate. In Atwater's model, the Arguello and Monterey plates broke from the Farallon plate in the middle of chron 10. Spreading slowed considerably and rotated 30° clockwise (see Figure 7 from Atwater, 1989). For Pacific-Monterey magnetics, she has identified the eastern branch of my proposed failed rift to be chron 9 compared to my chron 10 interpretation. Thus, her adjacent positive anomalies are chrons 8 and 7, respectively. However, when I forward modelled Atwater's anomaly interpretation it required an additional spreading rate change at the end of chron 8 that is not required by my model. In order to match her chron 7 with the data, the spreading rate needed to be reduced approximately by half between the end of chron 8 and the beginning of chron 7. Thus, I prefer propagating rifting as the method of ridge reorientation for the Pacific-Monterey spreading center. Furthermore, I think the rift propagation mechanism for ridge reorientation is also viable for the Pacific-Arguello and Pacific-Reyes spreading segments because my models exhibit excellent agreement with the data.

Some speculation regarding the "why's and wherefore's" of propagation is appropriate at this time. Previously, propagation rates have been reported to range

from 19 km/m.y. to 367 km/m.y. on the Pacific-Farallon spreading center during the Eocene reorganization (Caress et al., 1988). In the region between the Pioneer and Murray fracture zones, propagation rates in this study were modelled between 9 km/m.y. (PR 10 on the Pacific-Reyes ridge) and 422 km/m.y. (PR 2 on the Pacific-Farallon ridge). I have not included the exceptionally fast rate for PR 14 north of the Pioneer transform because even though it appears to be well documented in the magnetics data, its rate clearly lies well outside all previously published rates. I have also not included the exceptionally slow rate for PR 9 because this propagator existed only for triple junction adjustment between the Pacific, Vancouver, and Reyes plates. Prior to 30.0 Ma, the propagation direction was predominantly northward. This northward tendency occurred both south of the Pioneer FZ and north of the Mendocino FZ (Wilson, 1988). Moreover, during this time, the majority of propagation was fast (>100 km/m.y.).

At the beginning of chron 10 (30.33 Ma), a change in Farallon plate motion occurred north of the Mendocino FZ (Wilson, 1988); south of the Pioneer FZ, the Farallon plate was fractured into microplates. We interpret these events as the arrival of the Pacific plate at the North American trench and the initiation of strike-slip tectonics along the North American margin. The Pacific/North American plate meeting probably happened at the Pioneer transform fault which, due to its 300 km right-lateral offset, would have been the closest point of the Pacific-Farallon spreading system to the northwest-southeast trending trench. It is interesting to note that the Pacific-Vancouver ridge appears to have experienced only minor propagation (PR 14 at 27.95 Ma) from this event.

With the initiation of new rotation poles for the "fragments" of the Farallon plate, rift propagation was the primary mechanism for ridge reorientation in response to the relative motion change. The three prominent *V*-shaped features were formed as the rift segments with the old orientation were replaced by propagating segments with

the new orientation. After the break up of the Farallon plate, propagation rates slowed slightly from a range of 35 to 422 km/m.y. to a range of 9 to 389 km/m.y.. Prior to 30.33 Ma, the mean propagation rate was 150 km/m.y., with the median being 122 km/m.y.. After 30.33 Ma, the mean propagation rate was 96 km/m.y. and the median was 55 km/m.y.. Spreading rates also slowed down considerably, from an average of 55 km/m.y. half rate before chron 10 to 30 km/m.y. after the reorganization. Thus, the propagation/half spreading rate ratio remained approximately 3.

The fast propagation rates prior to chron 10 may have been driven by large stresses incurred on the Farallon plate from the nearby subduction zone -- a conclusion also reached by Hey and Wilson (1982). Stresses may have been released slightly after the fragmentation of the Farallon plate, possibly slowing down the propagation rate. Also, propagators PR 1 and PR 6 transferred large amounts of lithosphere to the Farallon plate, disrupting the age pattern. Approximately 10 percent of this portion of the Pacific plate was transferred to the Farallon plate by both northward and southward propagating rifts (but mainly northward propagators PR 1 and PR 6) from 36 to 30.3 Ma. The age disruption could have in turn affected the subduction rates and stresses.

Propagating rifts have been frequently associated with hotspot activity, particularly in the Galapagos and Juan de Fuca regions where active propagators are moving away from the hotspots. It has been proposed that propagating rifts could be driven by asthenospheric (sublithospheric) flow away from hotspots beneath the ridge axis (Hey and Vogt, 1977; Schilling et al., 1982). But, there is no evidence for a relationship between propagating rift tectonics and hotspot (melting anomaly) activity in the survey area. The only indication of any kind of melting anomaly is the Taney Seamount group, located at 36.7°N, 125.5°W. This elongated group of seamounts lying roughly parallel to the absolute Pacific plate motion, however, are in a region relatively undisturbed by propagation (except for the eastern end of the ridge). Phipps Morgan

and Parmentier (1985) argued that excess gravity stress is the force driving propagation and that "viscous suction" near the propagator tip limits the propagation velocity. This theory predicts that rifts propagate "downhill" from areas of anomalously shallow seafloor produced by excess magma supply as also proposed by Hey et al. (1980) in the Galapagos area. Wilson (1988) suggested that the magma supply was more robust at faster spreading rates, thus causing rifts to propagate down the gradient of the spreading rate. For the time prior to chron 10, the gradient would have sloped from the south towards the north. This may be a possible explanation for the prominence of northward propagation during this time although southward propagation also occurred.

The majority of the propagators were, in fact, initiated at transform faults, offsetting the ridge/transform intersection slightly. The reason why propagating rifts originate at transform faults is not understood, but it seems to be a common occurrence. In the model, the propagating rifts almost always initiated on the younger side of the transform fault near the ridge/transform intersection. A few propagators were initiated at kinks in a previously continuous ridge segment -- another frequent occurrence. Overall, it appears that the majority of the propagation episodes developed in response to changes in the direction of relative motion.

Hey (1977) and Hey and Wilson (1982) were the first to note that rift propagation is also a mechanism whereby sections of transform faults can be "instantaneously" changed to inactive fracture zones, freezing in the transform fault morphology. Several times in the model, mainly on the Farallon plate, portions of transform faults were abandoned when two propagating rifts intersected creating a FR-FR-AT (failed rift-failed rift-abandoned transform) triple junction-like feature in the oceanic crust. The size of the abandoned transform depends on the propagating/failing rift offsets before the propagators collided. Thus, it is important to keep in mind that not all triple-junction-like features in magnetic data are actual remnants of triple junctions. They could, instead, be a FR-FR-AT.

Menard (1978) proposed that the Farallon plate had been repeatedly fractured by ridge-trench transform faulting and by the intersection of the Pacific-Farallon ridge with the North American trench. He proposed that the Pioneer transform broke through to the trench at 37 Ma, and the resulting plate "swung erratically" (shown by the complex magnetic pattern of chron 13) for a few million years before it stabilized with a north-south ridge crest about 33 Ma. At approximately 32 Ma, when the ridge reached the trench off central California, it was oriented roughly north-south (chron 10) and was "continuous for long distances." However, within 1-2 m.y. after the collision, the ridge "swung" toward the northeast and fragmented by pivoting subduction into numerous shorter sections joined by new fracture zones (Menard, 1978). Rift propagation seems to offer a much better explanation for the complexity of chron 13. Furthermore, it appears that rift propagation reoriented the ridge segments towards the northeast after the Pacific/North American plate collision. It is important to note, however, that at the time of Menard's work, rift propagation was a new, relatively unknown concept.

VI. SUMMARY AND CONCLUSIONS

A detailed model for the tectonic evolution of the seafloor spreading system off the coast of California has been presented with the assumption that rift propagation provided the primary mechanism of ridge reorientation in the area. Excellent agreement between the model and the data provides strong support for this method. It also corroborates the ridge reorientation mechanism for the Juan de Fuca region (Hey and Wilson, 1982; Wilson et al., 1984; Wilson, 1988) and the Eocene reorganization of the Pacific-Farallon spreading center north of the Mendocino (Caress et al., 1988; Hey et al., 1988).

Analysis of the Raff-Mason magnetic data from this complex region of the Northeast Pacific has revealed that the Pacific plate interacted with five different plates during its spreading history offshore California (this does not include the North American plate). The final reconstructions are compilations of five separate spreading systems: Pacific-Farallon (chrons 13 through 11), Pacific-Vancouver (chrons 12 through 7), Pacific-Arguello (chrons 10 through 5E), Pacific-Monterey (chrons 10 through 6), and Pacific-Reyes (chrons 10 through 6A).

The proposed model begins at 36 Ma with three segments for the Pacific-Farallon ridge. Various propagators (PR 1 through PR 6) complicated the ridge geometry until a maximum of six ridge segments were formed by 33 Ma. At 32.25 Ma, a significant shift occurred in the Pacific-Farallon rotation pole causing the spreading direction to change from ENE-WSW to east-west. This caused the Pioneer transform fault to open slightly east of the Pioneer triple junction. By 30.3 Ma, several propagators (PR 7 and PR 8) and a ridge jump had simplified the ridge geometry to three segments once again. At the beginning of chron 10 (30.33 Ma), a major reorganization occurred when the Pacific plate arrived at the North American trench and strike-slip tectonics were initiated. Two new transforms, the Morro and the

Carmel, fractured through the Farallon plate to the trench creating three new microplates, the Arguello, the Monterey, and the Reyes; these microplates have since been subducted beneath North America. The new plate motions required ridge reorientation which was accomplished by rift propagation. As the microplates were reduced in size by subduction, instability led to complex propagation patterns, particularly for the Pacific-Arguello spreading center. At 27.95 Ma, another major pole change occurred. The Pacific-Vancouver relative motion rotation pole shifted to the east because of a change in the spreading direction from ENE-WSW to east-west, reducing the tension and compression in the Pioneer transform east and west of the triple junction, respectively. At 24.1 Ma, a new ridge segment with a NE-SW orientation propagated southward, terminating the main trend of the Murray fracture zone and offsetting it to the south. Additional propagation episodes (PR 20 and PR 21) reoriented the Pacific-Arguello spreading segment from NE-SW to north-south by 19 Ma, forming the fan shaped magnetic chrons 6A through 5E. At approximately 19 Ma, the Pacific-Monterey spreading center failed, leaving a "dead" ridge and a remnant piece of Monterey plate off the coast of San Francisco (Lonsdale, 1988; Atwater, 1989).

The research presented in this paper offers an initial model for the evolutionary history of the very complex region of seafloor offshore California. Despite the excellent match between model and data, there are still several questionable areas requiring further detailed analysis. This study has also strengthened the idea that rift propagation is a primary mechanism for ridge reorientation. However, there is still much to learn about propagating rifts, particularly the controlling mechanisms of their initiation and growth.

REFERENCES

- Atwater, T. M., Implications of plate tectonics for the Cenozoic tectonic evolution of western North America, *Geol. Soc. Am. Bull.*, 81, 3513-3536, 1970.
- Atwater, T. M., Plate tectonic history of the northeast Pacific and western North America, in *The Eastern Pacific Ocean and Hawaii, Vol. N, Geology of North America*, edited by E. L. Winterer, D. M. Hussong, and R. W. Decker, Geological Society of America, Boulder, CO, 1989.
- Bassinger, B. G., O. E. DeWald, and G. Peter, Interpretation of the magnetic anomalies off central California, *J. Geophys. Res.*, 74, 1484-1487, 1969.
- Caress, D. W., H. W. Menard, and R. N. Hey, Eocene reorganization of the Pacific-Farallon spreading center north of the Mendocino fracture zone, *J. Geophys. Res.*, 93, 2813-2838, 1988.
- Carlson, R. L., Late Cenozoic rotations of the Juan de Fuca Ridge and the Gorda rise, *Tectonophysics*, 77, 171-188, 1981.
- Chase, T. E., P. Wilde, W. R. Normark, C. P. Miller, B. A. Seekins, and J. D. Young, Offshore topography of the Western United States between 32° and 49° North latitudes, *Open File Rep.*, 81-443, U.S. Geological Survey, scale 1:864,518, 1981.
- EEZ-SCAN 84 Scientific Staff, *Atlas of the Exclusive Economic Zone, Western Conterminous United States, U. S. Geol. Surv. Misc. Invest. Ser., I-1792*, 1-152, 1986.
- Engebretson, D. C., A. Cox, and R. G. Gordon, Relative motions between oceanic plates of the Pacific basin, *J. Geophys. Res.*, 89, 10,291-10,310, 1984.
- Francheteau, J., J. G. Sclater, and H. W. Menard, Pattern of relative motion from fracture zone and spreading rate data in the northeastern Pacific, *Nature*, 226, 746-748, 1970.
- Hey, R. N., A new class of "pseudofaults" and their bearing on plate tectonics: A propagating rift model, *Earth Planet. Sci. Lett.*, 37, 321-325, 1977.
- Hey, R. N., and P. J. Vogt, Spreading center jumps and sub-axial asthenosphere flow near the Galapagos hot spot, *Tectonophysics*, 37, 41-52, 1977.
- Hey, R. N., and D. S. Wilson, Propagating rift explanation for the tectonic evolution of the northeast Pacific--The Pseudomovie, *Earth Planet. Sci. Lett.*, 58, 167-188, 1982.
- Hey, R. N., F. K. Duennebieer, and W. J. Morgan, Propagating rifts on midocean ridges, *J. Geophys. Res.*, 85, 3647-3658, 1980.
- Hey, R. N., M. C. Kleinrock, S. P. Miller, T. M. Atwater, and R. C. Searle, Sea Beam/Deep-Tow investigation of an active oceanic propagating rift system, Galapagos 95.5°W, *J. Geophys. Res.*, 91, 3369-3393, 1986.

- Hey, R. N., H. W. Menard, T. M. Atwater, and D. W. Caress, Changes in direction of seafloor spreading revisited, *J. Geophys. Res.*, 93, 2803-2812, 1988.
- Kent, D. V., and F. M. Gradstein, A Jurassic to recent geochronology, in *The Western North Atlantic Region, Vol. M, Geology of North America*, edited by P. R. Vogt, and B. E. Tucholke, pp. 45-58, Geological Society of America, Boulder CO, 1986.
- Lattimore, R. K., B. G. Bassinger, and O. E. DeWald, Magnetic map from the coast of California to 133°W longitude, *Misc. Geol. Invest. Map I-531A*, U.S. Geological Survey, 1968.
- Lonsdale, P., Structural patterns of the Pacific floor offshore of Peninsular California, in *Gulf and Peninsula Provinces of the Californias*, Amer. Assoc. Petroleum Geologists, Memoir, 1988 (in press).
- McKenzie, D. P., and R. L. Parker, The North Pacific: An example of tectonics on sphere, *Nature*, 216, 1276-1280, 1967.
- McKenzie, D. P., and W. J. Morgan, The evolution of triple junctions, *Nature*, 224, 125-133, 1969.
- Mason, R. G., A magnetic survey off the west coast of the United States between latitudes 32° and 36°N and longitudes 121° and 128°W, *Roy. Astron. Soc., Geophys. J.*, 1, 320-329, 1958.
- Mason, R. G., and A. D. Raff, A magnetic survey off the west coast of North America 32°N to 42°N, *Geol. Soc. Am. Bull.*, 72, 1259-1265, 1961.
- Menard, H. W., Fragmentation of the Farallon plate by pivoting subduction, *J. Geology*, 86, 99-110, 1978.
- Menard, H. W., and T. Atwater, Changes in the direction of sea floor spreading, *Nature*, 219, 463-467, 1968.
- Menard, H. W., and T. Atwater, Origin of fracture zone topography, *Nature*, 222, 1037-1040, 1969.
- Menard, H. W., and V. Vacquier, Magnetic survey of part of the deep sea floor off the coast of California, in *Research Reviews*, Office of Naval Research, pp. 1-5, 1958.
- Morgan, W. J., Rises, trenches, great faults, and crustal blocks, *J. Geophys. Res.*, 73, 1959-1982, 1968.
- Morton, W. T., and A. Lowrie, Regional geological maps of the Northeast Pacific: Standard Navy ocean area NP-9. *Naval Oceanographic Office, RP 16*, NSTL Station, MS. 39522, 1978.
- Nishimura, C., D. S. Wilson, and R. N. Hey, Pole of rotation analysis of present-day Juan de Fuca plate motion, *J. Geophys. Res.*, 89, 10,283-10,290, 1984.

- Phipps Morgan, J., and E. M. Parmentier, Causes and rate-limiting mechanisms of ridge propagation: A fracture mechanics model, *J. Geophys. Res.*, 90, 8603-8612, 1985.
- Pitman, W. D., III, E. M. Herron, and J. R. Heirtzler, Magnetic anomalies in the Pacific and sea-floor spreading, *J. Geophys. Res.*, 73, 2069-2085, 1968.
- Raff, A. D., and R. G. Mason, Magnetic survey off the west coast of North America, 40°N latitude to 50°N latitude, *Geol. Soc. Am. Bull.*, 72, 1267-1270, 1961.
- Riddihough, R., Recent movements of the Juan de Fuca plate system, *J. Geophys. Res.*, 89, 6980-6994, 1984.
- Rosa, J. W. C., and P. Molnar, Uncertainties in reconstructions of the Pacific, Farallon, Vancouver, and Kula plates and constraints on the rigidity of the Pacific and Farallon (and Vancouver) plates between 72 and 35 Ma, *J. Geophys. Res.*, 93, 2997-3008, 1988.
- Severinghaus, J., and T. M. Atwater, Cenozoic geometry and thermal state of the subducting slabs beneath western North America, in *Basin and Range Extension*, edited by B. Wernicke, Geol. Soc. Amer., Memoir, 1989 (in press).
- Shih, J., and P. Molnar, Analysis and implications of the sequence of ridge jumps that eliminated the Surveyor transform fault, *J. Geophys. Res.*, 80, 4815-4822, 1975.
- Sinton, J. M., D. S. Wilson, D. M. Christie, R. N. Hey, and J. R. Delaney, Petrologic consequences of rift propagation on oceanic spreading ridges, *Earth Planet. Sci. Lett.*, 62, 193-207, 1983.
- Smith, W. H. F., and P. Wessel, Gridding with continuous curvature splines in tension, *Geophysics*, 1989 (in press).
- Taylor, B., J. Sinton, L. Liu, and K. Crook, Extensional transform zone, Manus Back-arc Basin, *EOS Trans. Am. Geophys. Un.*, 67, 1228, 1986.
- Theberge, A. E., Jr., Magnetic survey off southern California and Baja California, Operational Data Report NOS DR-12, in ed., *National Oceanic Atmos. Adm., Mar. Geophys. Group*, 10 pp., Rockville, MD, 1971.
- Vacquier, V., Measurement of horizontal displacement along faults in the ocean floor, *Nature*, 183, 452-453, 1959.
- Vacquier, V., A. D. Raff, and R. E. Warren, Horizontal displacements in the floor of the northeastern Pacific Ocean, *Geol. Soc. Am. Bull.*, 72, 1251-1258, 1961.
- Vine, F. J., Spreading of the ocean floor: New evidence, *Science*, 154, 1405-1415, 1966.
- Vine, F. J., and D. H. Matthews, Magnetic anomalies over ocean ridges, *Nature*, 199, 947-949, 1963.
- Vine, F. J., and J. T. Wilson, Magnetic anomalies over a young oceanic ridge off Vancouver Island, *Science*, 150, 485-489, 1965.

- Vogt, P. R., and G. R. Byerly, Magnetic anomalies and basalt composition in the Juan de Fuca-Gorda Ridge area, *Earth Planet. Sci. Lett.*, 33, 185-207, 1976.
- Wessel, P., Xover: A cross-over error detector for track data, *Computers & Geosciences*, 15, 333-346, 1989.
- Wilson, D. S., Tectonic history of the Juan de Fuca Ridge over the last 40 million years, *J. Geophys. Res.*, 93, 11,863-11,876, 1988.
- Wilson, D. S., R. N. Hey, and C. Nishimura, Propagation as a mechanism of ridge reorientation: a model for the tectonic evolution of the Juan de Fuca Ridge, *J. Geophys. Res.*, 89, 9215-9225, 1984.
- Wilson, J. T., A new class of faults and their bearing on continental drift, *Nature*, 207, 343-347, 1965a.
- Wilson, J. T., Transform faults, oceanic ridges, and magnetic anomalies southwest of Vancouver Island, *Science*, 150, 482-485, 1965b.